Friction https://mc03.manuscriptcentral.com/friction
https://doi.org/10.26599/FRICT.2026.9441213

Review

Research progress and application prospects of nanocomposites in lubricants

Siyuan Wang[1, *], Hengyuan Liu[2], Gang Liu[1], Fang Xie[1], Ding Chen[3], Jingyi Liu[3], Bin Wang[3], Zhao Liang[4], Guanlin Ren[5, *]

[1] *Engineering Research Center of Additive Manufacturing Aeronautical Materials of Henan Province, Nanyang Institute of Technology, Nanyang 473004, China*

[2] *College of Advanced Materials Engineering, Zhengzhou Technology College, Zhengzhou 450010, China*

[3] *State Key Laboratory of Advanced Design and Manufacturing for Vehicle Body, Hunan University, Changsha 410082, China*

[4] *Institute of Micro/Nano Materials and Devices, Ningbo University of Technology, Ningbo 315211, China*

[5] *State Key Laboratory of Solid Lubrication, Lanzhou Institute of Chemical Physics, Chinese Academy of Sciences, Lanzhou 730000, China*

*Corresponding author: Siyuan WANG, E-mail: wangsy@nyist.edu.cn; Guanlin REN, E-mail: renguanlin@licp.cas.cn

Received: May 8, 2025; Revised: November 5, 2025; Accepted: January 5, 2026

Abstract: Nanocomposites have attracted significant attention as lubricant additives due to their advantages in reducing friction, enhancing wear resistance, and improving thermal and oxidative stability. In recent years, increasing research has explored how different types of nanomaterials (such as carbon-based materials, metallic nanoparticles, and ceramic phases) can use synergistic effects to achieve performance surpassing that of their single components. This review focuses on relevant studies published between 2020 and 2025, providing an updated overview of the advantages, synthesis methods, structures, dispersion stability, lubrication mechanisms, and tribological behavior of nanocomposites. Various structural types are discussed, including core-shell, layered, and in-situ hybrid systems, along with their fabrication routes such as sol-gel processing, hydrothermal synthesis, and surface modification strategies. The lubrication mechanism of nanocomposites is analyzed based on the material structure and the testing conditions. Particular attention is paid to the synergistic effects among multiple components within the nanocomposites and how these synergies enhance tribological performance. Furthermore, the challenges faced by nanocomposites and potential future developments are discussed. This review aims to clarify the current status of nanocomposites as lubricant additives and facilitate their future application in advanced lubrication systems.

Keywords: nanocomposite, lubricant additives, nanomaterial synthesis, synergistic effects, lubrication mechanism, research progress

1. Introduction

Lubricants play a crucial role in mechanical manufacturing and industrial production by reducing friction and wear, enhancing energy efficiency, and extending the service life of equipment [1, 2]. Over the past few decades, numerous researchers have explored the use of various nanomaterials as lubricant additives to break through the bottlenecks of traditional lubricant additives and meet the demands of modern industry for high-performance, environmentally friendly, and durable lubricants

(**Fig. 1**) [3-5]. However, a single type of nanomaterial often fails to meet multiple performance requirements, and this limitation has sparked interest in nanocomposites. Nanocomposites combine multiple nanomaterial components to achieve a synergistic enhancement of properties, providing a promising solution to the current challenges faced by lubricant additives [6-8].

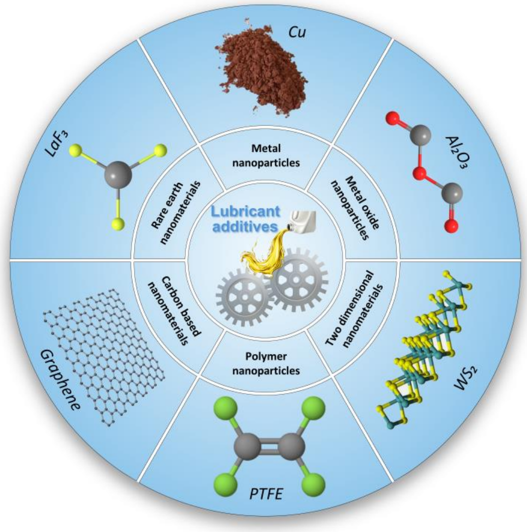

Fig. 1 Several common types of nanolubricant additives.

Nanocomposite lubricant additives typically integrate different types of nanomaterials to leverage their complementary advantages, such as metals, carbon-based phases, and ceramics. Metal nanoparticles (NPs) possess high thermal conductivity and load-bearing capacity but are prone to oxidation and agglomeration [9-12]. Carbon-based nanomaterials, including carbon nanotubes, graphene, and graphene oxide (GO), exhibit excellent mechanical strength and thermal conductivity, yet often suffer from poor dispersibility and weak interfacial compatibility [13-15]. Ceramic nanomaterials (e.g., TiO_2, ZrO_2, Al_2O_3) offer hardness and thermal stability, but may cause abrasive wear under certain conditions [16-19]. Instead of relying on a single-phase additive, nanocomposites allow for tailored design strategies to produce additives with enhanced stability, film-forming capability, and adaptive tribological behavior. For example, a “hard-soft” synergy can be achieved by combining metal and ceramic NPs, which reduces fluctuations in coefficients of friction (CoF) and improves adaptability under variable working conditions [20]. Similarly, incorporating both polytetrafluoroethylene (PTFE) NPs and cellulose nanofibers into lubricating oil has been shown to reduce wear and extend lubrication longevity: PTFE lowers CoF and wear scar diameter (WSD), while the long-chain cellulose structure helps retain oil at the contact interface [21]. These cases underscore the potential of nanocomposites to address multiple lubrication challenges through component synergy.

Nanocomposites with various structures, including core-shell structure, layered structure, and nanocapsules, have been synthesized and applied in the field of lubricant additives [22-27]. However, there are still many obstacles in developing the potential of nanocomposites for further applications, such as achieving long-term dispersion stability, clarifying the interfacial interaction mechanism, or developing more green and efficient preparation methods [28-30]. To quantify the research progress in this field, we conducted a literature search in the Web of Science database, as shown in **Fig. 2**. The results show that the number of relevant publications has significantly increased between 2010 and 2025, particularly after 2020. This trend reflects the growing interest in the research of nanocomposites for lubrication applications. However, existing research still exhibits fragmented properties, typically focusing on single materials or specific testing conditions. A comprehensive review of the construction of a comprehensive framework centered on nanocomposites is still scarce.

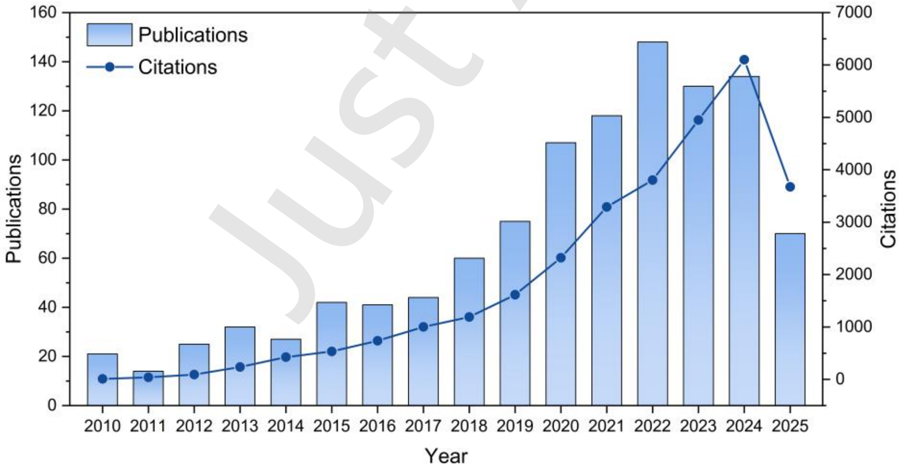

Fig. 2 Number of times cited and publications during 2010-2025. The data were compiled from the Web of Science database on July 16, 2025. The topic words for retrieval are (nanocomposites) AND (lubricants OR lubricating oils OR lubricant additives)

In response to these trends and research gaps, this review examines the latest advances (2020-2025) in nanocomposites as lubricant additives. It highlights the structure-property relationships, synthesis techniques, and lubrication mechanisms, and especially the synergistic effects among constituent components of nanocomposites. The challenges and future directions for industrial applications are also discussed, aiming to promote innovation and the application of nanocomposite-based lubrication technologies.

2. Advantages of nanocomposites

Nanocomposites have been a hot topic in the research of nanotechnology and materials science in recent years. Due to their unique multi-functionality, excellent mechanical and thermal properties, and chemical stability, they have been widely applied in various fields, including lubricants. Nanocomposites are typically composed of two or more different types of NPs, which are combined through physical or chemical interactions, generating a synergistic effect. This synergistic effect of the nanocomposites can usually significantly improve their performance in practical applications. Compared with traditional single-type nanomaterials, nanocomposites have significant advantages in multiple properties (**Fig. 3**), enabling the realization of various optimized characteristics of the materials to meet the requirements under different working conditions. In this section, the performance advantages of nanocomposites in lubricants will be systematically analyzed. Beyond their physicochemical, thermal, anti-corrosion, and dispersion-related properties, attention is also given to advanced strategies for performance enhancement, such as surface functionalization versus nanocomposite design, and to direct comparisons with widely used traditional additives. This comprehensive framework highlights not only the intrinsic strengths of nanocomposites but also their practical competitiveness, providing a basis for evaluating their potential as next-generation lubricant additives.

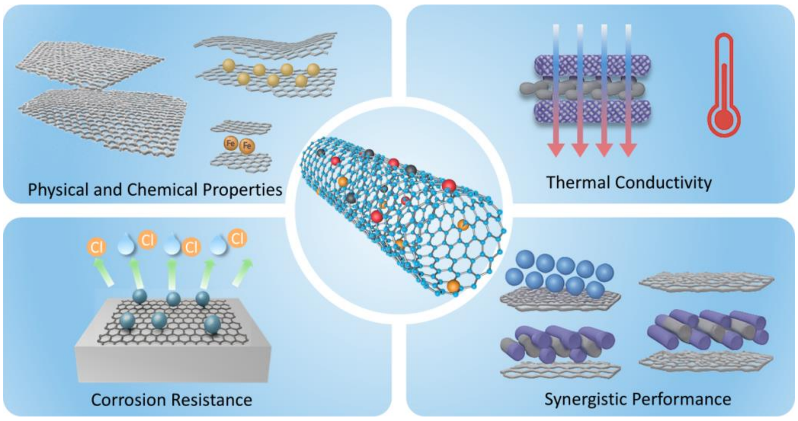

Fig. 3 Nanocomposites have a series of outstanding properties.

2.1. Advantages of physical and chemical properties

Nanocomposites can achieve comprehensive properties that single-type nanomaterials cannot reach. They usually possess a higher specific surface area, stronger surface activity, better electrical conductivity, and higher reactivity than single-type materials. Kumar et al. [31] examined CuO-TiO_2 hybrid nanofluids in EP 140 gear oil and showed complementary roles of the two phases. TiO_2 (spherical, hardness 5.5-7 Mohs) reduced friction through a nano-bearing effect, while CuO (hardness ~3.5 Mohs) enhanced wear resistance by tribo-sintering to fill defects and form protective films. Quantitatively, 0.3 wt% TiO_2+0.3 wt% CuO reduced the CoF by 19.33%, whereas 0.3 wt% TiO_2+0.1 wt% CuO decreased wear by 23.03% and increased load-carrying capacity by 89.24% compared to the base oil. These data confirm that synergy arises from the rolling action of TiO_2 combined with CuO-induced tribofilms. Kong et al. [32] reported TiO_2-Cu composite coatings on Ti6-Al-4V alloy, where TiO_2 dominated friction reduction and Cu acted as a binder. Increasing TiO_2 content from 80% to 90% decreased the CoF from 0.455 to 0.148 and wear rate from 101.70 to 6.15 $\mu m^3 \cdot N^{-1} \cdot mm^{-1}$. TiO_2 provided solid-lubricant tribo-films and debris lubrication, while Cu improved coating compactness but introduced adhesive wear at lower TiO_2 levels. The overall synergy thus stems from TiO_2 ensuring hardness and film formation, and Cu enhancing structural integrity. First-principles calculations show that the Cu binder reacts with TiO_2 to form Cu-Ti bonds, in which the

(001) crystalline surface of Cu grows on the (101) crystalline surface of TiO_2 to improve the mechanical properties of the coating (**Fig. 4**).

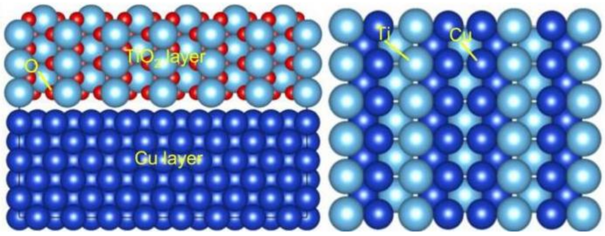

Fig. 4 Structures of TiO_2 and Cu layers on TiO_2-Cu composite coatings with different TiO_2 mass fractions by first-principle calculation. Reproduced with permission from Ref. [32], © Elsevier B.V. 2023.

The surface properties of nanocomposites are also one of their most remarkable advantages. Due to the interactions between different components, the surface of the nanocomposites can exhibit stronger surface activity than single-type nanomaterials. The physicochemical properties of nanocomposites can be regulated by adjusting the proportion, size, and shape of each component. For instance, by changing the ratio of metal particles to ceramic particles, the electrical conductivity and thermal stability of the nanocomposites can be adjusted. Momohjimoh et al. [33] prepared Al_2O_3-SiC and Al_2O_3-MWCNT nanocomposites via spark plasma sintering, achieving electrical conductivities of 2.65×10^{-5} S/m and 101.118 S/m, respectively, which represent several orders of magnitude improvement over pure Al_2O_3 (6.78×10^{-10} S/m). Such enhancements in electrical conductivity are not merely material attributes, but can actively facilitate electrochemical tribofilm formation and accelerate ion migration during current-assisted lubrication.

Recent studies further underscore the lubrication relevance of enhanced conductivity. Liu et al. [34] fabricated graphene nanosheets coated with silver nanorods and dispersed them in ionic liquid (ILs) LP108. The resulting lubricant exhibited 5.4-fold higher conductivity than pure LP108, which promoted rapid adsorption of nanocomposites on the friction interface and facilitated electrochemical reaction film formation under current-carrying conditions. Tribologically, the composite reduced the CoF to 0.0723 and decreased wear volume by 97.3% without current, while under 1 A current, the

CoF dropped further to 0.0687 with 90.2% wear reduction. Similarly, Zhang et al. [35] synthesized graphene nanosheet-silver nanosphere hybrids that enhanced conductivity by 11-fold compared to pure LP108. The improved conductivity accelerated protective tribofilm formation containing Ag and C elements, while the synergistic "rolling ball" effect of silver nanosphere and lamellar sliding of graphene nanosheet delivered CoF reductions to 0.07003 and wear reductions of over 92%. These findings clearly illustrate that enhanced electrical conductivity in nanocomposites not only improves charge transport but also directly translates into improved friction reduction and wear resistance under both neutral and current-carrying conditions.

In addition to electrical properties, the superior mechanical performance of nanocomposites plays a pivotal role in lubrication. Under high-temperature and high-load conditions, composites exhibit greater mechanical stability than single-component nanomaterials [36, 37]. They typically combine high hardness, tensile strength, compressive strength, and toughness, which enable them to resist deformation and wear while maintaining durability under severe contact stresses [38, 39]. For instance, the incorporation of carbon nanotubes (CNT) into metallic matrices has been shown to substantially enhance tensile strength [40-42], while metal-ceramic composites have been shown to overcome brittleness issues of single-phase ceramics under extreme conditions. Sharifianjazi et al. [43] further demonstrated that incorporation of MgO and SrO into bioactive glass markedly increased hardness and elastic modulus, highlighting the tunability of mechanical properties for nanocomposites.

The tribological implications of such mechanical reinforcement have been directly validated in recent studies. Szabó and Hasan [44] investigated the synergistic effects of CuO and ZnO nanoadditives in Group III automotive base oil. The hardness difference influenced their tribological roles: CuO (130-200 HV) formed stable tribofilms, while ZnO (1000-1200 HV), despite high hardness, tended to agglomerate. CuO-ZnO (2:1) mixture showed synergistic effects, achieving a 27% friction reduction and 54% wear reduction. This synergy arose from ZnO promoting CuO deposition into tribofilms while CuO mitigated the abrasive behavior of ZnO, with the hardness contrast facilitating balanced tribofilm formation and wear resistance. Sun et al. [45] further studied *h*-BN/ceramic composites, demonstrating that variations in Young's modulus and shear modulus directly controlled *h*-BN release efficiency and tribofilm stability. For example, *h*-BN/SiO_2 composites (Young's modulus=59.44 GPa, shear modulus=24.33 GPa) exhibited the lowest CoF (0.20) due to optimized lubricant extrusion and tribofilm continuity, while *h*-BN/Si_3N_4 composites (Young's modulus 58.55 GPa) exhibited a CoF of 0.21, benefiting from a strong *h*-BN-Si_3N_4 binding force that enhanced *h*-BN exfoliation and trapped abrasive debris, reducing wear. Thus, appropriate hardness and modulus balanced *h*-BN release and tribofilm stability, directly improving friction and wear performance. These results establish a direct link between tailored mechanical properties (hardness, modulus, toughness) and superior friction- and wear-reduction performance of nanocomposites.

Nanocomposites also exhibit remarkable fatigue resistance, particularly in applications requiring long-term cyclic loading [46]. Wang et al. [47] used GO and CNT along with styrene butadiene styrene (SBS) to modify asphalt binders (**Fig. 5(a)**). They characterized the modifiers and modified binders and evaluated their anti-aging, rheological, and fatigue properties. The results showed that both GO and CNT/SBS composites could improve the fatigue life of asphalt binders, with higher contents of GO or CNT enhancing fatigue resistance significantly (**Fig. 5(b)** and **(c)**). The introduction of NPs with high strength and toughness into composite systems can significantly enhance fatigue resistance and prolong service life [48]. In contrast, single-component nanomaterials may experience fatigue failure or fracture under prolonged operational loads due to structural homogeneity [49].

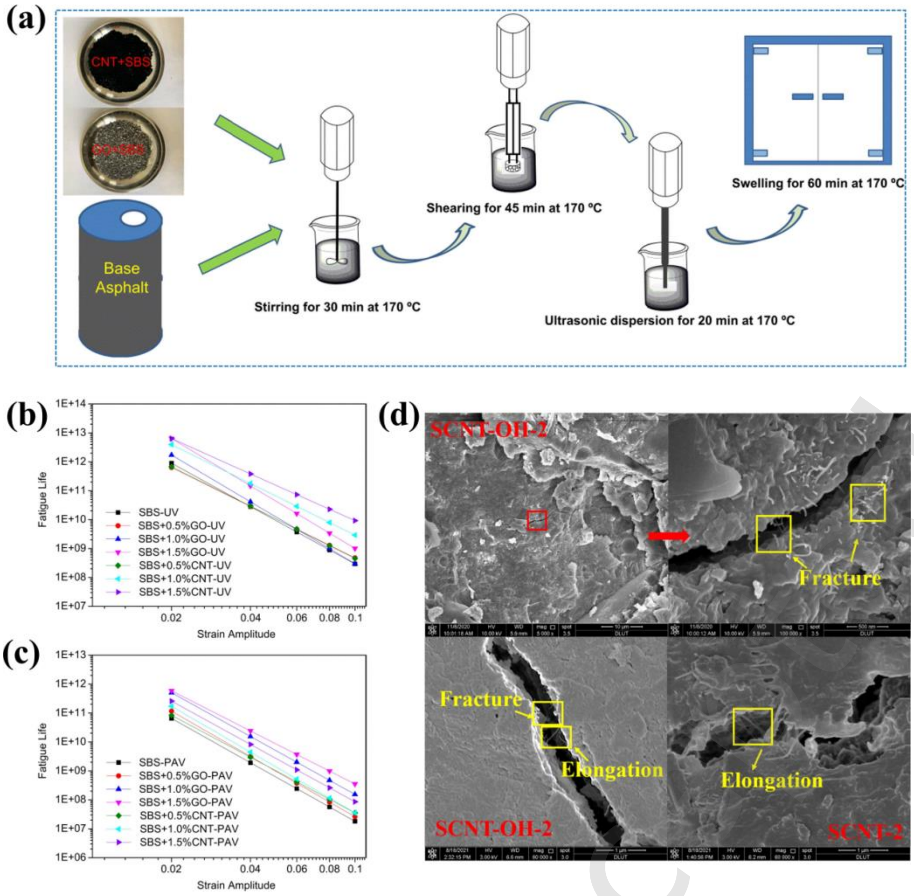

Fig. 5 (a) Schematic representation of preparing GO+SBS and CNT+SBS-modified asphalt binders. (b) Fatigue life predictions of the UV-aged asphalt binders modified with SBS/GO/CNT. (c) Fatigue life predictions of the PAV-aged asphalt binders modified with SBS/GO/CNT. (d) The bridging effect of CNT at the fatigue fracture surface of cementitious composites. Reproduced with permission from Ref.[47], © Elsevier B.V. 2021.

Somasundaram Prasadh et al. [50] observed that increasing hollow SiO_2 NPs content enhanced both yield strength and ultimate compressive strength of magnesium alloys, with Mg-1.5 vol.% SiO_2 demonstrating optimal mechanical properties. Additionally, the wear resistance and compressive performance of nanocomposites have been extensively validated. Carbon-based materials combined with ceramic particles exhibit improved stability under high-pressure environments through filling effects and synergistic interactions between particles, thereby enhancing wear resistance [51, 52].

The exceptional wear resistance and compressive properties of nanocomposites represent another significant advantage, particularly under high-load and high-pressure conditions. These characteristics make them particularly advantageous for lubricant applications, enabling better resistance to compressive stresses and wear in friction pairs while prolonging lubrication intervals [53].

2.2. Advantages in thermal properties

The thermal performance advantages of nanocomposites, particularly their stability and thermal conductivity under high-temperature conditions, constitute critical attributes for their application in lubricants [29, 36, 54]. Thermal stability ensures that the material retains its performance characteristics under extreme temperature conditions [55, 56]. Meanwhile, enhanced thermal conductivity improves the heat dissipation capacity of lubricants, thereby providing cooling effects during friction processes. This effectively reduces interfacial temperatures at contact surfaces, ultimately enhancing the performance, service life, and operational stability of lubricants [57, 58].

Nanocomposites generally exhibit superior thermal conductivity compared to single-component materials, with particularly notable improvements under elevated temperatures. Barani et al. [59] investigated the thermal properties of epoxy-based binary composites incorporating graphene and Cu NPs. Their study revealed that fillers with distinct dimensions synergistically enhanced the thermal conductivity of the composite. The incorporation of graphene significantly improved heat transfer efficiency, enabling rapid thermal dissipation in lubricants under high-temperature conditions and preventing lubrication failure caused by localized overheating [60, 61].

In contrast, single-component materials such as TiO_2 or Al_2O_3 demonstrate relatively low thermal conductivity, which may be insufficient to meet heat dissipation requirements in high-temperature environments [62-64]. Additionally, nanocomposites typically exhibit excellent high-temperature stability and oxidation resistance, effectively preventing material degradation while maintaining performance integrity under thermal stress [65, 66]. For instance, in ceramic-based composites, ceramic particulates enhance mechanical properties and thermal stability at elevated temperatures. Sun et al. [67] fabricated polyetherimide-based nanocomposites containing SiO_2 NPs via a solution casting method. Their findings indicated that SiO_2 NP incorporation reduced electrical conductivity while substantially improving high-temperature breakdown strength. Hu et al. [68] prepared boron nitride nanosheets (BNNS) graphene hybrid fillers using the in-situ exfoliation method (**Fig. 6**). After incorporating them into a polyethylene glycol (PEG) matrix, the thermal conductivity of the nanocomposites significantly increases while maintaining electrical insulation.

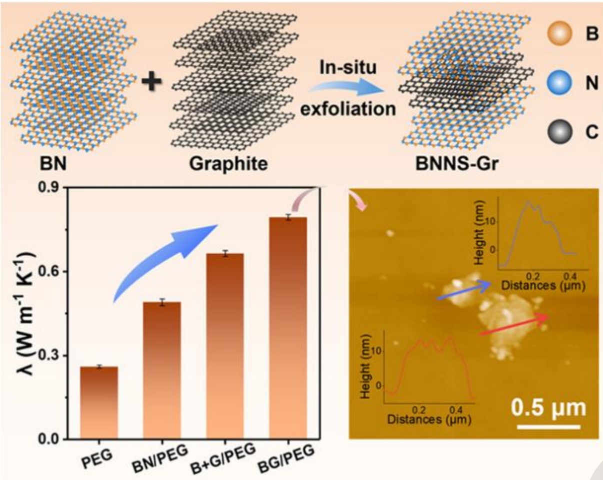

Fig. 6 The composite of graphene and BN reduces the interfacial thermal resistance of polymer composites. Reproduced with permission from Ref.[68], © American Chemical Society 2025.

Jiang et al. [69] synthesized manganese ferrite on BNNS by the hydrothermal method, forming a layered structure of BNNS@M Magnetic responsive nanohybrid materials (**Fig. 7**). Integrate this material into a water-based polyurethane solution and shape it under a magnetic field to prepare a thermally conductive film. The film achieved an in-plane thermal conductivity of 8.5 $W \cdot m^{-1} \cdot K^{-1}$ and an out-of-plane thermal conductivity of 1.8 $W \cdot m^{-1} \cdot K^{-1}$, exhibiting significant anisotropic thermal conductivity. Furthermore, rational selection of particle types and optimization of composite ratios can mitigate thermal fatigue or degradation in nanocomposites under harsh thermal conditions, ensuring stable and sustained lubrication efficacy [70, 71].

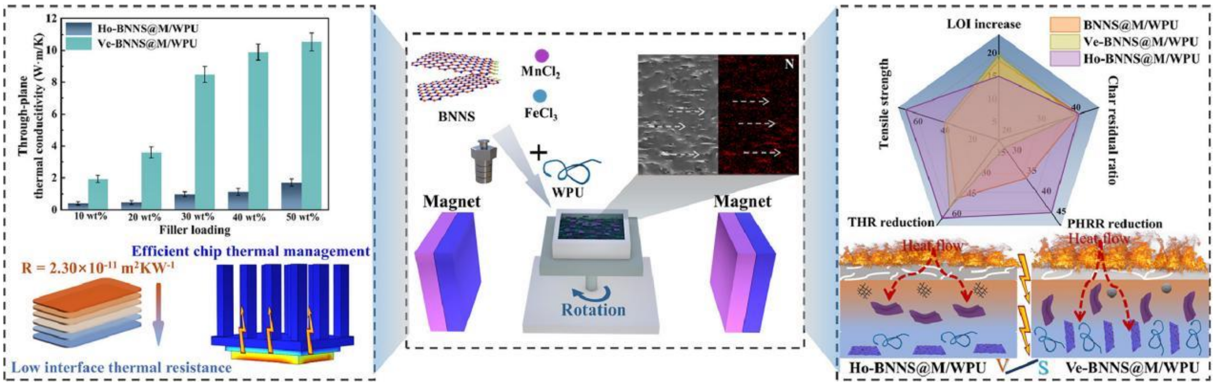

Fig. 7 Schematic diagram of the preparation, thermal conductivity, and lubrication mechanism of BNNS@M nanohybrids. Reproduced with permission from Ref.[69], © Elsevier 2025.

2.3. Advantages of corrosion resistance

The superior corrosion resistance of nanocomposites enables their exceptional performance in extreme environments [72]. By optimizing the selection of constituent phases, these composites demonstrate significantly enhanced oxidation resistance, acid-alkali tolerance, and chemical erosion resistance, particularly under harsh conditions involving high temperatures, humidity, or aggressive chemical exposure [73].

Certain nanomaterials (e.g., silver NPs, nano-alumina) exhibit intrinsic oxidation resistance that effectively inhibits substrate oxidation reactions, making them ideal candidates for composite reinforcement. Yang et al. [74] improved the oxidation resistance of Fe nanowires by coating them with Ag. Similarly, Han et al. [75] developed Ti_3C_2-TiO_2 composites through the in situ growth of TiO_2 NPs on MXene surfaces, achieving both enhanced photoelectrochemical properties and oxidation resistance. To address the brittleness and oxidation vulnerability of $MoSi_2$ coatings, Wang et al. [76] incorporated Al_2O_3 whiskers and particles. After 76 hours of oxidation at 1450 °C, the Al_2O_3 whisker-reinforced $MoSi_2$ coating (1 wt%) exhibited minimal mass loss (0.17%) with retained structural integrity, failing via penetrative cracking rather than catastrophic oxidation. Such nanomaterial-enhanced oxidation resistance ensures sustained lubricant performance under high-temperature or corrosive gaseous environments, thereby extending maintenance intervals.

Beyond oxidation resistance, nanocomposites also display robust chemical corrosion resistance[77, 78]. For instance, carbon-based and ceramic particles within composites can shield lubricants from chemical degradation, improving operational stability in extreme chemical environments [72, 79, 80]. Chen et al. [81] developed a uniform BTA@ZIF-8 (1H-Benzotriazole@Zeolitic Imi-dazolate Framework-8) layer via a one-step in-situ one-pot method, which was applied in sol-gel coatings on AA2024-T3 (**Fig. 8**). The 2.6 μm thick composite coating showed excellent corrosion resistance, with $|Z|_{0.01\ Hz}$ remaining 10^6 Ω·cm^2 after 30 days immersion in 3.5 wt% NaCl solution and no visible corrosion pits even after 60 days. The mechanism involves the barrier property of the uniform BTA@ZIF-8 layer and pH-induced release of inhibitors (BTA and 2-Methylimidazole) from BTA@ZIF-8 particles, where strong adsorption between BTA and Cu-rich phases promotes heterogeneous nucleation of BTA@ZIF-8 crystals, enhancing coating integrity and active protection. Zafar et al. [82] synthesized silane-functionalized titania-GO nanocomposites for PU coatings on steel, which showed superior corrosion resistance with a maximum impedance of 0.821 TΩ·cm^2 (99.9% inhibition efficiency) after 4 weeks in 3.5 wt% NaCl and delayed corrosion in salt spray tests, via electrolyte diffusion barrier of GO, TiO_2-derived $FeTiO_3$ passive layer, and silane-enhanced adhesion through Si-O bonds.

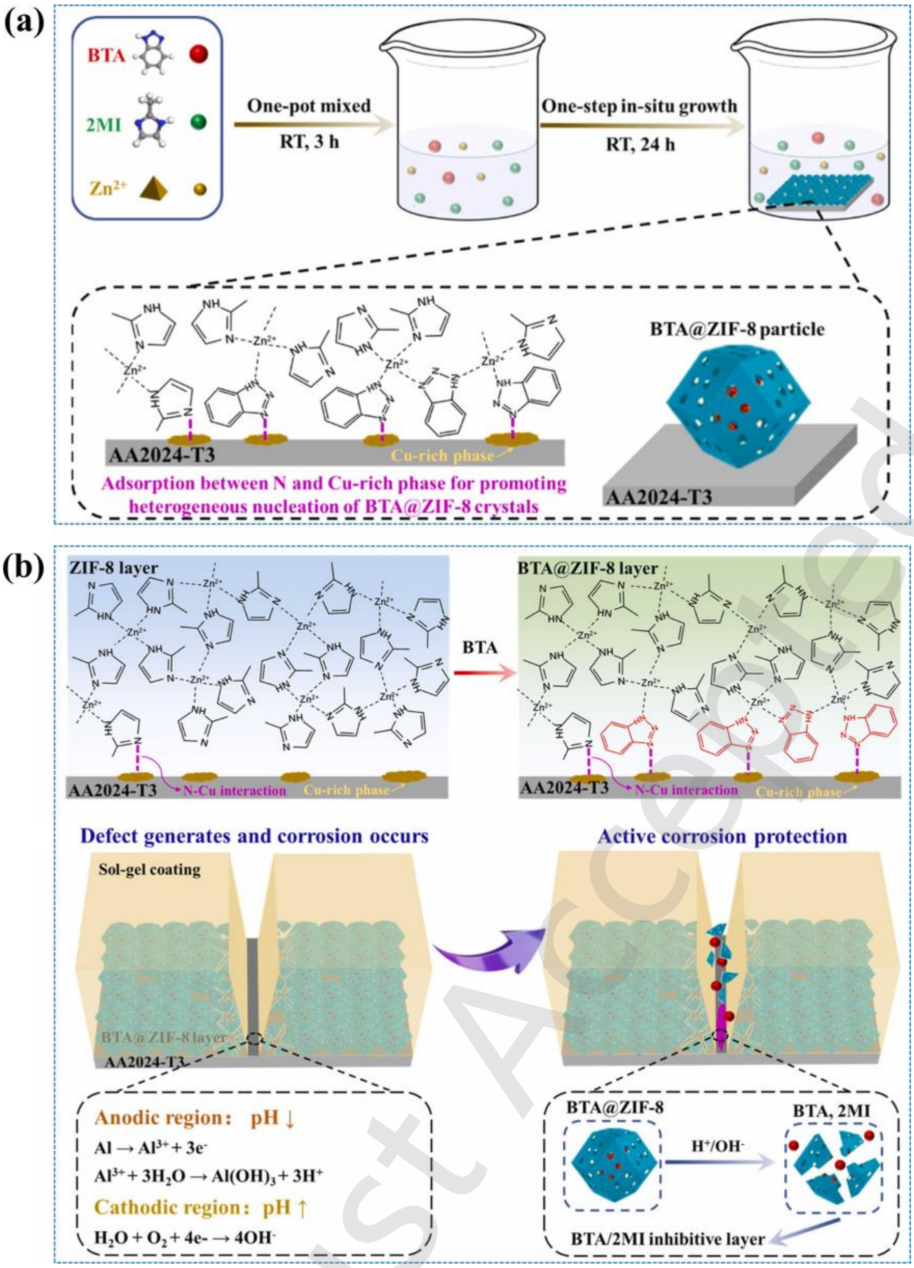

Fig. 8 (a) Schematic representation of one-step in-situ growth by one-pot method for preparation of BTA@ZIF-8 layer. (b) The mechanism of BTA promotes the uniform growth of the BTA@ZIF-8 layer, and the BTA@ZIF-8 layer improves the corrosion protection of sol-gel coatings. Reproduced with permission from Ref.[81], © Elsevier B.V. 2025.

2.4. Advantages in dispersion stability

The dispersion stability of nanocomposites represents a critical advantage for practical applications, particularly in lubricants where NPs dispersion directly governs both performance and system reliability. Nanocomposites effectively address the dispersion challenges inherent to single-component NPs in media. For instance, monophasic NPs (e.g., CNTs, graphene) tend to aggregate due to high surface energy, compromising their dispersion in lubricants [83, 84]. By combining two or more nanomaterials with complementary physical and chemical properties, nanocomposites can modulate interparticle interactions, improve compatibility with the lubricant medium, and thus significantly enhance dispersion stability.

Structural design of nanocomposites plays a central role in improving dispersion. Kamae and Drzal [85] achieved uniform coatings between CNTs and carbon fibers by immersing fibers in CNT/water suspensions, where balanced repulsive and attractive forces between the components enabled superior dispersion efficiency. Such optimized dispersion not only improves nanomaterial stability in lubricants but also enhances tribological properties. Core-shell architectures further enhance stability by tailoring surface chemistry. Wei et al. [86] synthesized TiO_2-core/CTAB-shell nanocomposites, where the hydrophobic CTAB shell facilitated stable dispersion in base oils while protecting the TiO_2 core from environmental degradation. This architecture demonstrated significant potential for extending diesel engine service life and ensuring operational safety. The interfacial engineering has proven highly effective in improving stability. Samanta and Sahoo [87] fabricated covalently linked *h*-BN-GO nanocomposites using (3-aminopropyl) trimethoxysilane as a bifunctional linker, achieving stability without sedimentation for over 60 days, which is substantially longer than oleic-acid-modified *h*-BN/GO (14 days). This improvement was attributed to stronger interfacial bonding, which resisted particle separation under high shear stress and enabled sustained tribofilm formation during operation.

Several recent studies provide quantitative evidence that nanocomposites can achieve markedly better dispersion stability than single-component counterparts, and that improved stability correlates with superior tribological behavior. Gong et al. [88] synthesized MoS_2@CNT, MoS_2@graphene, and MoS_2@C_{60} nanocomposites and showed that these systems remained stably dispersed in polyalkylene glycol (PAG) for over two weeks, whereas pure MoS_2 rapidly aggregated. The enhanced dispersion enabled the formation of protective tribofilms and resulted in wear-volume reductions exceeding 96% relative to the base oil. Sun et al. [89] reported GO-Fe_3O_4 nanocomposites that resisted sedimentation for 24 hours in water-based lubricants, outperforming single GO (agglomerated) and Fe_3O_4 (rapid settling); These synergistic combinations not only enhanced stability but also improved friction reduction and wear resistance by promoting continuous tribofilm generation, leading into ~34% lower friction and ~32% smaller wear scars. Yang et al. [90] studied the tribological properties of GO/modified SiO_2 as a composite additive. The modified SiO_2 attached to GO can prevent GO aggregation, which also improves the dispersibility of modified SiO_2. This synergistic effect is more conducive to forming a dense and thick friction film, thereby improving the tribological performance. Compared with pure GO lubricant and pure modified SiO_2, the minimum average CoF of GO/modified SiO_2 lubricant decreased by 48.7% and 46.09%, respectively, and the highest the maximum non-seizure load (P_B) increased by 1.43% and 1.38%, respectively.

Nanocomposites are also effective in non-oil systems. Morshed et al. [91] prepared *h*-BN/TiO_2 nanocomposites stabilized with glycerol and SDBS, achieving no visible stratification after 7 days in water-based lubricants and a 70 % reduction in CoF compared to water alone. Jin et al. [92] demonstrated that Mn_3O_4/graphene nanocomposites remained uniformly dispersed in lithium grease, sustaining lubrication up to 120 ℃ while pure grease failed at 80 ℃. In the above cases, stable dispersion ensured continuous additive supply to the contact interface, allowing the full exploitation of lubricant additives such as rolling, polishing, and mending effects.

A comparative summary of dispersion stability performance is presented in **Table 1**, illustrating the differences between various nanocomposite systems and their single-component counterparts in terms of sedimentation time, particle-size stability, and tribological improvements.

Table 1 Comparison of dispersion stability and tribological performance of representative nanocomposites.

Nanocomposites	Media	Stability	Comparison with a single	Key tribological

			component	improvements
MoS_2@CNT, MoS_2@Gr, MoS_2@C_{60} [88]	PAG	>14 days	Pure MoS_2 aggregated within hours	wear volume ↓ >96 %
h-BN-GO [87]	Paraffin oil	>60 days	GO sedimented within days	CoF ↓50.7 %, very low wear rate
h-BN/TiO_2 [91]	Water-based	7 days	*h*-BN or TiO_2 alone is unstable for hours	CoF ↓70 %, wear area ↓79.6 %
GO-Fe_3O_4 [89]	Water-based	24 h	Fe_3O_4: 12 h settling; GO: wall adhesion	CoF ↓33.6 %, WSD ↓32.3 %
N-C/Ag [93]	Liquid paraffin	Stable during test	CNT/Ag without OA: partial sedimentation	CoF ↓27.3 %, WSD ↓25.3 %
Mn_3O_4/graphene [92]	Lithium grease	Stable at 120 ℃	Pure grease failed above 80 ℃	CoF ↓35 %, wear depth ↓76 %
Mn_3O_4-graphene [94]	G-III oil	Stable	Single-phase phases are less effective	Wear depth ↓50 %, area ↓64 %
g-C_3N_4/rGO [95]	poly-alpha-olefin (PAO)-10 base oil	>3 days	Single-phase phases are less effective	CoF ↓62.3 %, wear volume ↓96 %
Ag/graphene [96]	Paraffin liquid	>60 days	Ag or graphene alone is less effective	CoF ↓40 %, wear volume ↓36.4 %

Nanocomposites enhance dispersion stability through a combination of physical hindrance, interfacial chemical modification, and synergistic structural design. Stable dispersion ensures sustained delivery of active components to the contact interface, enabling continuous tribofilm formation, defect healing, and rolling effects. While substantial progress has been made, there remains a need for standardized stability evaluation protocols, including accelerated sedimentation tests and long-term particle-size monitoring, to facilitate cross-study comparisons and accelerate industrial adoption.

Beyond static dispersion, long-term stability under dynamic conditions such as shear cycling and temperature fluctuations has become an increasingly critical parameter for assessing real-world applicability. Yi et al. [97] reported a sugar-assisted mechanochemical exfoliation approach for boron nitride nanosheets, which demonstrated that covalent grafting of sucrose molecules can maintain ultrastable dispersion for over 28 days and sustain ultralow friction (CoF≈0.001) even under continuous sliding. This finding highlights the importance of chemical anchoring and hydration-layer stabilization in preventing nanoparticle aggregation and structural degradation during prolonged operation. Nevertheless, comprehensive evaluation under combined mechanical and thermal stresses remains limited, and developing nanocomposites with robust long-term structural integrity and performance retention continues to be a key challenge for their industrial implementation.

2.5. Advantages of nanocomposites vs. surface functionalization

Nanoparticles have been extensively explored as lubricant additives owing to their ability to reduce friction, mitigate wear, and promote the formation of protective tribofilms. However, their practical efficacy is strongly dependent on stability within the lubricant medium and on their interactions with sliding interfaces. To address these issues, two main approaches have been pursued: surface functionalization, which modifies NPs at the molecular level to improve their interfacial affinity and stability, and nanocomposite design, which integrates multiple components into a hybrid structure to exploit synergistic physical and chemical effects. A comparison of these two strategies reveals not only distinct pathways to enhanced performance but also opportunities for their combination.

Surface functionalization represents one of the most widely adopted methods for improving the tribological properties of NPs. Kumara et al. [98] synthesized thiol-modified Ag NPs using 4-(tert-butyl)benzylthiol (TBBT) and dodecanethiol (C12) ligands, achieving stable dispersion in PAO oil and demonstrating reductions in both friction (up to 35%) and wear (up to 85%), which were attributed to the formation of a silver-rich tribofilm with ligand-controlled adsorption. Building on this concept, Wang et al. [99] reported oleylamine-modified Fe_3O_4 NPs that remained dispersed in mineral oil for over 12 months, with an optimal loading of 5 wt%, reducing wear volume by 93.8%

through micro-bearing effects and the formation of protective oxide layers. Further studies have shown that particle morphology can modulate the effect of functionalization: Wang and Ye [100] found that oleic-acid-modified Fe_3O_4 nanospheres exhibited superior dispersion and tribological behavior compared with nanowires and nanosheets, highlighting the combined roles of rolling, self-healing, and interlayer sliding in wear reduction. In aqueous lubricants, Gong et al. [101] demonstrated that sodium-oleate-functionalized *h*-BN nanosheets exhibited excellent dispersion stability and significantly lowered the CoF to 0.077, with the improvement linked to enhanced compatibility and the formation of continuous lubricating films. Taken together, these studies confirm that surface functionalization provides a versatile and scalable route to performance improvement by optimizing dispersion, interfacial adsorption, and morphology-dependent lubrication mechanisms.

Nanocomposite strategies, in contrast, are designed to combine complementary properties into a single additive, thereby enabling multifunctional lubrication effects. Zhang et al. [102] prepared Ag@polydopamine (PDA) core-shell NPs, where the PDA layer imparted electrostatic repulsion and stable dispersion, resulting in an 18.7% reduction in friction and negligible wear at low concentrations. Similarly, Ghasemy-Piranloo et al. [103] developed Fe_3O_4/TiO_2 core-shell structures that mitigated magnetic agglomeration and reduced wear volume by 44.5% through a synergistic combination of hard-shell support and tribo-chemical film formation. Dong et al. [104] demonstrated that BPQDs@SiO_2 nanocomposites achieved wear reductions of 83.0% in aqueous lubricants by coupling the polishing effect of SiO_2 with the extreme-pressure resistance of BPQDs. More recently, Ao et al. [105] reported carbon-silver microspheres that remained dispersed for several days and decreased wear by 88%, with tribological performance arising from the ability of the Ag shell to form protective layers under frictional heat and the role of the carbon core in defect filling. Advanced designs such as molybdenum disulfide quantum-dot/graphene crumpled balls (MGCB) [106] have further demonstrated long-term stability and superior high-temperature performance compared with conventional additives, underscoring the potential of composite structures to deliver robust lubrication under demanding conditions. Collectively, these examples show that nanocomposites not only address dispersion challenges but also provide structural and chemical synergies that extend functionality beyond what can be achieved by functionalization alone. However, their practical deployment is often limited by challenges such as complex and costly synthesis routes, sensitivity to reaction conditions, and difficulties in precisely controlling parameters like shell thickness in core-shell systems, which remain critical barriers to scalability and industrial translation.

Recent research has also highlighted the benefits of integrating functionalization within nanocomposite architectures, thereby combining molecular-level stabilization with structural synergy. Jia et al. [107] fabricated SiO_2-PDA@Ag nanospheres that exhibited both improved dispersion and enhanced load-bearing capacity, resulting in significant reductions in friction and wear. Li et al. [108] reported that the GO@pPTFE hybrid material exhibits superhydrophilicity and excellent water dispersibility, and can reduce friction and wear by more than 60% due to the complementary effect of the low shear force of PTFE and the mechanical reinforcement of GO. Xu et al. [109] developed BP/Fe_3O_4-PDA nanocomposites that delivered friction reductions exceeding 55% by combining the interlayer sliding of BP, the rolling of Fe_3O_4, and the self-healing capacity of PDA. Other examples, such as citric acid-modified 3D porous graphene/carbon black (CC) composites [110] and surface-carbonated BN nanosheets [111], further demonstrate that dual approaches can yield long-term stability and superior tribological outcomes. These studies emphasize that hybrid strategies can overcome the limitations of either method when applied alone.

Overall, both surface functionalization and nanocomposite design have been demonstrated as effective strategies to enhance the tribological performance of NPs in lubricants. Functionalization primarily improves compatibility with the base oil and promotes stable adsorption films, offering a direct and relatively cost-effective route to improving performance. In contrast, nanocomposite design provides additional benefits through synergistic structural effects, such as core-shell protection, rolling lubrication, and tribo-chemical film formation, thereby achieving superior robustness under complex conditions. In some cases, a combination of both approaches further reinforces dispersion stability and durability, particularly under severe operating environments. To provide a clearer comparison of these strategies, **Table 2** summarizes representative examples in terms of dispersion stability, tribological performance, and underlying mechanisms. The emerging trend of integrating functionalization with nanocomposite design highlights a promising pathway toward next-generation lubricant additives, where both molecular-scale tuning and structural engineering are leveraged to achieve durable friction and wear reduction.

Table 2 Representative examples of surface functionalization and nanocomposite strategies for lubricant additives.

Additive	Media	Surface functionalization reagents	Stability	Key tribological improvements
Surface Functionalization				
Ag [98]	PAO base oil	TBBT and C12	Stable in PAO	CoF ↓35%, wear ↓85%.
h-BN [101]	Water-based fluid	Sodium oleate	7 days	CoF:0.077 at 0.05 wt%; roughness ↓88%.
Fe_3O_4 [99]	Mineral oil (150 N)	Oleylamine	12 months	Wear ↓93.8% at 5 wt%
Fe_3O_4 NPs (nanospheres, nanowires, nanosheets) [100]	Liquid paraffin	Oleic acid	Nanospheres dispersed best; nanowires agglomerated	CoF ↓~42%, wear ↓86.88%-91%
Nanocomposites				
TiN@SiO_2-RC (SiO_2-	85W90 gear oil	\	20 days	CoF ↓14.6%, wear

coated TiN NPs) [112]				↓23.2% at 0.4 wt%
MGCB [106]	PAG base oil	\	12 months	CoF ↓47%, wear ↓30% at 0.05 wt% (vs. tricresyl phosphate)
Fe_3O_4/TiO_2 core-shell composites [103]	Base oil	\	8 h	CoF ↓7.8%, wear ↓44%.
C@Ag core-shell microspheres [105]	G1830 ester base oil	\	5 days	CoF ↓15.5%, wear ↓88% at 0.5 wt%
BPQDs@SiO_2 core-shell materials [104]	Ultrapure water	\	7 days	CoF ↓46%, wear ↓83% at 0.05 wt%
Ag@PDA core-shell NPs [102]	PAO6 base oil	\	20 days	CoF ↓18.7%; negligible wear at 0.25 wt%
Nanocomposites & Surface Functionalization				
GO@pPTFE core-shell nanohybrids [108]	Water (hydro-based lubricant)	P(MMA-GMA-AM-St)	Ultra-hydrophilic, dispersed instantly in water.	CoF ↓69%, wear ↓62% at 0.05 wt%
SiO_2-PDA@Ag core-shell nanospheres [107]	PAO base oil and SiO_2-based shear thickening fluids	PDA	Dispersed in PAO without agglomeration	CoF ↓44%, wear ↓95% at 3 wt%
CC composites [110]	Castor oil	Citric acid	6 months.	CoF ↓25-33%, wear ↓57-70% at 0.2 wt%
Surface-carbonated boron nitride nanosheets (C-HPC-BNNSs) [111]	Water-glycol solution	Hydroxypropyl cellulose (HPC)	>30 days.	CoF ↓52%, wear ↓85% at 0.5 wt%
BP/Fe_3O_4-PDA [109]	Soybean oil and grease	PDA	15 days	CoF ↓55-64% in oil/grease at 0.12-0.15 wt%

2.6. Advantages compared with traditional additives

Traditional additives such as zinc dialkyldithiophosphate (ZDDP) and molybdenum dithiocarbamate (MoDTC) have long been employed in lubricants due to their ability to form protective tribofilms and reduce wear. However, the drawbacks of these traditional additives cannot be ignored. For ZDPP, its sulfur, phosphorus, and zinc components can deposit oxides and inorganic salts on catalysts and particulate filters, polluting exhaust gas post-treatment systems. In addition, ZDDP tends to increase friction under mixed lubrication by forming a rough pad-like friction film, reduce break-in by maintaining the peak roughness, and intensify abrasive corrosion wear when interacting with smoke or dispersants [113]. While MoDTC has limited high-temperature stability, short service life, easy precipitation formation, and high cost [114]. These limitations have prompted people to explore hybrid additives based on nanomaterials as supplements or alternatives to ZDDP and MoDTC.

Some research work highlights the synergistic effect between NPs and ZDDP or MoDTC. Lei et al. [115] demonstrated that oleylamine-modified CeO_2 NPs combined with ZDDP produced an exceptionally thick nanocomposite tribofilm (≈2 μm) containing $CePO_4$, which reduced WSD by 56.8% and increased load capacity to 1700 N, outperforming the individual additives. Mittal et al. [116] showed that tert-butoxy-functionalized *h*-BN nanosheets synergized with ZDDP to provide up to 91% wear reduction on Al-Si alloys, overcoming the shortcomings of both ZDDP alone and ZDDP+MoDTC. Segu and Kim [117] reported that ZrO_2/MoDTC composites reduced friction by over 70% compared with base oil, as ZrO_2 acted as micro-bearings while MoDTC supplied low-shear MoS_2 tribofilms. Similarly, Zhang and Li [118] found that graphene combined with MoDTC maintained low-friction tribofilms while enhancing wear resistance, particularly at elevated temperatures. Environmentally friendly approaches have also been reported: Zhang et al. [119] synthesized ZnO-based ZODDP NPs, which reduced sulfur and phosphorus contents by ~80% relative to ZDDP while achieving superior anti-wear performance in Al contacts. Wang et al. [120] further showed that combining organic molybdenums with ZDDP generated composite tribofilms containing MoS_2 and phosphates, reducing friction and wear while lowering sulfur/phosphorus dependency.

Beyond improving ZDDP and MoDTC, recent research has attempted to replace them altogether. Maurya et al. [121] evaluated hybrid ILs-NPs systems (*h*-BN or ZnO) in PAO oil, directly comparing them with ZDDP. These hybrids outperformed ZDDP in both friction reduction (30% vs. 20%) and wear reduction (57% vs. 25%), and enhanced extreme pressure resistance by 65-75%. Importantly, they contained only half the phosphorus and no sulfur, thus addressing the environmental drawbacks of ZDDP. The superior performance arose from dual mechanisms: ILs contributed chemical protection by forming phosphate-based tribofilms, while NPs provided physical reinforcement through tribosintering and regenerative sacrificial layers.

In summary, while ZDDP and MoDTC remain the most widely used additives in commercial lubricants, their inherent drawbacks in terms of environmental compatibility and tribological performance highlight the necessity for improved or alternative solutions. Nanomaterial-based hybrids not only enhance the efficiency of traditional additives by combining rapid film formation with mechanical reinforcement, but also open avenues for sulfur- and phosphorus-free systems that address regulatory challenges. To provide a clearer overview of these comparative advantages, **Table 3** summarizes representative results of ZDDP, MoDTC, and nanocomposite-based additives in terms of dispersion stability, tribological performance, and key mechanisms, thereby offering a quantitative context for evaluating their practical applicability.

Table 3 Summary of dispersion stability and tribological performance of ZDDP, MoDTC, and nanocomposite lubricant additives.

Additive	Media	Test condition	Key tribological improvements
ZDDP [122]	PAO4	load: 392 N; temperature: 75±2 °C; speed:1200 rpm	CoF ↓10%, wear lower than pure PAO4
MoDTC [122]			CoF ↓60%, wear lower than pure PAO4

ZDDP/MoDTC [122]			CoF ↓25%, wear ↓50%
ZODDP (modified ZnO NPs) [119]	Diisooctyl sebacate	Load: 2 N; frequency: 2 Hz; time: 30 min; temperature: RT; steel-aluminum contacts.	CoF ↓10.37%, wear ↓71.74% (vs. ZDDP)
MODE/MGMO (sulfur- and phosphorus-free organic molybdenums)+ZDDP [120]	PAO6	Concentration: 0.75 wt% (optimal ratio 1:2); load: 100-500 N; speed: 1450 rpm; time: 30 min.	CoF ↓31.6%, WSD ↓39.3%
ZrO_2/MoDTC composite [117]	Mineral base oil (BO)	Mass ratio 1:2; concentration: 0.25-0.75 wt%; load: 14-92 N; speed: 0.08-0.3 m/s; steel-steel contacts.	CoF ↓71.64% (vs BO), 67.80% (vs ZrO_2 alone), 47.22% (vs MoDTC alone); wear ↓75.36% at 0.5 wt%
CeO_2 NPs+ZDDP [115]	PAO6	Four-ball tester: 1200 rpm, 392 N, 75 ℃, 60 min; P_B test: 1770 rpm, 25 ℃, 10 s.	P_B ↑, CoF stable at ~0.06; load-carrying capacity up to 1700 N
h-BN-TBO (tert-butoxy-functionalized *h*-BN)+ZDDP [116]	MAK 65 base oil	Temperature: 110 ℃; contact pressure: 0.43-0.64 GPa; sliding time: 90 min; Al-Si alloy	CoF ↓~42%; wear volume ↓91% (Al matrix) and 86% (Si phase)

Sections 2.1-2.6 show that nanocomposite strategies deliver system-level gains beyond single-component additives. The controllable multi-component structure (such as core-shell structure, heterostructure, layered mixture) enhances physical and chemical activity, thermal stability, and corrosion resistance, while improving key dispersibility properties. Meanwhile, surface functionalization offers a cost-effective route to improve compatibility with base oils and to promote durable adsorption films; when combined with nanocomposite design, a dual stabilization effect emerges that further strengthens performance and longevity. The comparative evidence with ZDDP/MoDTC indicates that nanomaterial-based hybrids can match or surpass commercial additives while mitigating sulfur- and phosphorus-related constraints. As the application scope of

nanocomposites in lubricants continues to expand, the development of diverse synthesis methods has become essential to realize these multifunctional systems in practice.

3. Synthesis methods of nanocomposites

Nanocomposites, which integrate the advantageous properties of disparate materials, demonstrate broad application prospects in catalysis, electronics, energy, environmental remediation, and biomedicine. Compared to conventional single-component nanomaterials, composites achieve multifunctionality through synergistic effects, meeting operational demands under diverse conditions. The selection of synthesis methods critically determines the structural characteristics, performance metrics, and application efficacy of the nanocomposite. This section reviews common synthesis techniques, analyzes their merits and limitations, and provides theoretical guidance for practical implementations.

3.1. Hydrothermal synthesis

Hydrothermal synthesis is a widely adopted method for fabricating nanocomposites through reactions of precursors in sealed autoclaves under elevated temperatures and pressures, typically using water or organic solvents as media. This approach enables precise control over particle size, morphology, and crystallinity by adjusting temperature, reaction duration, and solvent composition [123, 124]. Due to its aqueous solvent system, the method is considered environmentally benign and cost-effective, and it is particularly suitable for the preparation of nanocomposites [125]. The technique offers high purity, uniformity, and structural tunability, making it a versatile strategy for producing functional composites across various application fields [126, 127]. In recent years, hydrothermal synthesis has been increasingly applied to the preparation of nanocomposites for lubrication purposes. Its mild reaction conditions, high controllability, and ability to integrate multiple functional components make it well-suited for tailoring tribological performance.

One representative class of materials is carbon-based nanocomposites, which particularly benefit from the capacity of the method to integrate carbonaceous structures with layered or fibrous substrates, yielding stable tribofilms under load. Zhang and Chang [128] prepared a hydrothermal amorphous carbon-coated nano-magnesium silicate hydroxide core-shell structure (MSH@C) by the hydrothermal method, which improved the anti-wear rate by 75.43% compared to pure MSH. The synergistic effect stems from MSH transporting carbon layers and friction-induced structural rearrangement, enhancing tribological performance. MSH/graphene hybrids fabricated similarly exhibited near-zero wear under contact pressures up to 3.91 GPa, where graphene provided mechanical reinforcement and MSH contributed to a self-repairing tribofilm [129]. Hydrothermal has also been applied to prepare biochar nanocomposites derived from renewable materials. Mou et al. [130] synthesized carbon polymer dots (CPDs-c) from renewable sugar sources in green solvents via a hydrothermal route. CPDs-c showed excellent dispersion stability in PEG200 for over 6 months, and 0.12 wt% CPDs-c reduced the CoF by 47.6% and wear volume by 50.7% due to the synergistic effect of interfacial adsorption of polymeric shells, nano-lubrication of carbon cores, and formation of tribofilm. These examples show that hydrothermal processing enables carbon to be uniformly anchored onto functional substrates, enhancing both load-bearing capacity and interfacial stability during operation.

MoS_2-based composites also gain significant advantages from hydrothermal assembly, which allows nanosheets to be integrated with 2D carbides or silicate frameworks for synergistic lubrication. Liu et al. [131] prepared multilayer $Ti_3C_2T_x$@MoS_2 composites via hydrothermal growth of MoS_2 nanosheets on $Ti_3C_2T_x$, followed by deposition as solid lubrication coatings on silicon substrates (**Fig. 9(a)**). Compared with individual $Ti_3C_2T_x$, MoS_2, and their mechanical mixtures, the composite coatings reduced CoF by 75 %, 69 %, and 58 %, respectively, and exhibited superior wear resistance, attributed to the synergistic lubrication of $Ti_3C_2T_x$ and MoS_2. Guan et al. [132] synthesized MSH-MoS_2 nanocomposites through a two-stage hydrothermal method (**Fig. 9(b)**) and applied them as additives in PAO. The composites outperformed PAO, PAO-MSH, and PAO-MoS_2, with a 27.7 % reduction in friction and a 37.4 % reduction in wear, and they also exhibited surface repair capabilities during operation. These findings underline the ability of the hydrothermal method to engineer interfaces that preserve dispersion stability and facilitate continuous tribofilm regeneration.

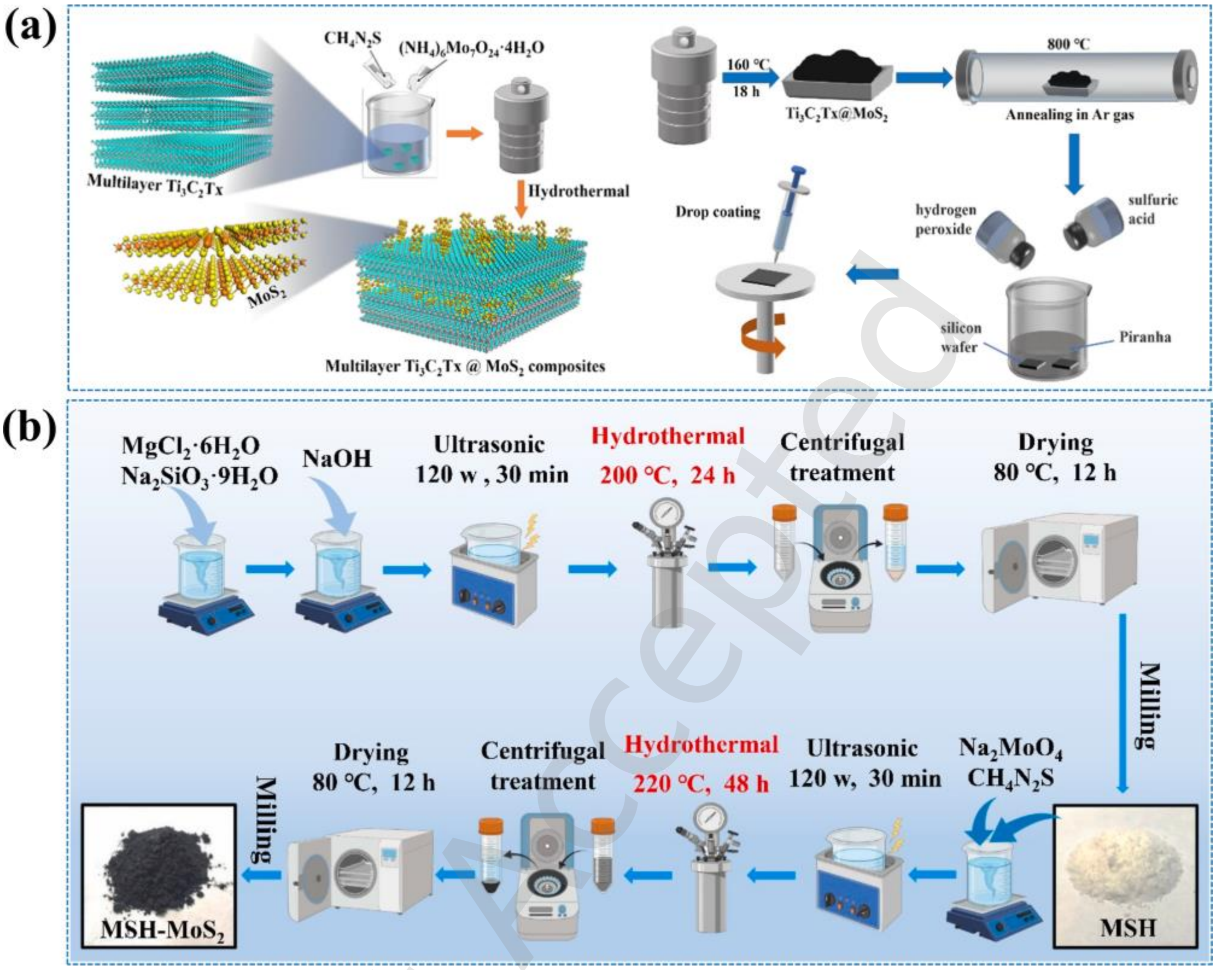

Fig. 9 (a) Schematic illustration of the synthesis of multilayer $Ti_3C_2T_x@MoS_2$ composites and $Ti_3C_2T_x@MoS_2$ solid lubrication coating[131], © Elsevier B.V. 2024; (b) Schematic of the fabrication route of $MSH-MoS_2$ powders. Reproduced with permission from Ref.[132], © Elsevier B.V. 2022.

Ceramic-based nanocomposites, valued for their hardness and thermal stability, also benefit from hydrothermal integration with carbonaceous or layered phases to improve lubrication under extreme conditions. Xiong et al. [133] employed hydrothermal stirring to synthesize nano-BN/Si and BN/Al_2O_3 composites using BN, Si, and Al_2O_3 as raw materials, with PEG and dodecyl alcohol ester as dispersants; these composites reduced the CoF to a minimum of 0.0652 and significantly decreased wear via a synergistic effect where layered BN provided sliding lubrication and Si/Al_2O_3

particles promoted the formation of a protective film containing BN, Si, Al_2O_3, and Fe_2O_3. In another approach, Zhao et al. [134] used a hydrothermal method to in-situ grow TiO_2 NPs (4-9 nm) on rGO sheets, achieving a 28.4% reduction in average CoF and 70.7% reduction in wear volume at 0.08 wt% concentration, with synergistic effects from the protective tribofilm of rGO and nano-bearing action of TiO_2. Meng et al. [135] prepared the BN coated with a carbon layer by a novel hydrothermal coating method, which at 0.2 wt% reduced the CoF by 19% and WSD by 22%, maintaining performance even after 5 days of storage through synergistic lamellar sliding of BN and tribofilm formation by the carbon layer. These examples highlight hydrothermal synthesis as an effective means of constructing ceramic-based hybrids with enhanced mechanical durability and interface compatibility.

Overall, the hydrothermal method not only enables the integration of diverse material components but also allows precise control of their microstructure. The resulting composites exhibit stable dispersion, sustained tribofilm formation, and notable reductions in friction and wear across a range of lubrication environments. Nevertheless, some limitations remain, including the need for high-pressure reactors, relatively long reaction durations, and scalability constraints due to reactor volume. Addressing these challenges will be essential for broader industrial adoption of this technique, such as by developing continuous-flow hydrothermal systems or optimizing reaction efficiency.

3.2. Sol-Gel synthesis

Sol-gel synthesis, a wet-chemical method, fabricates metal oxide composites through hydrolysis and polycondensation of organometallic precursors, followed by gelation and calcination [136-138]. This technique offers exceptional control over size, morphology, and chemical composition [139], with scalability for both laboratory and industrial production [140, 141]. The resulting composites exhibit enhanced optical, electrochemical, and magnetic properties [142, 143]. Beyond metal oxides, sol-gel methods enable the fabrication of fluorescent composites and ceramic coatings[144, 145]. Ge et al. [145] developed red-emissive Cu nanocluster composites in one-pot syntheses, and Sang et al. [146]

produced SiO_2-B_2O_3-Li_2O-ZnO-Al_2O_3 glass-ceramic coatings on diamonds, addressing wettability issues and enhancing flexural strength. Haldorai et al. [147] developed a simple sol-gel-assisted synthesis method for the preparation of CuO NPs dispersed on reduced graphene oxide (rGO) composites to achieve sunlight-assisted removal of methylene blue dye and nanofluid applications (**Fig. 10**).

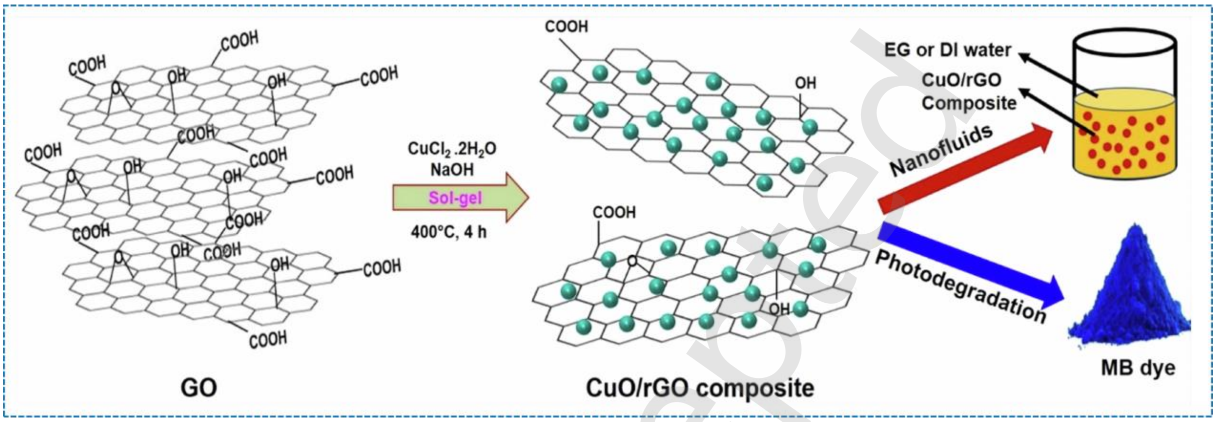

Fig. 10 Schematic representation of the synthesis of CuO/rGO composite. Reproduced with permission from Ref.[147], © Springer 2024.

As a low-temperature wet-chemical synthesis technique, the sol-gel method has demonstrated distinctive advantages in the preparation of nanocomposites, particularly within the domain of lubricating additives. Wang et al. [148] prepared multi-layer graphene/silicon dioxide composite coatings via the sol-gel method, where SiO_2 NPs were uniformly grafted on multi-layer graphene surfaces (**Fig. 11**); these coatings exhibited tribological properties with average CoF first decreasing (to 0.3663 at 600 °C) then increasing in 400-800 °C, and the lubrication mechanism involved low interlayer shear of MLG, ball-bearing effect of SiO_2, and protection from tribo-chemical reaction films. Zhang et al. [149] synthesized water-soluble Cu/SiO_2 nanocomposites via a sol-gel method. As a water-based additive, 1.0 wt% of it increased P_B to 108 N (vs. <88 N for pure water), P_D (welding load) to 3875 N (vs. 1190 N), reduced WSD from 0.702 mm to 0.440 mm at 50 N, and enhanced load-carrying capacity to 300 N, via Cu NP filling micro-pits and forming a protective film with Cu, FeS, $FeSO_4$, and SiO_2. Further, López et al. [150] synthesized functionalized SiO_2 NPs via the sol-gel method. Functionalized improved the stability of SiO_2 NPs, while reducing friction by up to 40%, via protective hydrophobic buffers, rolling action, and surface asperity filling. This work highlighted the direct correlation between SiO_2 surface functionalization and lubrication performance. Bokov et al. [140] reviewed the application of the sol-gel method in the synthesis of nanomaterials and pointed out that due to its mild synthesis conditions and low cost, the sol-gel method has great potential for industrial applications, especially in the synthesis of metal oxides, composite carbon materials, and electrolyte systems.

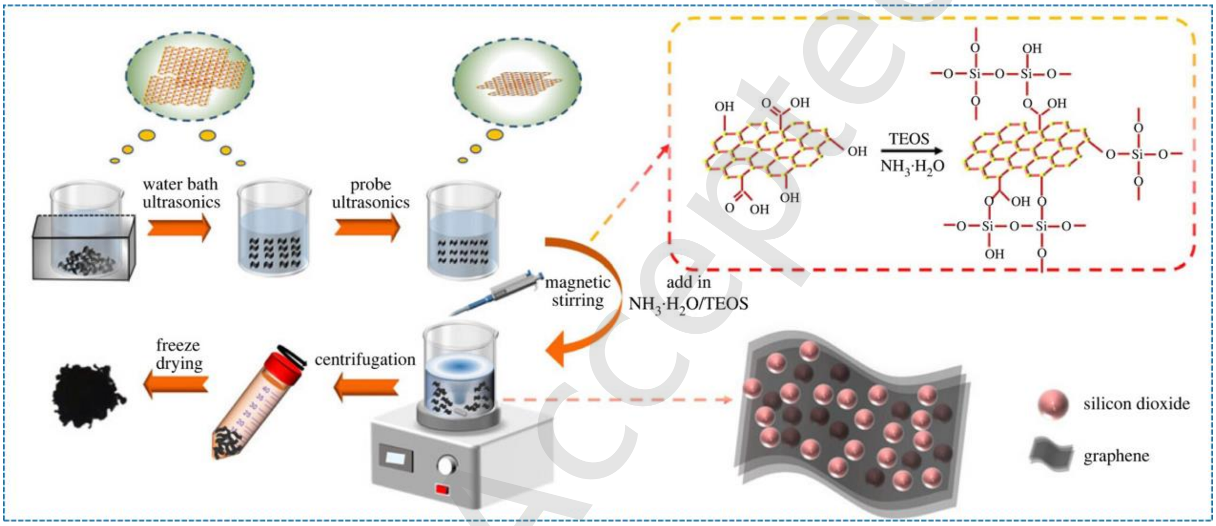

Fig. 11 The scheme of the preparation process of multi-layer graphene/silicon dioxide composites. Reproduced with permission from Ref.[148], © Royal Society of Chemistry 2023.

Although the sol-gel method has the advantages of a simple process, controllable composition, and low-temperature reaction in the preparation of nanocomposites, research in recent years has gradually revealed some limitations of this method in the field of lubricant application. Firstly, the sol-gel method has the problems of solvent residue and particle agglomeration in the process of preparing a nanocomposite. Although the sol-gel method can produce a uniform nanocomposite, the residual solvent may affect the purity of the materials during high-temperature drying [151, 152]. In addition, the composite is prone to particle aggregation during heat treatment, which affects its dispersion. In summary, although the sol-gel method has certain advantages in the preparation of lubricating nanomaterials, it still faces challenges in crystallization control, scale-up, and interface stability. Future development needs to further improve the practicability and reliability of this method through auxiliary modification, the introduction of interfacial agents, and fine control of reaction parameters.

3.3. Co-precipitation method

As an economical, efficient, easy-to-operate, and scalable wet chemical synthesis technique, the coprecipitation method offers a core advantage: it enables the synchronous precipitation and atomic-level uniform mixing of multi-component metal ions by precisely regulating key parameters of the reaction system, such as pH, temperature, and concentration, thereby allowing precise control over the chemical composition and phase structure of the products. This method features a simple operation process and low equipment requirements, making it highly promising for large-scale industrial production. Additionally, its excellent ability to adjust the compositional uniformity of multi-component composite systems renders it an ideal choice for constructing composite nanostructures in lubricating additives. Process measures such as introducing surfactants and optimizing the feeding method can further tailor the particle size, morphology, and dispersibility of NPs to meet the special requirements for the interfacial properties of nanomaterials in the lubrication field.

In practical research, numerous scholars have used this method to prepare a series of nanocomposites with excellent properties, which have been successfully applied in lubricating oil systems.

Yang et al. [153] prepared Fe_3O_4@PEG core-shell nanocomposites via co-precipitation (**Fig. 12(a)**), which contained 1.0 wt% in aqueous glycerol, reduced the CoF by 41.4% and wear volume by 24.1%. TEM images show Fe as the nucleus, which is wrapped in PEG (**Fig. 12(b)**), where PEG improved dispersion and the core-shell structure formed boundary lubricating films, with Fe_3O_4 acting as micro-bearings. Zhang et al. [154] fabricated Fe_3O_4@CNTs via co-precipitation (**Fig. 12(c, d)**); 0.5 vol% nanofluids on textured TiC ceramics reduced contact angle by 29.17%, CoF by 44.69%, and flashpoint temperature by 48.28%, with synergistic effects of nanofluids and micro-textures enhancing wettability, lubricating film formation, and heat dissipation. Xiang et al. [155] synthesized Ni-Fe layered double hydroxide (LDH) nanosheets via room-temperature co-precipitation; 0.3 mg/mL Ni-Fe LDH (Ni/Fe=6) in GTL base oil reduced the average CoF by 51.3%, wear volume by 78.4%, with a lubrication mechanism involving initial physical adsorption films transforming into tribo-chemical films containing iron oxides and NiO. Lawal et al. [156] developed nano-Al_2O_3-based gear oil from lube oil effluent via co-precipitation with oleic acid modification; 0.4 wt% Al_2O_3 improved anti-wear property by 26.14% through forming tribo-films, enhancing thermal stability and lubrication performance. These research achievements highlight the unique advantages of the coprecipitation method in regulating particle structure and interfacial functions, enhancing dispersion stability, and improving tribological properties, providing a theoretical foundation and practical pathway for the green preparation of high-performance lubricating materials.

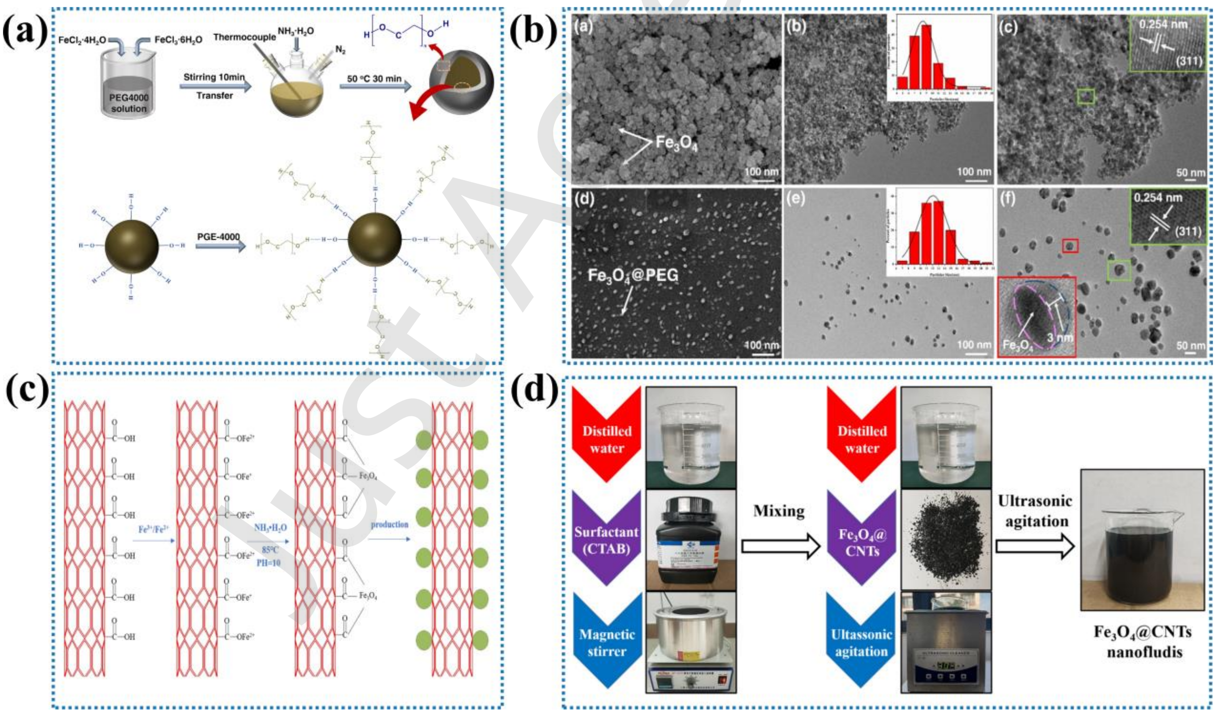

Fig. 12 (a) Schematic diagram of the synthesis method of Fe_3O_4@PEG core-shell nanospheres. SEM images of Fe_3O_4 and Fe_3O_4@PEG nanospheres; (b) TEM images of Fe_3O_4 and Fe_3O_4@PEG nanospheres. Reproduced with permission from Ref.[153], © Springer 2022; (c) Schematic of Fe_3O_4@CNTs magnetic composites prepared by co-precipitation method; (d) A double-step method

for the preparation of Fe_3O_4@CNTs based nanofluids. Reproduced with permission from Ref.[154], © Springer 2022.

However, recent studies have revealed several limitations of the coprecipitation method in material structure regulation and performance enhancement. Dipping et al. [157] review the synthesis methods and applications of MFe_2O_4 (M=Co, Cu, Mn, Ni, Zn) NPs, found that the MFe_2O_4-type composites prepared by co-precipitation are prone to aggregation, non-uniform particle size distribution, and difficulty in obtaining a single-phase structure, thus limiting further improvements in their magnetic properties. Sobhani et al. [158] synthesized $CuMn_2O_4$/CuMnO composites and found that the coprecipitation process is often accompanied by problems such as impurity phase formation and difficult crystal structure control, affecting the electrocatalytic stability of the material. Patil et al. [159] emphasized in their review that although the coprecipitation method is suitable for doping and compositing metal oxides, it has insufficient control over morphology and nucleation rate, especially in complex reaction systems, where multi-phase coexistence and aggregation are prone to occur. In addition, Mirkazemi et al. [160] compared $CoFe_2O_4$ composites synthesized by the coprecipitation method and the solvothermal method, and found that the former (co-precipitation) produced larger particle sizes, lower specific surface areas, and poorer dispersion, resulting in inferior energy storage and sensing application performance compared to the latter (solvothermal method). These studies indicate that while the coprecipitation method has cost and operational advantages, it still faces challenges in structural uniformity, dispersibility control, and impurity phase suppression. Future improvements in its comprehensive performance can be achieved by introducing surface modifiers or coupling with other techniques. In summary, the method still has technical bottlenecks in controlling the uniformity, crystal stability, structural regulation, and precise compositional design of the nanocomposite, requiring further advancements through auxiliary technologies or optimization strategies.

In conclusion, the coprecipitation method, with its advantages of controllable composition, tunable structure, and large-scale production, holds irreplaceable technical value in the field of lubricating additives, particularly in constructing multiphase synergistic systems such as metal oxides/graphene. Despite challenges in compositional regulation and dispersibility control, its application potential continues to be unlocked through process optimization and technical coupling, providing a solid technical pathway for the design of high-performance lubricating materials and driving the lubrication field toward the goals of low friction, long service life, and environmental friendliness.

3.4. Chemical deposition method

As a highly controllable synthesis strategy for constructing structurally ordered composites, the chemical deposition method is widely used due to its ability to generate films or nanomaterials on substrate surfaces through chemical reactions. This method includes forms such as chemical vapor deposition, electrochemical deposition, and solution chemical deposition, offering advantages like dense film layers, uniform composition, and strong, particularly suitable for preparing nanocomposites with uniform structures and excellent interfacial properties in lubrication systems. By flexibly adjusting reaction parameters such as temperature, pressure, and reaction time, chemical deposition holds significant application value in constructing high-performance functional materials for lubricants.

In recent years, researchers have successfully used chemical deposition to prepare various nanocomposites for lubrication systems. Wu et al. [161] prepared ZnO@SiO_2 core-shell NPs via chemical deposition (**Fig. 13(a)**), which exhibited better dispersibility than physically mixed particles, benefiting from the solid-liquid composite film formed by long-chain molecule adsorption on the SiO_2 shell. Adding 1 wt% ZnO@SiO_2 reduced the CoF of lithium-based grease by 11.5% and the wear amount by 25%. Subsequently, Wu et al. [162] further prepared two core-shell structures (ZnO@SiO_2 and SiO_2@ZnO), where ZnO@SiO_2 decreased the CoF by 18% and wear amount by 22% under light load, while SiO_2@ZnO reduced the CoF by 15% and wear amount by 28% under heavy load, demonstrating that core-shell structures enhance lubrication performance through synergistic effects between soft and hard components (**Fig. 13(b)**). Yang et al. [163] synthesized TiO_2@SiO_2 core-shell NPs through chemical deposition. TiO_2 was dispersed in ethanol, coated with silica sol derived from ethyl silicate, and then sintered. These NPs were incorporated into PTFE grease. At a concentration of 1 wt%, the composite reduced the CoF by 13.8% (steel-steel contacts) and 38.2% (Cu-Cu contacts), decreased wear width by 25.3% and wear diameter by 26.2%, and increased contact resistance by 24% to enhance insulation performance. The lubrication mechanism involves the high hardness of SiO_2 improving load-bearing capacity, TiO_2 and SiO_2 forming a protective film (containing CuO) to fill surface pits and reduce direct contact, and the electron-capturing ability of SiO_2 enhancing insulation. Additionally, Fang et al. [164] synthesized SiO_2/SnO_2 nanocomposite via chemical methods, as additives in rapeseed oil, 2.5 wt% of the composites increased P_B from 500 N to 980 N, P_D from 1250 N to 1960 N, reduced WSD from 0.67 mm to 0.35 mm and CoF from 0.071 to 0.065, with the lubrication mechanism involving adsorption/deposition of NPs to form a low-shear boundary layer and tribo-chemical reactions forming SnO_2 films, which repair worn surfaces.

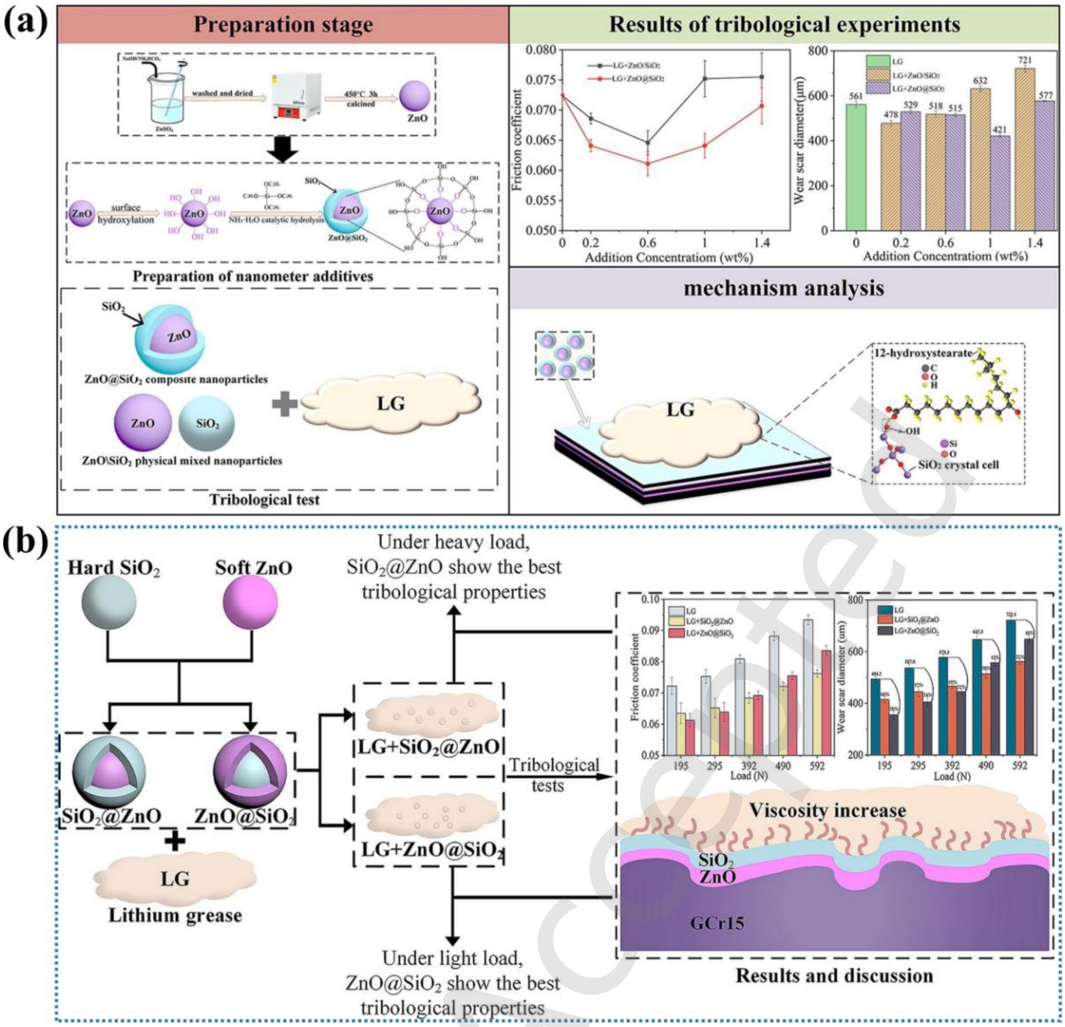

Fig. 13 (a) Schematic diagram of the synthesis, tribological properties, and lubrication mechanism of ZnO@SiO2. Reproduced with permission from Ref.[161], © Elsevier B.V. 2023. (b) Tribological behavior of ZnO@SiO2 and SiO2@ZnO in lithium grease. Reproduced with permission from Ref.[162], © Elsevier B.V. 2024.

However, the chemical deposition method still faces practical challenges. The chemical vapor deposition equipment is expensive and has a narrow reaction window, making it unsuitable for large-scale, low-cost production[165]. Moreover, issues such as uneven deposition, compositional segregation, and film cracking often occur in multi-component systems, limiting long-term stability in high-load lubrication scenarios[163]. Therefore, maintaining microstructural stability and dispersibility while improving preparation efficiency has become a key research direction.

In conclusion, the chemical deposition method, with its excellent structural regulation and film-forming capabilities, demonstrates broad application prospects in lubricating additives. Through technical integration and process optimization, its potential in constructing high-performance composite nano-lubricating materials will be further unlocked, providing solid technical support for the development of low-friction, high-stability, and environmentally friendly lubrication systems.

3.5. Microwave synthesis

Microwave synthesis is a chemical synthesis technique that utilizes microwave irradiation to accelerate reaction kinetics through rapid and uniform volumetric heating. This method enables instantaneous heating of reaction systems, significantly reducing processing time while enhancing synthesis efficiency. The homogeneous thermal profile achieved via microwave penetration ensures consistent internal temperatures, facilitating the preparation of a uniform nanocomposite. A distinctive advantage of microwave synthesis lies in its selective heating capability, where differential microwave absorption by materials induces localized thermal gradients. This property allows preferential activation of highly microwave-responsive components, enabling tailored synthesis of composites with specific architectures and functionalities [166, 167]. By leveraging rapid heating kinetics and spatial energy localization, precise control over nanomaterial growth parameters, including temperature, gas flow rates, and catalytic activity, can be achieved, yielding composites with tunable structural and performance characteristics [168].

Microwave irradiation has been successfully applied in graphene fabrication via microwave-assisted exfoliation and reduction of GO [167, 169]. Furthermore, its utility extends to graphene-based composites. Fu et al. [170] developed a microwave-assisted strategy for synthesizing MoS_2/graphene composites, where ultrafine MoS_2 NPs were uniformly anchored on graphene sheets, endowing the composite with exceptional capacitive performance. Core-shell architectures have also been fabricated using microwave techniques. Sun et al. [171] synthesized CNT@$NiMn_2O_4$ core-shell nanocomposites through microwave-hydrothermal methods, demonstrating low charge-transfer resistance and high specific capacitance. The material exhibited 93.0% capacity retention after 5,000 cycles, with the assembled supercapacitor achieving an energy density of 46.8 Wh·kg^{-1}, highlighting its potential as an advanced energy storage electrode. Sahoo et al. [172] synthesized a g-C_3N_4/rGO/MoS_2 composite via a microwave-assisted method by mixing graphite oxide, MoS_2, and ammonium thiocyanate, followed by microwave irradiation at 700 W for 120s, enabling ultrafast formation of the heterostructure with improved electrocatalytic properties for water splitting (**Fig. 14**).

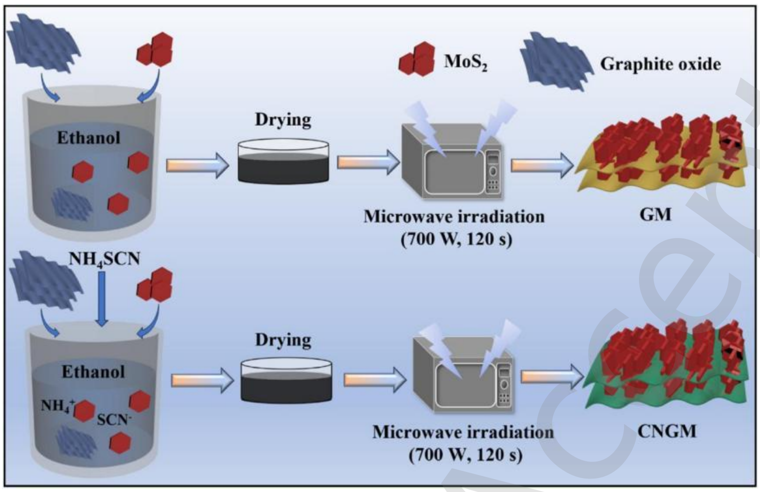

Fig. 14 Schematics of the synthesis processes of rGO/MoS_2 and g-C_3N_4/rGO/MoS_2. Reproduced with permission from Ref.[172], © Elsevier B.V. 2025.

Although the application of microwave synthesis in the field of lubricating additives is still in its infancy, preliminary studies have demonstrated its potential. Microwave synthesis is particularly suitable for preparing nanocomposites with high dispersibility and structural stability required for lubricating additives. Liu et al. [173] Synthesized FeOCl/Zn MOF composites through the microwave-assisted strategy, and successfully introduced them into the PEG200 lubrication system (**Fig. 15**). The results showed that the additive significantly reduced the CoF (48%) and wear diameter (88%), reflecting the optimization effect of the synergistic effect between two-dimensional materials on the interface lubrication behavior.

Jaiswal et al. [174] synthesized TiO_2-reinforced boron-nitrogen co-doped rGO via microwave-assisted method (for doped graphene) and sol-gel method (for TiO_2), followed by composite formation; as additives in paraffin oil at 0.15% w/v, it reduced mean WSD from 0.733 mm to 0.366 mm, CoF from 0.0756 to 0.0564, steady-state wear rate by 67-fold, and increased seizure load from 1078 N to 1470 N, with the mechanism involving in-situ formation of a tribofilm containing boron nitride, adsorbed graphene layers, and tribosintered TiO_2 NPs (acting as nanobearings). Salah et al. [175] combined microwave-synthesized CuO nanosheets with CNT for sunflower oil systems, finding that a 0.05 wt% concentration enabled the NPs to stably suspend for months while reducing the CoF by approximately 43%, demonstrating excellent friction reduction, anti-wear properties, and dispersion stability. Kumar et al. [176] grafted polyacrylamide onto the surface of functionalized GO via microwave-assisted polymerization to prepare FGO-PAM water-based lubricating additives, which achieved a 46-55% reduction in CoF and a 13-37% improvement in anti-wear performance in friction tests. Saxena et al. [177] prepared g-C_3N_4 via urea calcination and g-C_3N_4/MoS_2 nanocomposite through microwave-assisted synthesis, the 9 wt% g-C_3N_4 composite exhibited optimal tribological performance, reducing wear depth (e.g., ~66% lower than uncoated steel) and CoF (lowest at 15 N load), with enhanced wear life, due to synergistic effects: g-C_3N_4 improves adhesion and support, while MoS_2 provides low-shear lubrication, forming a protective tribofilm.

Fig. 15 Schematic diagram of the synthesis of FeOCl/Zn-MOF hybrid. Reproduced with permission from Ref.[173], © Elsevier B.V. 2023.

Although microwave synthesis has advantages in efficient synthesis and performance control, this method still has technical limitations, such as high requirements for reaction equipment and difficulty in achieving uniform nucleation in some multi-component systems. Meng et al. [178] compared the special properties and applications of functional nanomaterials prepared by microwave-assisted hydrothermal method with other methods. Subsequently, it is proposed that in the microwave hydrothermal system, the control of heat conduction and pressure balance is the key to the preparation of high-quality composites, and its future development depends on the upgrading of process equipment and the deepening of mechanism research.

In conclusion, the microwave-assisted synthesis method, characterized by high efficiency, environmental friendliness, and strong tunability, demonstrates great potential in the preparation of lubricating additives. By optimizing reaction parameters and precursor selection, this technology is expected to play a key role in constructing high-performance, environmentally friendly composite nano-lubricating materials in the future, providing a new pathway for the development of high-performance lubrication systems.

3.6. Other methods

In addition to the traditional synthesis methods of nanocomposites mentioned above, researchers have gradually adopted various new or composite synthesis strategies to prepare nanocomposites for lubrication in recent years, to achieve better dispersibility, structural controllability, and lubrication performance.

In situ reduction is a widely used method. Kim et al. [179] proposed an improved liquid-phase reduction method, which significantly reduced the oxidation degree of Cu NPs by adding volatile organic solvents (such as phenylene). The Cu particles in the obtained lubricating oil can reduce the CoF by 60%. Cui et al. [180] first prepared single or few-layer MXene nanosheets by etching Ti_3AlC_2 MAX with a mixed HCl-LiF solution (**Fig. 16(a)**), as additives in 500 SN base oil at 2.4 wt%, they reduced the CoF from 0.572 to 0.108, wear volume by 73.7%, and increased load capacity to 800 N, with the mechanism involving synergistic effects of interlayer sliding (MXene), rolling bearing action (SiO_2), and formation of physical adsorption films and tribo-chemical films (containing TiO_2, Fe_2O_3). Wu et al. [181] synthesized a silver/graphene nanocomposite (SGN) by sulfonating GO first, followed by electrostatic adsorption of Ag ions and in situ reduction (**Fig. 16(b)**). They characterized the SGN and investigated its tribological performance as an aqueous lubricant additive for Si_3N_4/Al_2O_3 tribo-components. The results showed that the SGN significantly improved friction reduction and wear resistance, for example, at 150 rpm and 3 N, it contributed to 52.2% and 54.2% improvement in these aspects, respectively.

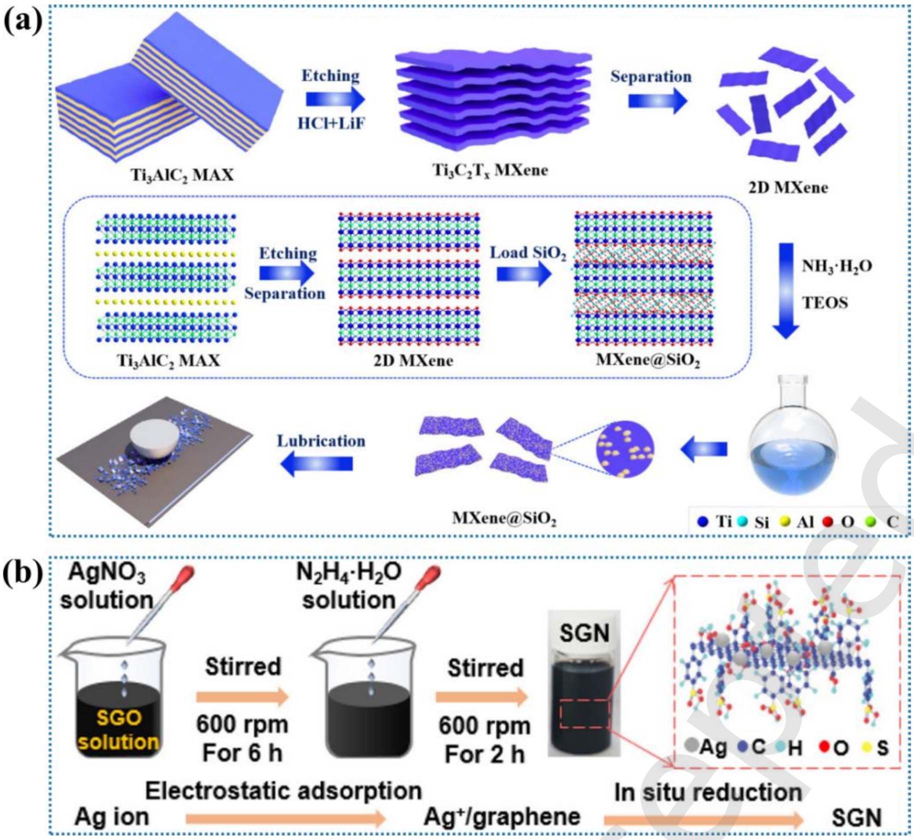

Fig. 16 (a) Schematic diagram of the preparation process of MXene@SiO_2. Reproduced with permission from Ref.[180], © Tsinghua University Press 2024; (b) Preparation procedure of the SGN aqueous solution. Reproduced with permission from Ref.[181], © American Chemical Society 2023.

Self-assembly and supramolecular oil gel strategies are also becoming emerging hot spots. Liang et al. [182] prepared supramolecular oil gels by self-assembly of amphiphilic telechelic polymers ($H_mS_{2n}H_m$) to stabilize 2D nanomaterials (GO, *h*-BN, g-C_3N_4); in PAO-10, *h*-BN@$H_6S_{50}H_6$ composite gel reduced CoF by 48.0%, wear volume by 98.4%, forming 60-90 nm thick tribofilms, with the mechanism relying on gel networks stabilizing nanomaterials and forming composite tribofilms containing Fe oxides and B_2O_3. The composite gel solid lubrication system is more promising. Zhang et al. [183] built a new composite lubrication system for space equipment by combining MoS_2 solid lubrication film with a supramolecular gel. The system still exhibits excellent anti-wear (e.g., from 1.33×10^{-6} to 7.1×10^{-7} $mm^3/N\cdot m$ in vacuum) and creep resistance in extreme environments, significantly extending its lubrication life and demonstrating its potential in high-reliability lubrication systems. Wang et al. [184] prepared gallium-based liquid metal (GLM)-based nano-oleogels by combining alkylthiol self-assembled GLM nanodroplets (C12@GLM) and α-lipoic acid ester-based dynamic covalently linked supramolecular gels (**Fig. 17**). Compared with the base oil, the nano-oleogel GLM@G-0.5 significantly reduced the CoF from 0.216 to 0.108, decreased the wear volume loss by 73.04%, and increased the load-carrying capacity from 50 to 550 N.

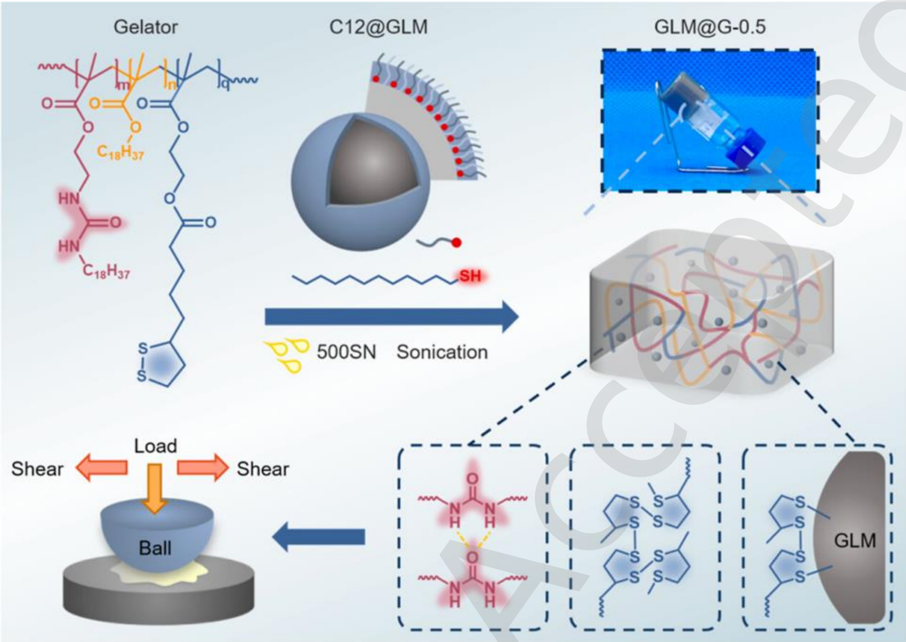

Fig. 17 Preparation process of glm-based nano-oleogels. Reproduced with permission from Ref.[184], © American Chemical Society 2024.

Some researchers have also used the ILs composite method. Wang et al. [185] synthesized dendritic fibrous nano silica (DFNS) via bi-continuous microemulsion polymerization, then prepared DFNS@ILs composites by vacuum impregnation to adsorb ILs; as additives in PAO6, they reduced the CoF by 18% and volume wear rate by 65% compared to pure PAO6, outperforming ZDDP and nano-SiO_2, with the mechanism involving synergistic effects of DFNS (as rolling bearings) and ILs (releasing to form chemical adsorption films) and formation of a protective transfer film. Wang et al. [186] fabricated GLM-based ionic supramolecular oleogels by incorporating ultrasonicated GLM nanodroplets and vinyl-containing ILs into a free radical polymerization system (**Fig. 18**); in PAO10, GLM@IGel-2 reduced the CoF from 0.192 to 0.097 (49.5% reduction) and wear volume from 100.10×10^4 μm^3 to 9.69×10^4 μm^3 (90.3% reduction), with a load capacity of 550 N, via synergistic effects of GLM nanodroplets and gel networks forming a tribo-chemical film containing iron oxides, sulfides, and fluorides.

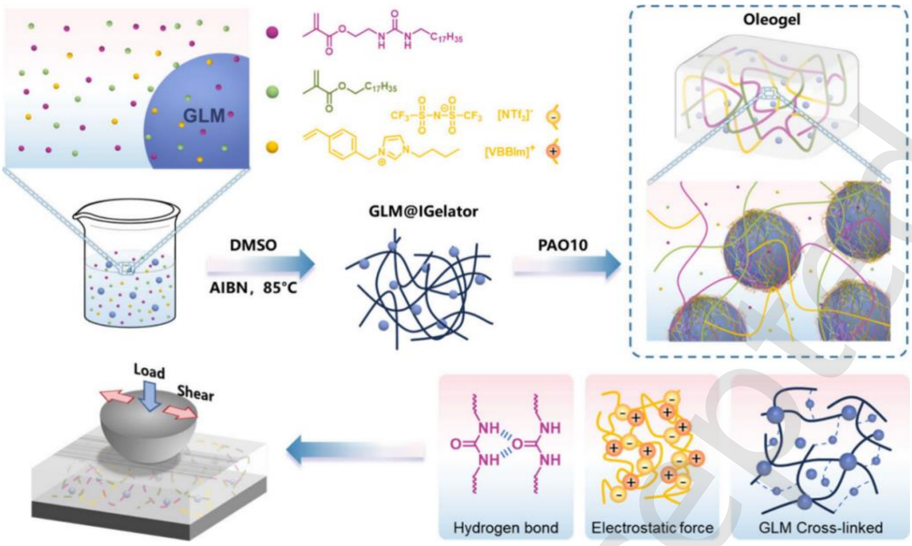

Fig. 18 Preparation process of glm-based ionic oleogels. Reproduced with permission from Ref.[186], © American Chemical Society 2024.

In addition to the microwave, some other auxiliary fields are also used to synthesize nanocomposites as lubricating additives. As shown in **Fig. 19**, Jin et al. [187] prepared N, S-codoped CDs (N, S-CDs)-based lubricants in PEG base oil by directional ultrasonic treatment of BTA and benzothiadiazole (BTH). The synthesized N, S-CDs had good dispersion stability. Compared with pure PEG, the N, S-CDs (BTH)-based lubricant reduced the CoF from 0.292 to 0.108, decreased the wear volume by 91.2%, and increased the maximum load-carrying capacity from 150 to 450 N.

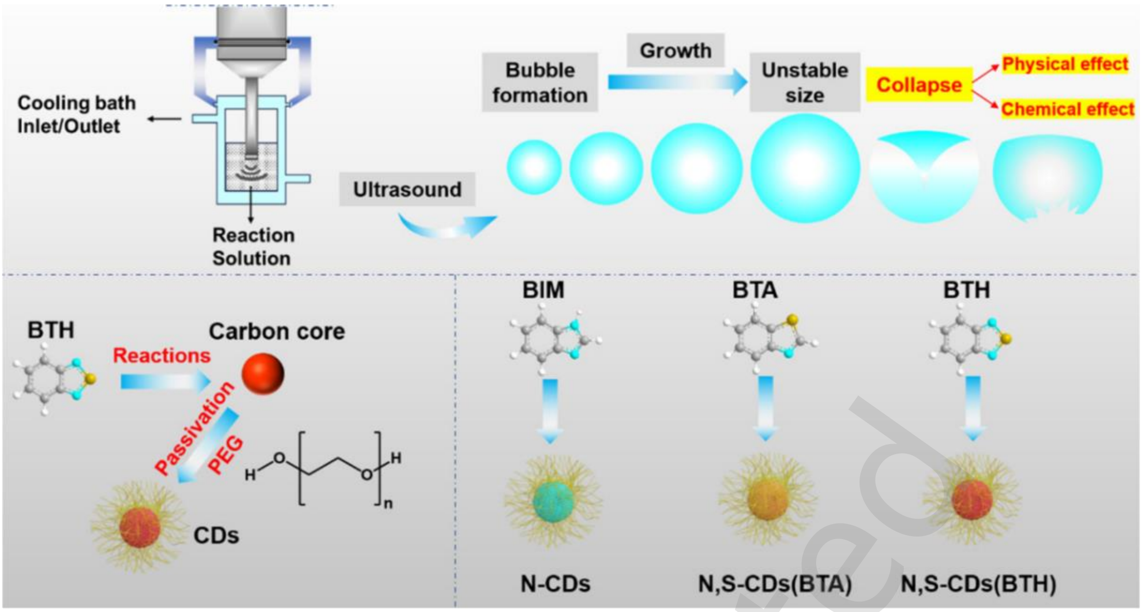

Fig. 19 Preparation Process of CDs by directional ultrasonic treatment. Reproduced with permission from Ref.[187], © American Chemical Society 2024.

Wei et al. [188] synthesized multilayer graphene-reinforced TiO_2 composite (MGTC) via dielectric barrier discharge plasma-assisted ball milling (**Fig. 20**), where expanded graphite was exfoliated into multilayer graphene and TiO_2 particles (size reduced from 1 μm to ~150 nm) were bonded to graphene with oleic acid modification; 1.0 wt% MGTC in base oil reduced the CoF by 18.34%, WSD by 39.37%, increased oil film thickness by 167% (to 27.5 nm) and P_B value by 37.5% (to 653 N), with the mechanism involving interlayer sliding of graphene, nano-bearing action of TiO_2, and formation of carbon protective films, TiO_2 deposition films, and transfer films, along with NPs filling of surface pits for repair.

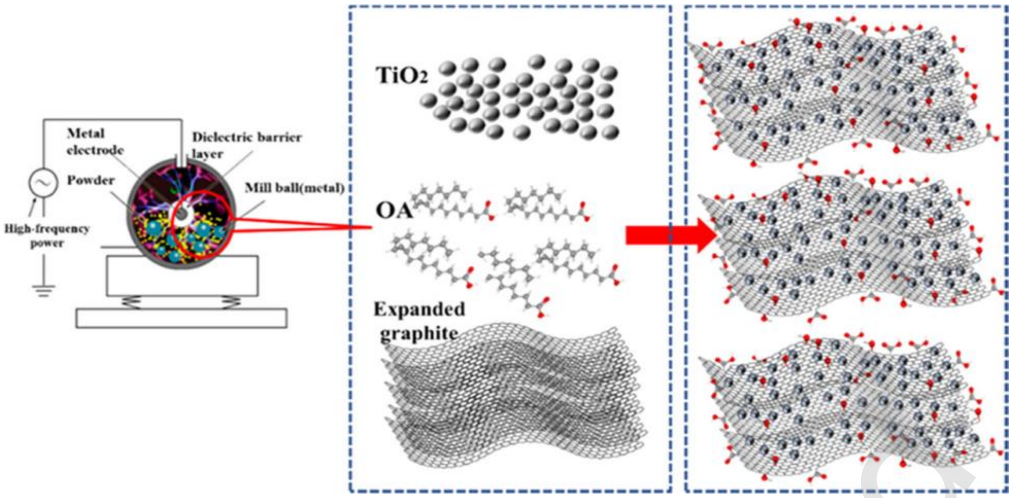

Fig. 20 Schematic diagram of the preparation of MGTC nanocomposites by using dielectric barrier discharge plasma-assisted ball milling. Reproduced with permission from Ref.[188], © American Chemical Society 2022.

Krim et al. [189] reviewed the fundamental mechanisms of NPs additives in lubricants, emphasized the new trend of electromagnetic response-assisted synthesis (such as electric field-induced regulation of friction), demonstrating the cutting-edge exploration of external field-induced structural control in lubricating additives. Meng et al. [190] used supercritical carbon dioxide-assisted deposition to uniformly deposit ultrafine nickel NPs on the surface of oxidized graphene, forming Sc Ni/GO nanocomposites. When used as a lubricant additive, it can reduce the CoF and wear spot diameter by 32% and 42%, respectively. The significant performance improvement is attributed to the dense transfer film structure formed by the synergistic formation of Ni and GO. Jiang et al. [191] reviewed the research progress of nano additives in lubricants in recent years, pointing out that electrostatic self-assembly, template-assisted method, microwave-assisted synthesis, laser ablation, etc., have gradually become new methods for constructing composite nanostructures, especially suitable for constructing multiphase synergistic lubrication systems.

In summary, these emerging nanocomposite synthesis methods demonstrate unique advantages in regulating particle size distribution, constructing synergistic interfaces, and enhancing material dispersibility, providing innovative paths for the green and functional development of high-performance lubricants. With the continuous optimization and industrialization of these technologies, their application prospects in the field of lubrication will become even broader.

4. Lubrication mechanisms of nanocomposites

The paramount advantage of nanocomposite additives in tribological applications lies in their synergistic effects, where the complementary interactions between distinct components collectively enhance comprehensive lubrication performance.

4.1. Film formation mechanism

4.1.1 Physical adsorption films

Physical adsorption films represent a fundamental lubrication mechanism in which NPs or nanocomposites adsorb onto friction surfaces through van der Waals forces, electrostatic interactions, or other weak bonding, forming a protective barrier that minimizes direct asperity contact and thereby reduces friction and wear [192-194]. Compared with single-component NPs, nanocomposites often exhibit enhanced adsorption capability due to their synergistic surface chemistry and multi-scale structural features, enabling the formation of more stable and effective lubricating films.

For instance, Wang et al. [96] prepared mono-dispersed Ag/graphene nanocomposites via a one-step laser irradiation strategy, where Ag nanospheres uniformly decorated rGO sheets. When used at 0.1 wt% in liquid paraffin, nanocomposites reduced the CoF and wear spot diameter by 40% and 36%, respectively, surpassing the performance of individual GO, Ag NPs, and commercial additives. The enhancement was attributed to a continuous physical adsorption film that prevented direct mechanical contact, while the layered rGO facilitated easy shear, and Ag NPs acted as micro-bearings and self-repair agents within wear grooves. Similarly, Guo et al. [195] synthesized a novel nanomaterial named aminated silica modified graphene oxide (SAG) by combining GO and hydrophilic nano-silica with 3-aminopropyltriethoxysilane (**Fig. 21(a)**), which in water-based lubrication achieved a stable CoF of ~0.07 at 0.2 wt% and significantly lowered wear rates compared to pure water. The combined nano-bearing effect of SiO_2 and the high mechanical strength of GO enabled the rapid formation of a physical adsorption film that filled surface valleys and reduced high-pressure asperity collisions (**Fig. 21(b)**). These studies demonstrate how hybrid structures combining hard and lamellar phases can synergistically enhance the integrity and durability of physical adsorption layers.

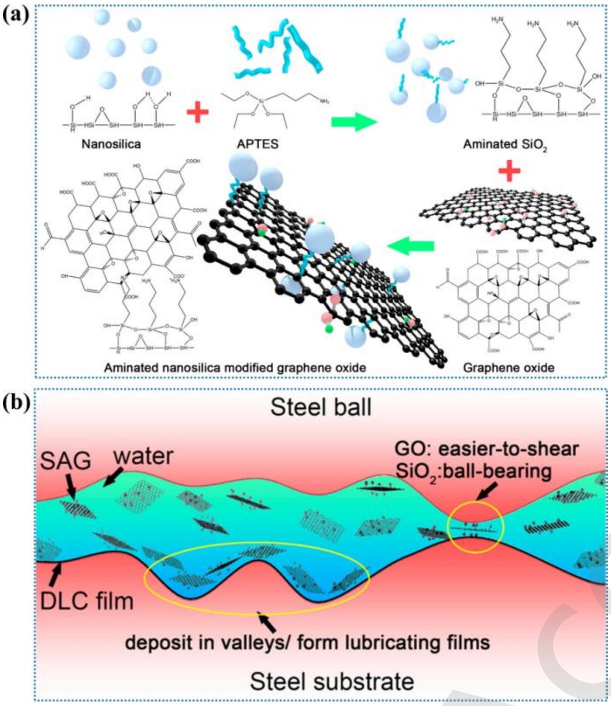

Fig. 21 (a) Schematic diagram for the synthesis of SAG by APTES. (b) The lubricating mechanism of SAG during the friction process. Reproduced with permission from Ref.[195], © American Chemical Society 2018.

Recent work has further diversified this mechanism by introducing novel material architectures. Wang et al. [196] synthesized Zr-MOF@FG composites via covalent bonding and van der Waals assembly, achieving reductions of 70.2% in average CoF and 62.7% in wear track width at optimal concentration. The adsorption film of iron fluoride and Zr-MOF@FG tribo-film can enhance the friction-reduction and antiwear effect in coordination, thus realizing the outstanding tribological properties. Wei et al. [86] fabricated TiO_2@CTAB core-shell NPs using a dielectric barrier discharge plasma-assisted ball milling method, where the CTAB shell electrostatically adsorbed onto steel surfaces to form uniform physical films, resulting in a 41.7% reduction in CoF and a 25.8% decrease in wear spot diameter in base oil. Gao et al. [197] developed MoS_2@FG nanocomposites through ILs crystal-assisted exfoliation, showing Cof reductions of 76-80% in water and PAO4. In this case, FG contributed oxidation resistance and physical barrier effects, while interlayer sliding of MoS_2 enhanced lubrication stability; both acted cooperatively to form continuous physical adsorption layers across diverse lubrication media.

Collectively, these findings highlight that physical adsorption films in nanocomposite lubrication are not solely passive barriers; rather, they are dynamic, adaptive layers whose formation, stability, and performance can be tailored through rational selection of component phases, surface functionalization, and particle morphology. The synergy between hard NPs, lamellar structures, and surface-active agents ensures improved load-bearing capacity, reduced shear strength, and prolonged service life of lubricating films under a wide range of operating conditions.

4.1.2 Chemical reaction films

Chemical reaction films are generated when specific elements or functional groups in nanocomposites undergo tribo-chemical reactions with the friction surface, forming compound layers that lower shear stress and mitigate wear. Compared with single-component systems, nanocomposites often produce more complex and stable reaction films owing to the synergistic interaction of their constituents, thereby delivering markedly improved tribological performance.

Recent studies on functionalized carbon materials demonstrate that they can effectively engage in tribo-chemical interactions with metallic substrates to generate dense and robust chemical reaction films, thereby markedly improving tribological performance. For instance, Hou et al. [198] synthesized potassium borate/graphene nanocomposites via dielectric barrier discharge plasma-assisted ball milling. When incorporated at 0.05 wt% into base oil under a 100 N load, the CoF and wear rate were reduced by 29.1% and 35.8%, respectively. XPS and Raman analyses revealed the formation of a tribo-chemical film composed of C, FeO, Fe_2O_3, and B_2O_3; the high thermal conductivity of graphene, coupled with the synergistic effects of potassium borate and graphene, enhanced the integrity and stability of the film. Similarly, Yu et al. [199] developed a sustainable lubrication system in which cyclopropanecarboxylic acid (CPCa) underwent tribo-chemical reactions catalyzed by Ni or Cu particles in PAO-4 base oil, producing graphene in situ. The CPCa/Cu system reduced the average CoF and WSD by 48.0% and 36.2%, respectively, relative to pure base oil. The generated graphene, together with Fe_3O_4, formed a protective tribofilm that inhibited direct metal-to-metal contact and could be recycled as an additive, enhancing sustainability. In another example, Zhang et al. [200] synthesized silver/PDA-modified GO nanocomposites as additives for DTE 32# oil. At 0.2 wt%, the CoF and wear rate decreased by 53.57% and 68%, respectively. The tribofilm containing C, O, N, and Ag exists and plays an important role in reducing friction and increasing wear resistance. Sun et al. [201] reported CeO_2-decorated reduced graphene oxide (CeO_2@rGO), which achieved a 31.9% reduction in CoF compared to pure oil. XPS and Raman spectroscopy identified Fe_2O_3 and Ce-O-Ce bonds in the tribofilm, with CeO_2 NPs filling surface defects and rGO providing interlayer shear, jointly improving film stability and shear resistance. Overall, functionalized carbon-based materials generate tribo-chemical films with diverse compositions and high compactness, delivering significant reductions in friction and wear alongside exceptional durability under demanding conditions.

MoS_2-based composites also form multifunctional reaction films combining sulfides, oxides, and carbonaceous layers. Wang et al. [202] introduced modified reduced graphene oxide (MRGO) and modified MoS_2 (MMD) into PAO-6 base oil at a 5:5 ratio. At an optimal concentration of 0.3 wt%, the CoF and WSD decreased by 48.53% and 31.71%, respectively. XPS and Raman analyses confirmed the formation of FeS, MoO_3, and SO_4^{2-} species within the reaction film, which, together with MRGO/MMD adsorption layers, synergistically enhanced anti-friction and anti-wear performance. Similarly, Gou and Chen [203] reported that adding a composite of 0.05 wt% graphene and 0.05 wt% MoS_2 to PAO-6 reduced the wear rate of polycrystalline diamond compact (PDC) cutters by 41% compared to graphene alone and by 20% compared to MoS_2 alone, while also lowering the CoF. MoS_2 decomposed into Mo and S during sliding, forming Mo oxides and sulfides such as $FeSO_4$, whereas graphene contributed to a carbonaceous transfer film; these layers acted synergistically to protect the PDC surface. Lu et al. [204] synthesized MoS_2/C_{60} nanocomposites via in situ hydrothermal methods, achieving reductions of 54.5% in CoF and 62.7% in wear rate at 0.5 wt% in dioctyl sebacate. The reaction film contained MoS_2, MoO_3, $FeSO_4$, and $Fe_2(SO_4)_3$, indicating that MoS_2-driven sulfuration, combined with the load-bearing capability of C_{60}, enhanced film stability. He et al. [205] developed N-doped carbon quantum dots (N-CQDs) combined with MoS_2 as water-based lubricant additives. At 0.4 wt%, the CoF and wear rate decreased by 30.4% and 31.0%, respectively. The resulting $FeSO_4$ and $Fe_2(SO_4)_3$ tribofilms exhibited an average thickness of ~13.9 nm, with O- and N-containing functional groups from N-CQDs improving film compactness and adhesion. Collectively, MoS_2-based materials form chemically diverse and structurally stable reaction films, maintaining low friction and wear even under high-load, complex operating conditions.

Metal oxide NPs are capable of forming tribo-chemical films through surface reactions with metallic substrates, yielding oxides, fluorides, or mixed compound layers with high hardness and stability. Lv et al. [206] investigated α-Al_2O_3/PTFE and SiO_2/PTFE composites under loads ranging from 1 to 10 MPa. α-Al_2O_3/PTFE exhibited stable wear rates on the order of ~10^{-6} $mm^3/N{\cdot}m$, while the wear rate of SiO_2/PTFE increased significantly at higher loads. FTIR and XPS analyses detected tribo-chemical species such as carboxylates, metal fluorides, and iron oxides. α-Al_2O_3 facilitated more intense tribo-chemical reactions, forming thicker, shear-resistant films, as shown in **Fig. 22(a),** whereas SiO_2 produced thinner films with reduced stability under heavy loads. In another example, Nassef et al. [207] modified palm grease with ZnO and rGO nano-additives. Incorporating 1 wt% rGO or 0.1 wt% ZnO lowered the CoF by 60% and increased the load-carrying capacity by 60% and 30%, respectively, compared to unmodified grease. XPS characterization confirmed the presence of Zn-containing compounds from the reaction of ZnO with the steel surface, together with rGO layers, forming a protective hybrid tribofilm. Such films effectively prevented direct asperity contact and enhanced lubricant stability. Overall, metal oxide-based systems produce robust and chemically stable tribofilms, contributing to long-term wear protection and friction reduction across a wide range of load and temperature conditions.

$Ti_3C_2T_x$ MXene and its composites have attracted considerable attention in lubrication research due to their unique two-dimensional layered structure, high electrical conductivity, and rich surface functional groups, which promote both interlayer shear and tribo-chemical film formation. Wen et al. [208] prepared Ti_3C_2 MXene and tetradecylphosphonic acid-functionalized MXene (TDPA@MXene) through water-molecule-assisted intercalation and surface modification, respectively, and evaluated their performance as additives in PAO8 base oil. At an optimal concentration of 0.01 wt% under a 100 N load (1.37 GPa contact pressure), MXene reduced the CoF by 20.9% and wear rate by 99.5%, while TDPA@MXene achieved reductions of 16.3% and 99.8%, respectively, compared with pure PAO8. XPS analysis revealed the presence of iron oxides and $FePO_4$ within the tribofilm, with TDPA modification improving dispersion stability and enabling uniform, compact film formation. In another study, Feng et al. [209] synthesized few-layer $Ti_3C_2T_x/MoS_2$ heterojunctions via hydrothermal methods for use as additives in mineral oil (150N). At 0.3 wt%, the composite decreased the CoF and wear volume by 38.85% and 83.52%, respectively, surpassing the performance of either $Ti_3C_2T_x$ or MoS_2 alone. Tribo-chemical analysis revealed a multi-component film containing MoO_3, $FeSO_4$, iron oxides, and C-O bond-rich compounds, which exhibited strong adhesion and high load-bearing capacity (**Fig. 22(b)**). $Ti_3C_2T_x$-based materials demonstrate excellent synergistic effects between mechanical protection via interlayer shear and chemical protection via triboreaction films, enabling outstanding friction- and wear-reduction under demanding conditions.

Overall, these studies demonstrate that chemical reaction films serve not only as physical barriers but also as integrated tribo-chemical layers, combining the properties of the reaction products with those of the nanocomposites constituents. This synergy delivers substantial, quantifiable improvements in friction reduction, wear resistance, and load-bearing capability under diverse lubrication regimes.

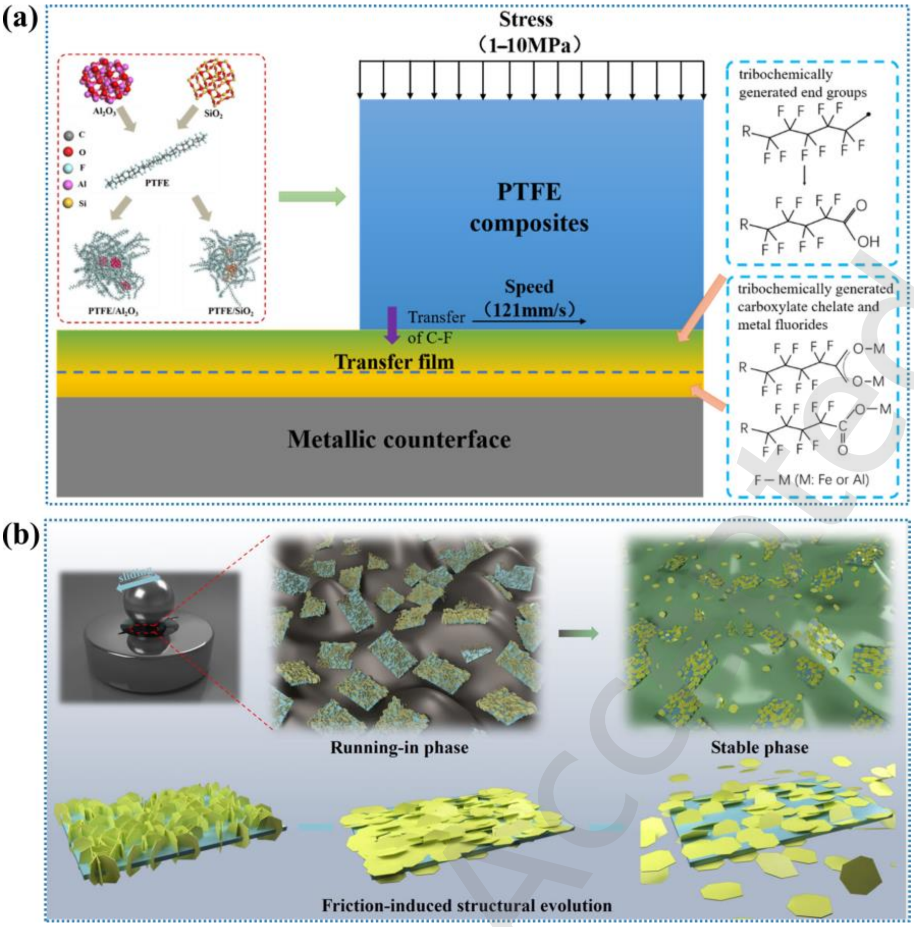

Fig. 22 (a) The mechanism of mechanochemical reactions and tribo-film formation between PTFE nanocomposites and metallic counterparts. Reproduced with permission from Ref.[206], © MDPI 2024. (b) The schematic diagram of the lubrication mechanisms of a few-layer $Ti_3C_2T_x/MoS_2$ heterojunction. Reproduced with permission from Ref.[209], © Tsinghua University Press 2022.

4.2. Micro-bearing effect

Nanoparticles can act as micro-bearings between friction pairs, converting sliding friction into rolling friction and thus reducing the CoF. Well-dispersed spherical NPs fill interfacial gaps and roll between contact surfaces, mitigating direct asperity contact and lowering frictional resistance [210]. Their effectiveness, however, depends strongly on operating conditions [211]. Under low-speed and light-load conditions, particles remain stably embedded and maintain low friction and wear. At high speed or heavy load (e.g., >300 MPa contact pressure), excessive shear and thermal stresses can fracture or expel particles from the interface, causing lubrication failure and potential surface damage [212].

Compared to single-component NPs, nanocomposites often demonstrate superior micro-bearing performance because of their combined structural and functional advantages. In this context, Gu et al. [213] developed carbon microspheres/poly(methyl methacrylate) (CMS/PMMA) core-shell microparticles as lubricant additives. At an optimal concentration of 0.2 wt%, the nanocomposites reduced the CoF by 28.3% under an 8 N load and decreased wear scar width and wear rate by 30.4% and 41.42%, respectively, under a 30 N load. The rigid CMS core acted as the primary rolling element, while the flexible PMMA shell enhanced dispersion stability and conformed to surface asperities, thereby reducing abrasive wear. This combination provided stable rolling lubrication under mixed lubrication regimes (**Fig. 23**).

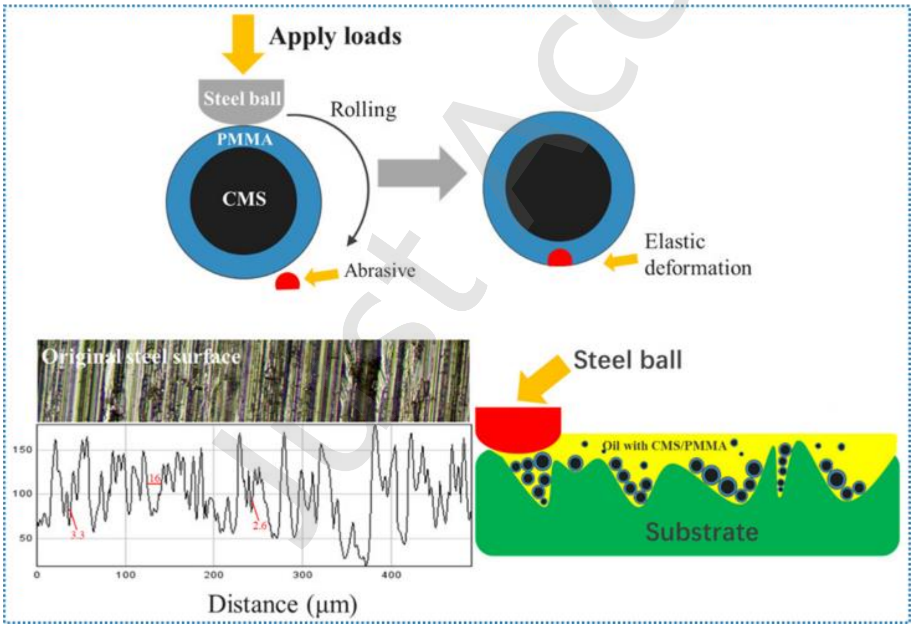

Fig. 23 Schematic of the rolling bearing effect of CMS/PMMA composites as oil additives. Reproduced with permission from Ref.[213], © American Chemical Society 2019.

Building upon this design concept, similarly, Chen et al. [26] prepared Ag/BN nanocomposites by depositing Ag NPs onto BN surfaces, used at a 2 wt% concentration in lithium-based grease. Under a

10 N load and 50 mm/s sliding speed, the nanocomposites reduced the average CoF by 35.2% (to 0.33) and the wear rate by 41.6% (to 1.08×10^{-14} $m^3/(N\cdot m)$) compared with pure grease. The Ag NPs acted as micro-bearings to convert sliding friction into rolling friction, while BN offered structural rigidity to sustain high loads, resulting in a durable lubricating film. Similarly, Shan et al. [214] reported cellulose-armored CNT/Ag hybrids in sunflower oil, where the cellulose layer maintained a uniform dispersion of CNTs and Ag NPs. At 0.4 wt%, this system reduced friction and wear by 61.9% and 79.5%, respectively. The CNTs and Ag particles rolled between surfaces while cellulose fragments filled wear scars, ensuring long-term lubrication stability, as shown in **Fig. 24**. These studies demonstrate how incorporating both hard rolling cores and stabilizing shells can significantly enhance the durability and effectiveness of the micro-bearing effect.

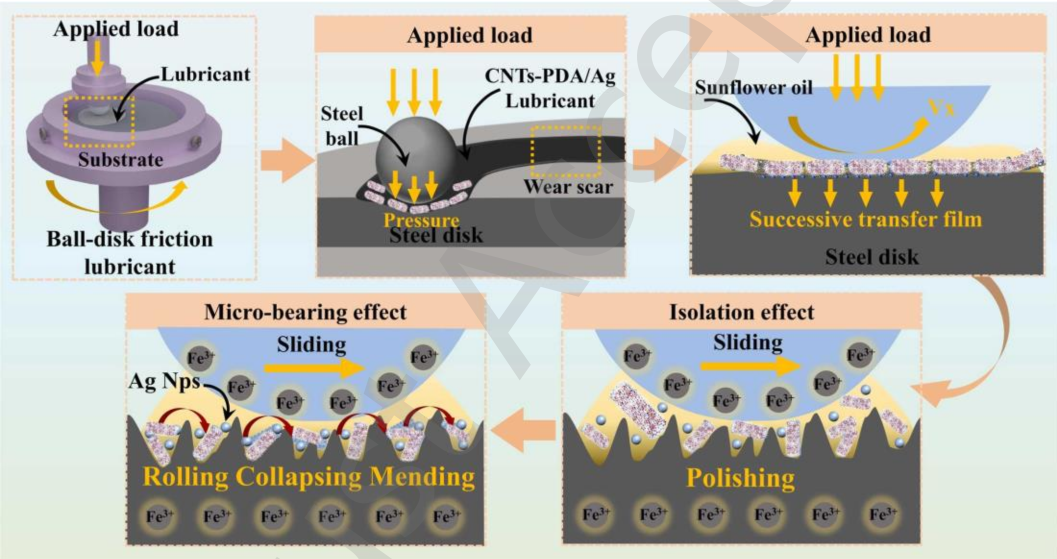

Fig. 24 The lubrication mechanism diagram of C-[CNTs-PDA/Ag] as a lubricant additive. Among them, the CNTs and Ag NPs can be used as microscopic bearings to turn sliding friction into rolling friction (lower left quarter). The collapsed Ag NPs adhere to the friction surface to produce a protective film and repair the worn surface (bottom right corner). Reproduced with permission from Ref. [214], © Elsevier B.V. 2024

Beyond carbon-based composites, core-shell architectures incorporating magnetic or ceramic materials also show remarkable performance. Wang et al. [215] synthesized oleic acid-modified

Fe_3O_4@C microspheres, which reduced the CoF by 10% and wear rate by 91.51% compared to base oil. The hard Fe_3O_4 core sustained load while enabling rolling motion, and the carbon shell exfoliated during friction to release lubricating fragments into wear grooves. Similarly, Xue et al. [216] developed nano-SiO_2/GO composites for engine oil. At only 0.125 wt%, the CoF and WSD were reduced by 38.6% and 29.7%, respectively. In this system, spherical SiO_2 particles provided the rolling effect, while the GO layers formed a low-shear sliding interface. Such synergistic designs demonstrate that combining micro-bearing action with secondary lubrication mechanisms can deliver both low friction and high wear resistance.

Overall, the micro-bearing effect in nanocomposites arises from the interplay between particle geometry, mechanical strength, and interfacial stability. Rigid cores enable rolling motion under load, while flexible or layered components enhance film continuity and reduce shear resistance. These combined attributes allow nanocomposites to maintain effective rolling lubrication across a wider range of operating conditions than single-component systems.

4.3. Repair mechanism

Nanomaterials in lubricants possess intrinsic self-healing capabilities that enable the restoration of worn surfaces, which is critical for sustaining low friction and minimizing material loss [217]. During friction, metal NPs transported by lubricants infiltrate surface scratches or micro-damage zones, where they deposit and gradually fill defects. Maurya et al. [218] evaluated γ-AlOOH NPs (0.25-1.0 wt% in PAO-6) under four-ball antiwear tests (ASTM 4172, 392 N, 1200 rpm, 60 min) and extreme-pressure tests (IP 239, 1450 rpm). At 0.5 wt%, the additive lowered the average CoF by ~15%, reduced WSD by ~24%, and increased P_B by ~40%. SEM images and EDS maps show that the grooves on the worn surface are narrower, the pits are fewer, and Al (0.79 wt%) and O (8.32 wt%) are detected, confirming that γ-AlOOH is involved in the formation of the friction film. The XPS spectra (**Fig. 25**) detected peaks corresponding to the iron oxide film (710.8 eV and 724.5 eV), and the peaks of O 1s (530.9 eV) and Al 2p (74.0 eV) also confirmed the dehydration of γ-AlOOH to form Al_2O_3. It is indicated that the two jointly form a dense oxide friction film, repairing defects and reducing wear.

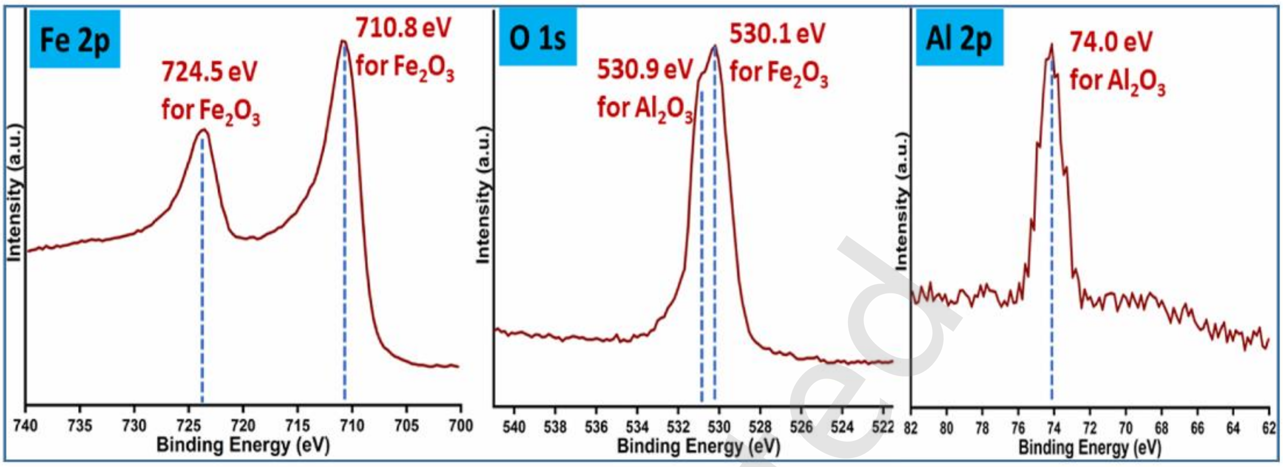

Fig. 25 XPS spectra of Fe 2p, O 1s, and Al 2p for the worn surface lubricated with 0.5 wt% γ-AlOOH nanolubricant under ASTM 4172 test conditions. XPS analysis was performed using a Thermo Fisher Scientific K alpha+ system with monochromatic Al Kα radiation (beam current 6 mA, 1486.7 eV) and a pass energy of 150 eV over a 200 μm spot size; core-level spectra for Fe 2p, Al 2p, and O 1s were acquired with a 30 eV pass energy. Reproduced with permission from Ref.[218], © Elsevier B.V. 2022.

Nanocomposites outperform single-phase counterparts in surface restoration due to synergistic interactions. Yang et al. [95] fabricated g-C_3N_4/rGO nanocomposites via electrostatic self-assembly. The heterojunction between g-C_3N_4 and RGO suppressed particle agglomeration, while the high surface area of 2D materials enabled efficient adsorption. At an optimal concentration of 2.0 wt%, the nanocomposites reduced the CoF by 62.3% (to 0.103) and wear volume by 96.0% (to 0.86×10^5 μm^3) compared to pure PAO-10. Under shear stress, g-C_3N_4/RGO nanosheets fragmented into nanoscale debris (10-20 nm), filling surface depressions and achieving ultralow roughness (**Fig. 26**).

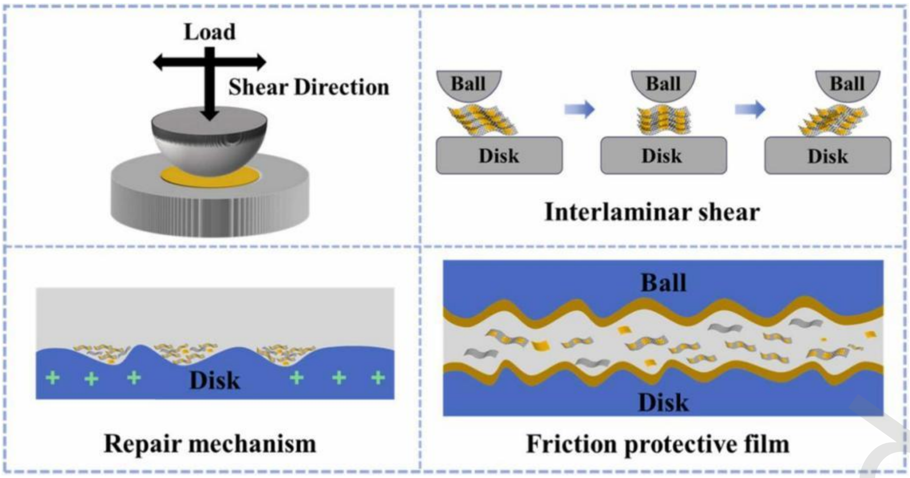

Fig. 26 The lubrication mechanism of g-C_3N_4/RGO as a lubricant additive, including repair mechanism and protective film. Reproduced with permission from Ref.[95], © Elsevier B.V. 2024.

MXene-based systems offer another promising route to self-healing lubrication. Ma et al. [219] modified $Ti_3C_2T_x$ with dodecyl phosphonic acid and used them as OSP-46 oil additives. At 100 N load and 50 °C, the additive reduced the CoF by 24% and wear rate by 85%. The repair mechanism involved both interlayer sliding of $Ti_3C_2T_x$ to replace direct asperity contact and the formation of TiO_2 NPs via tribo-chemical oxidation, which combined with MXene nanosheets to create a continuous protective film capable of maintaining stability under variable loads and temperatures. Similarly, Wang et al. [220] designed CNUS-2@MQDs nanocomposites for PAO-10 lubrication. At 3.0 wt%, the CoF (0.097) and wear volume (1.48×10^5 μm^3) were reduced by 46.7% and 92.6%, respectively. Here, MXene quantum dots filled wear grooves while oxygen-containing functional groups on CNUS-2 promoted strong adsorption and tribo-film formation, with interlayer slip enhancing lubrication stability under extreme conditions.

Repair mechanisms are not limited to 2D materials; spherical and core-shell architectures also show strong potential. Wu et al. [221] developed 2D Cu-MOFs surface modified (CS@Cu(BDC)) composites by coating carbon spheres (CS) with 2D Cu-MOF nanosheets. At 0.5 wt% in base oil, the CoF decreased by 62.2% and the wear rate by 33.9%. The CS served as micro-bearings to reduce sliding friction, while Cu(BDC) layers enabled interlayer slip and debris-filled wear grooves, together forming a protective tribo-film that minimized abrasive wear. Zhang et al. [222] developed core-shell C@MoS_2 particles as PAO 40 additives. At 0.5 wt%, the CoF and wear track width were reduced by 11.7% and 20.3%, respectively. The Repair Mechanism operates in three stages: shell crushing (rolling bearing effect), core-shell separation (CS filling and MoS_2 sliding), and core-shell recombination (forming a dense protective film). This synergistic action of CS (load-bearing) and MoS_2 (low shear) repairs worn surfaces effectively.

Inorganic mineral-based systems can also provide metallurgical-level surface restoration. Jin et al. [223] employed MSH/MoS_2 NPs in PAO6 for gray cast iron-Cr-coated steel pairs, achieving 25% friction reduction, 30.78% wear rate reduction, and 40% wear volume recovery after 8 h. The repair process relied on isomorphic replacement, where MSH was dehydrated to form silicates that reacted with Fe oxides to produce a metallurgically bonded repair layer firmly anchored to the substrate.

Overall, repair mechanisms in NPs and nanocomposite lubrication rely on a combination of defect filling, tribo-film formation, and, in some cases, chemical bonding with the substrate. Synergistic material designs, including integrating high-load-bearing cores, low-shear layers, and functional groups for strong adhesion, enable more robust and long-lasting surface restoration than single-component systems.

4.4. Synergistic effects

The superior performance of nanocomposites in tribological applications stems from their ability to integrate multiple lubrication mechanisms into a unified, cooperative action. Such synergistic effects arise when distinct structural components and physicochemical functions of each phase complement one another, resulting in enhanced dispersion stability, load-bearing capacity, protective film integrity, and self-repair capability. Zhao et al. [224] developed Mn_3O_4/graphene nanocomposites with sandwich-like nanostructures via in situ synthesis. In the steel-steel sliding friction test (0.075 wt% added to PAO-6 base oil, 125 °C), the material reduced the CoF by 75% and the wear depth by 97%. **Fig. 27**(a) shows the Raman spectra of wear tracks at different lubrication temperatures. the

Mn_3O_4 peak (645.1 cm^{-1}) at 125 °C is higher than that at 25 °C, indicating stronger adsorption of Mn_3O_4 NPs on the surfaces. **Fig. 27**(b) shows the TEM cross-sections, revealing a tribo-film 200-300 nm thick between the steel substrate and protective Pt coating, and EDS maps confirm high C, O, and Mn concentrations within the film. The Synergistic Effects are illustrated in **Fig. 27(c)**. Mn_3O_4 NPs prevent graphene agglomeration and increase interlayer spacing, while graphene carries Mn_3O_4 into contact zones, enabling a "sliding or rolling" mechanism that enhances lubrication stability. In a subsequent study, Zhao et al. [225] used a similar method to synthesize a sandwich-shaped CuO@G nanocomposite, with CuO NPs uniformly anchored on and intercalated between rGO nanosheets. At 0.5 wt% in PAO-6, CuO@G reduced CoF by over 50% and nearly eliminated wear scars. The synergy originates from CuO NPs preventing rGO restacking and rGO inhibiting CuO aggregation, resulting in a "slide-roll" interaction where rGO provides low-shear sliding and CuO functions as micro-bearings.

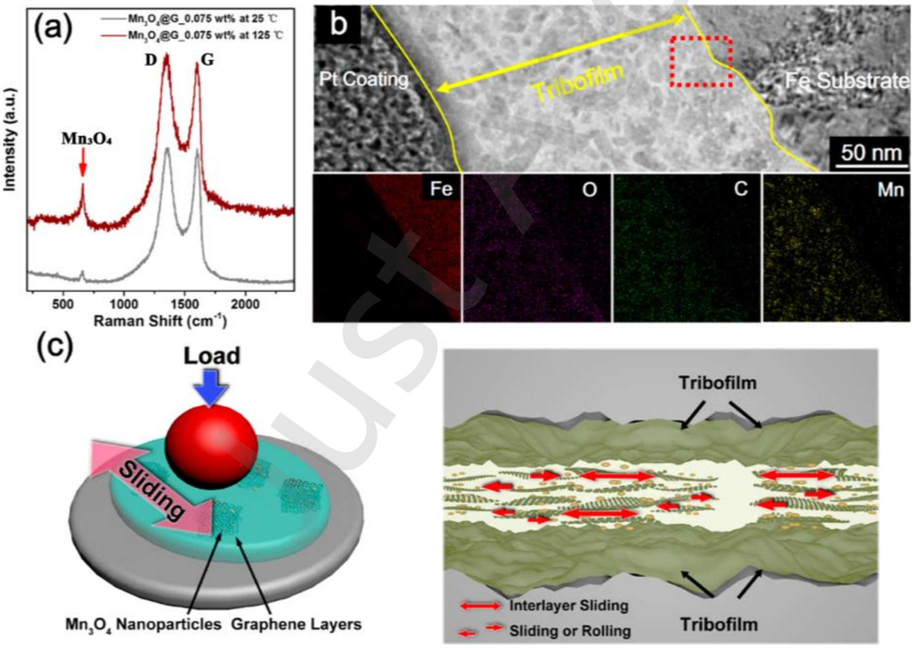

Fig. 27 (a) Raman spectra of wear tracks lubricated with 0.075 wt% Mn_3O_4/graphene nanocomposites in PAO base oil after ball-on-disk testing (2 N, 2.4 mm/s, 25-150 °C, 40 min), showing graphene D- and G-bands and the Mn_3O_4 peak (645.1 cm^{-1}). (b) FIB cross-sectional TEM image and EDS elemental maps (Fe, O, C, Mn) of the tribofilm from the same test, revealing a 200-

300 nm-thick layer. (c) Schematic illustration of the synergistic lubrication mechanism, based on the Raman, EDS, and tribological observations reported by Zhao et al. [224], showing graphene nanosheets undergoing interlayer sliding assisted by Mn_3O_4 NPs, inducing a "sliding or rolling" effect. Reproduced with permission from Ref.[224], © American Chemical Society 2019.

Composite NPs can form different types of lubricating films, thereby promoting each other and enhancing tribological properties. Xiang et al. [155] prepared Ni-Fe LDH nanosheets with a Ni/Fe ratio of 6:1, used at 0.3 mg/mL in GTL base oil. The CoF, WSD, and wear volume decreased by 51.3%, 30.8%, and 78.4%, respectively. As shown in **Fig. 28**, the lubrication process begins with a physical adsorption film formed by LDH nanosheets, which is later replaced by a tribo-chemical film of iron and nickel oxides generated under heat and plastic deformation, offering more durable surface protection.

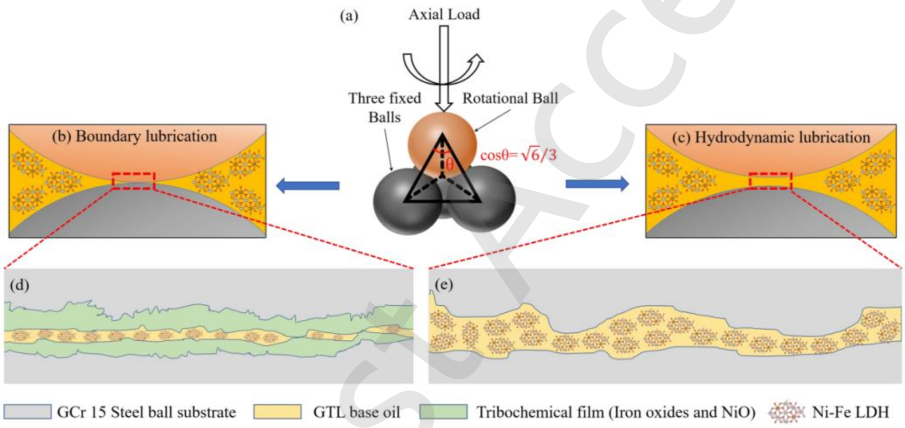

Fig. 28 Schematic diagrams of the lubrication mechanism for GTL base oil enhanced with Ni-Fe LDH with Ni/Fe. (a) schematic illustration of the four-sphere point contact model, (b, d) boundary lubrication between two sliding surfaces of solid rough peaks and ridges, (c, e) hydrodynamic lubrication in fluid contact. Reproduced with permission from Ref.[155], © MDPI 2024.

In more cases, the synergistic lubrication effect of nanocomposites includes multiple interactions of lubrication mechanisms such as the film formation effect, ball-like effect, and repair effect. Wei et al. [188] developed MGTC via plasma-assisted ball milling, as additives in a 500 N base oil. At 1.0 wt%, the average CoF decreased by 18.34%, WSD by 39.37%, and the oil film thickness increased by 167%

(to 27.5 nm). The synergistic Effects are driven by the interlayer sliding of graphene and the nano-bearing effect of TiO_2. Graphene forms carbon protective films, TiO_2 deposits to repair wear, and their combination reduces direct metal contact, improving tribological stability. Cui et al. [180] developed core-rim structured MXene@SiO_2 composites via in-situ hydrolysis of TEOS, used as additives in 500 SN base oil. At 2.4 wt% concentration, the CoF decreased from 0.572 to 0.108, wear volume was reduced by 73.7%, and the load capacity increased to 800 N. The Synergistic Effects stem from interlayer slip of MXene and rolling bearing effect of SiO_2, SiO_2 increases interlayer spacing of MXene to avoid agglomeration, enhances load-bearing capacity, and together they form physical adsorption films and tribo-chemical reaction films (containing TiO_2, Fe_2O_3), improving lubrication stability. In the work of Wu et al. [181], SGN was used as an aqueous lubricant additive. At 0.2 wt%, under 150 rpm and 3 N, friction reduction and wear resistance improved by 52.2% and 54.2%, respectively. The Synergistic Effects include rolling friction of Ag NPs and interlayer shearing of graphene; collapsed Ag NPs form protective coatings on worn surfaces, while graphene enhances load-bearing, collectively reducing friction and repairing damage (**Fig. 29**). Chen et al. [226] prepared mono-dispersed Ag NPs decorated graphitic carbon nitride as additives in polyphthalazinone ether sulfone ketone (PPESK) nanocomposite films. At 0.3 wt% concentration, the CoF and wear rate were reduced by 68.9% and 97.1%, respectively, compared to pure PPESK. The Synergistic Effects involve interlayer sliding of g-C_3N_4, micro-bearing effect of Ag NPs, and the formation of a transfer film, which together limit shear deformation of PPESK and enhance interfacial compatibility, maintaining excellent performance under heavy loads and high speeds.

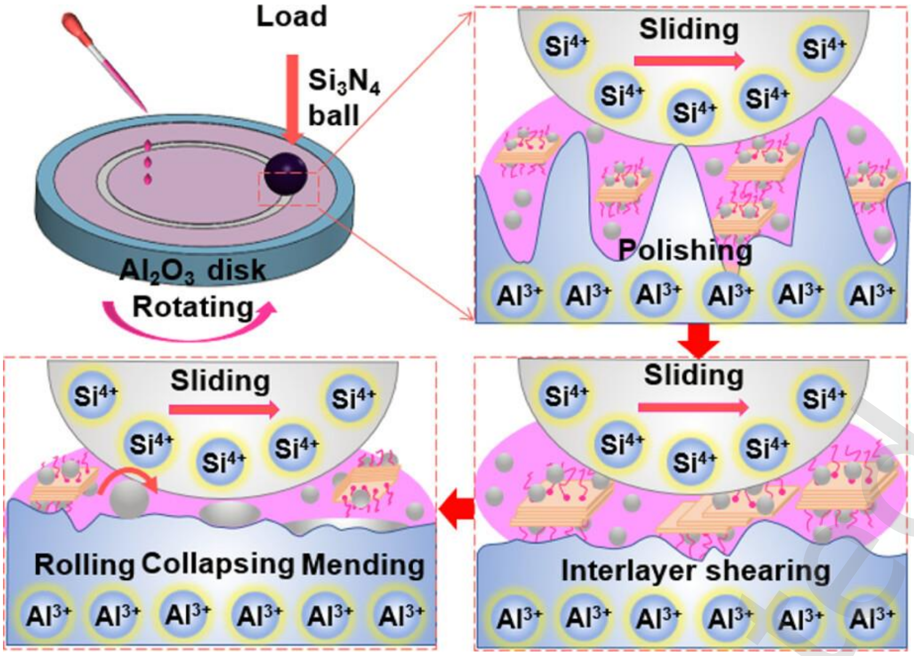

Fig. 29 Lubrication mechanisms of SGN, including polishing, rolling, filling, and film-forming effects. Reproduced with permission from Ref.[181], © American Chemical Society 2023.

Core-shell nanostructures offer another route to synergy by spatially integrating distinct functions. Liu et al. [227] synthesized hybrid carbon nanospheres encapsulating vanadium and wolframium nanocrystals (V/W@NCNs) via one-pot domino synthesis. At 0.2 wt% in 500 SN base oil, CoF reached 0.09, wear volume decreased by 91.5%, and extreme pressure capacity reached 1250 N. The N-doped carbon shell ensured dispersion and formed physical adsorption films, while the metal nanocrystals enhanced mechanical strength, thermal conductivity, and catalyzed tribo-chemical protective layers (**Fig. 30(a)**). Ao et al. [105] produced C@Ag core-shell microspheres, which at 0.5 wt% in G1830 base oil reduced CoF and wear volume by 15.5% and 88%, respectively. **Fig. 30(b)** shows the synergistic lubrication mechanism includes the rolling filling of core-shell particles to repair micro damage, the compression deformation of the Ag shell under friction, and the melt bonding of Ag particles to form a tribo-film, which effectively separates the friction pair and reduces wear. Ma et al. [228] fabricated SiO_2@Cu and SiO_2@MoS_2 microspheres for PAO 40. Under 2.72 GPa, SiO_2@Cu reduced friction by 32.47% and wear by 67.86%, outperforming SiO_2@MoS_2 and single additives. As illustrated in **Fig. 30**(c), the superior performance of SiO_2@Cu is due to the rolling action of SiO_2 combined with the easy-shearing and self-repairing Cu shell, forming a dense, stable film that also delays NPs agglomeration. In contrast, the MoS_2 shell yielded less stable films, underscoring the importance of core-shell compatibility.

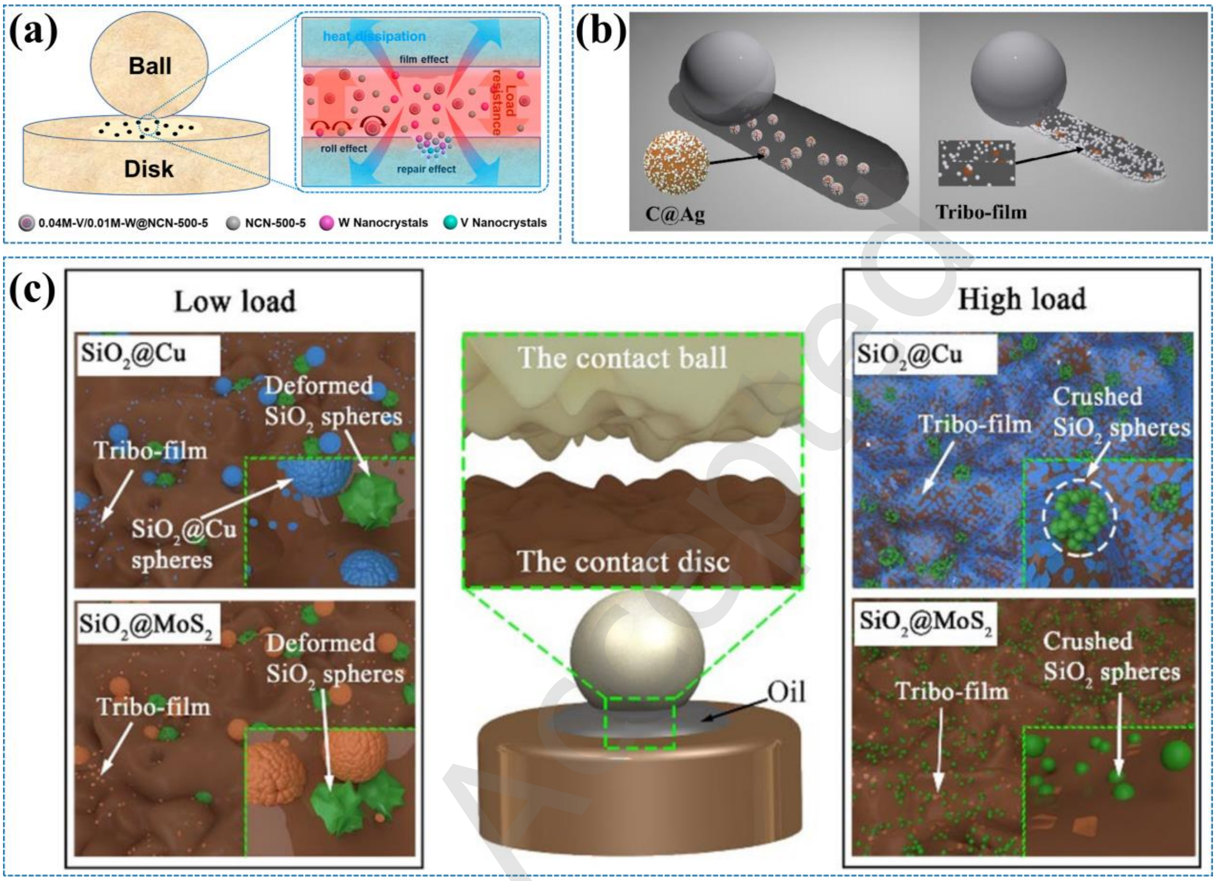

Fig. 30 (a) Lubrication Mechanism of V/W@NCNs as Additives. Reproduced with permission from Ref.[227], © American Chemical Society 2024. (b) Self-healing mechanism of C@Ag core-shell additives, including rolling fill and friction film formation. Reproduced with permission from Ref.[105], © Tsinghua University Press 2024. (c) Lubrication mechanism of SiO_2@Cu and SiO_2@MoS_2 under different loads. Reproduced with permission from Ref.[228], © Springer 2021.

In addition, the synergistic effect of nanocomposites also shows some promising applications in the field of electronically controlled friction. Wang et al. [229] synthesized porous Cu-BTC@Ag nanocrystals for ILs. At 0.5 wt% without voltage, CoF and wear volume decreased by 8.3% and 16%, respectively, while at 20 V and 2.0 wt%, the reductions were 18.8% and 32.7%. As shown in **Fig. 31**, under combined contact stress and electric fields, the nanocrystals released lubricant and deposited active elements to form repair layers, offering simultaneous friction reduction, anti-wear protection, and self-healing. In a similar approach, Shang et al. [230] synthesized sodium iron Prussian blue analogue (NaFe-PBA) NPs modified with PDA for use in polydimethylsiloxane base oil. At 1 wt%, the NaFe-PBA@PDA nanocomposites reduced wear volume by 49.04% compared to pure polydimethylsiloxane, and under electric-tuned conditions (0.5 A), the CoF was further reduced by 6% without compromising wear resistance. The cubic-to-rod transformation of NaFe-PBA under shear and current produced micro-rollers that decreased interfacial shear and enhanced load-bearing capacity, while Na^+ ions facilitated surface repair; PDA modification improved dispersion, amplifying the combined effects of rolling, load-bearing, and repair. Hou et al. [231] prepared intercalated graphene/carbon nanotube (GC) nanocomposites as additives in hexadecane (C16) base oil. At 0.3 wt%, GC-C16 reduced CoF and wear volume by 45% and 43.75%, respectively, compared to pure C16, and under intelligent electric current control, the 1.0 wt% formulation achieved an additional 18% CoF reduction. This enhancement was attributed to CNTs intercalated within graphene layers, providing load-bearing reinforcement while graphene offered low-shear sliding; under current, the additives fragmented into finer structures that filled worn surfaces, reinforcing the synergy of CNT rolling, graphene sliding, and interfacial load support to optimize tribological performance.

These examples demonstrate that the integration of electric-field or current-responsive nanocomposites with conventional lubrication strategies can further amplify synergistic effects, enabling precise, on-demand control over friction and wear, and expanding the functional scope of nanomaterial-based lubricants.

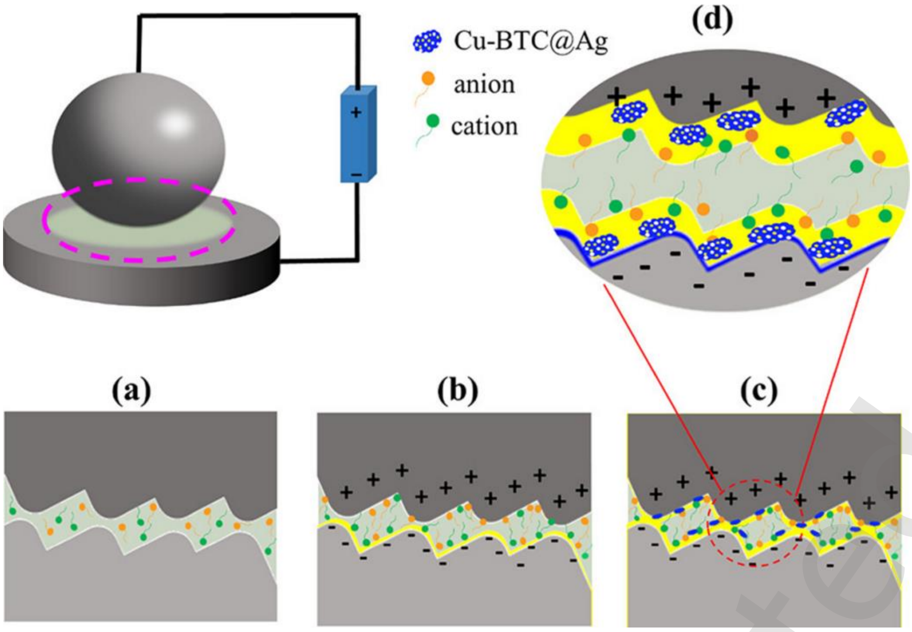

Fig. 31 Diagram of electrically excited friction mechanism of Cu-BTC@Ag nanocrystal lubricant additive: (a) ILs at no voltage applied, (b) ILs at 20 V applied voltage, (c) ILs with Cu-BTC@Ag nanocrystal additive at 20 V applied voltage, and (d) locally enlarged image of ILs with Cu-BTC@Ag nanocrystal additive at 20 V applied voltage. Reproduced with permission from Ref.[229], © American Chemical Society 2023.

To consolidate the above discussion, **Table 4** presents representative nanocomposite systems, allowing a concise comparison of their synergistic lubrication mechanisms across diverse material architectures and operating conditions. Recent studies have further quantified these synergistic behaviors, providing concrete evidence of the cooperative effects between different structural components. For instance, $Ti_3C_2T_x$ MXene nanosheets dispersed in glycerol achieved macroscale superlubricity with an ultralow friction coefficient of 0.002 through the co-formation of dual tribofilms and mixed lubrication regimes [232]. Similarly, alkyl-functionalized black phosphorus nanosheets exhibited stable superlubricity (CoF≈0.006) and over 90% wear reduction due to the synergistic interfacial interactions between surface functionalization and Si-DLC coatings [233]. More recently, Mo_2CT_x MXene nanoparticles in ionic liquids achieved a friction coefficient as low as 0.004 under contact pressures exceeding 1.4 GPa, attributed to the co-deposition of Mo_xO_y/P_xO_y

tribofilms and enhanced load-bearing capacity [234]. Collectively, these findings underscore that the integration of multiple functional components can generate pronounced synergistic effects, whether through surface modification, hybrid assembly, or tribo-chemical coupling, where physical rolling, interfacial adsorption, and tribofilm formation act cooperatively to achieve ultralow friction and superior wear protection.

Despite these advances, several key issues remain unresolved. For instance, determining the optimal additive concentration becomes more challenging when multiple NPs are introduced; the influence of mixed NPs on lubricant stability is not yet fully understood; and whether the incorporation of three or more NP types can yield further performance gains remains an open question. Addressing these challenges will be essential for translating the promising laboratory-scale results of nanocomposite lubricants into robust, large-scale industrial applications.

Table 4 Nanocomposite systems and their synergistic lubrication mechanisms classified by mechanism combinations.

Nanocomposites system	Base lubricant	Concentration	Test conditions	Tribology Performance improvement	Film formation	Micro-bearing	Repair
3D graphene/nano-TiO_2 [235]	Castor oil	0.1 wt%	Four-ball; 304 stainless steel balls; load 392 N; speed 1450 r/min; temperature 25 ℃; time 1800 s	Extreme pressure ↑150%; CoF ↓25.13%, wear rate ↓30.63%	●	●	●
h-BN nanosheets [236]	Sunflower oil	0.05 wt%	Four-ball; AISI 52100 balls; load 147 N; speed 1200 rpm; time 3600 s; temperature 50 ℃	CoF ↓21%, WSD ↓9%	●	●	●
Ag NPs [236]	Soybean oil	0.01 wt%		CoF ↓28%			
MgO NPs [236]	Soybean oil	0.01 wt%		CoF ↓15%			
nano-ZnO/TiO_2 [237]	No. 100 oil (viscosity	0.5 wt%	Four-ball; G10 bearing steel balls; load 300 N;	CoF ↓52%; wear amount ↓66%	●	●	●

	index 68)		speed 1000 rpm; time 1200 min; temperature 50 °C				
CNT/g-C_3N_4/MoS_2 [238]	Paraffin oil	0.2 wt%	Ball-on-disc; GCr15 ball, 45# steel disc; load 5 N; speed 300 rpm; time 30 min	CoF ↓39.23%, wear rate ↓91.97%	●	●	●
PTFE/*h*-BN [239]	Jatropha oil	0.5 wt% PTFE+0.8 wt% *h*-BN	Ball-on-flat; AISI 52100 steel balls; load 20 N; speed 10.5 m/s; time 15-30 min	CoF ↓8.67%-10.98%, wear rate ↓	●	●	●
GO/modified SiO_2 [90]	L-TSA-46A turbine oil	0.03 wt% GO+0.12 wt% modified SiO_2	Four-ball/Timken; GCr15 steel; load 392 N (four-ball); time 1200 s	CoF ↓48.70%, wear ↓60.56%, P_B ↑1.43% (vs. pure GO)	●	●	×
Graphene-encased Cu [240]	Semi-solid lubricant	0.5 wt%	Ball-on-plate; Si_3N_4 ball; load 20-30 N; cycles 2000-20000	Wear rate ↓60.3%-62.5%	●	●	×
N-doped GO quantum dots (NGOQDs)-MoS_2 and NGOQDs-Al_2O_3 [241]	Aqueous glycerol (90% glycerol+10% water)	0.1 wt%	Ball-on-plate; AISI 52100 steel; load 100 N; frequency 10 Hz; stroke 10 mm; time 60 min	CoF ↓32.3%, wear rate ↓54.5%	●	●	×
Graphene/Al_2O_3 [242]	Oleic acid-based nanofluid	1-3 wt%	Nanofluid Minimum Quantity Lubrication grinding; Ti-6Al-4V/ZrO_2 workpieces	Specific grinding energy ↓73.92%; CoF ↓46.57%; surface roughness ↓60.53% (ZrO_2) and 48.66% (Ti-6Al-4V)	●	●	×
Al_2O_3/graphene	Coconut oil	0.1 wt%	Linear reciprocating;	CoF ↓28%; specific fuel	●	●	×

[243]			load 120-200 N; frequency 15-50 Hz; temperature 140 °C	consumption ↓8%; exhaust emissions ↓			
Polycarboxylate superplasticizer modified 3D porous graphene/SiO_2 [244]	cutting fluid	0.03 wt%	Four-ball; GCr15 balls; load 392 N; speed 800 r/min; temperature 25 °C; time 1800 s	P_B ↑39.7%, P_D ↑86.3%; CoF ↓35%, wear rate ↓72.2%	●	●	×
MoS_2 quantum dot/graphene crumpled ball [106]	PAG	0.05 wt%	Reciprocating ball-on-disc; GCr15 steel ball/disc; load 100 N; frequency 5 Hz; amplitude 5 mm; time 2 h; temperature 150 °C	CoF ↓47%, wear rate ↓30% (vs. tricresyl phosphate)	●	●	×
Citric acid modified 3D porous graphene/carbon black [110]	Castor oil	0.2 wt%	Four-ball; GCr15 balls; load 392 N/588 N; speed 1200 rpm; time 1800 s	At 392 N: CoF ↓24.57%, wear ↓70.27%; at 588 N: CoF ↓32.59%, wear ↓56.54%; P_B ↑125.26%	●	●	×
MSH/MoS_2/C [245]	PAO6	1.0 wt%	Reciprocating ball-on-disc; GCr15 disc/ball; load 5-40 N; frequency 15 Hz; temperature 25 °C; time 1-6 h	CoF ↓39.4% (0.104 to 0.063), wear rate ↓56.3% (5.91×10^{-7} to 2.22×10^{-7} $mm^3N^{-1}\cdot m^{-1}$)	●	×	●
Nitrogen-doped graphene/C_{60} [246]	PAO6	0.4:0.5 wt%	Rotary; austenitic stainless steel ball/plate; load 10-20 N; speed 150 rpm; time 30 min	CoF ↓60%, wear volume ↓57%; Z-axis vibration acceleration ↓81%, noise ↓19%	●	×	●
Ricinoleic acid-modified graphene/nanodiam	PAO6	0.1:0.1 wt%	Rotary; austenitic stainless steel ball/plate; load 10 N; speed 120	CoF ↓64%, wear rate ↓71%; average noise sound pressure level ↓3.6 dB(A)	●	×	●

ond [247]			rpm; time 30 min				
GO/CeO_2 nanohybrid [248]	Rapeseed oil	0.1 wt%	Ball-on-disc; 440C stainless steel ball; load 6 N; speed 200 rpm; time 20 min	CoF ↓36.5%, wear rate ↓62.4%	●	×	●
MoS_2/AlOOH nanosheets [249]	PAO4	0.5 wt%	Four-ball; GCr15 steel balls; load 78-118 N; speed 1400 rpm; time 30 min	CoF ↓50.47%, WSD ↓42.34%, wear volume ↓86.57%	●	×	●
γ-AlOOH/*h*-BN composites [25]	Water-based lubricant	0.09-0.12 wt%	Four-ball; GCr15 balls; load 100 N; speed 120 r/min; time 30 min	CoF ↓55.44% (water-glycol), WSD ↓39.45%	●	×	●
Functionalized WS_2/SiO_2+phosphonium ILs [250]	PAO6	0.1 wt% NPs+1 wt% IL	Pure sliding/rolling-sliding; 100Cr6 steel; temperature 120 ℃; load 9.43 N (pure sliding)/50 N (rolling-sliding)	CoF ↓25%, wear area ↓84%	●	×	●
MoS_2-graphene nanohybrid [251]	20W40 diesel-based engine oil	0.05 wt%	Four-ball; GCr15 balls; load 392.5 N; speed 1200 rpm; time 3600 s; temperature 75 ℃	CoF ↓58.82%, WSD ↓36.26%	●	×	×
$Ti_3C_2T_x$ nanoflakes [232]	Glycerol	1 wt%	Ball-on-disk; Si_3N_4-sapphire; load 1-4 N; speed 0.004-0.326 m/s; 25 ℃; a relative humidity of 15%	CoF as low as 0.002 (↓96.90% vs. pure glycerol and ↓97.87% vs. pure MXene)	●		
DTEOS-BP nanosheets [233]	PAO	0.2-0.4 wt%	Reciprocating ball-on-disk; GCr15 balls/Si-DLC film; load 1-4 N; speed 0.014-0.126 m/s;	CoF as low as 0.006 (↓90% vs. Pure BP)	●		

				25 ℃; a relative humidity of 15%		
Mo_2CT_x [234]	MXene	$LiPF_6$-EG ionic liquid	0.083-0.332 wt%	Ball-on-disk; Si_3N_4-sapphire; load 1-6 N; speed 0.004-0.375 m/s; 25 ℃; a relative humidity of 20%-25%.	CoF can maintain at 0.004 for 4.5 hours and achieve superlubricity at a contact pressure of 1.42 GPa.	•

5. Challenges and development trends

Although significant progress has been made in the application of nanocomposites in lubricants, there are still some obstacles and challenges, and there are many aspects worth further research and exploration.

5.1. Fundamental structure and property correlation

The relationship between the composition, structure, and properties of nanocomposites still requires systematic investigation to enable more precise performance optimization. By finely controlling parameters such as particle size, morphology, and crystal structure, as well as the proportion and spatial distribution of each constituent phase, it is possible to achieve targeted regulation of mechanical, thermal, and tribological behaviors. Such control allows for the tailoring of nanocomposites to meet specific lubrication requirements, for example, by balancing load-bearing capacity with interfacial shear reduction, or by enhancing thermal stability without sacrificing dispersion stability.

The integration of computer simulations with advanced material characterization techniques offers an effective approach to accelerating this optimization process. Computational modeling can predict how structure variations influence interfacial interactions, while high-resolution characterization, such as electron microscopy, X-ray spectroscopy, and in situ tribological testing-can validate these predictions and reveal structure-property correlations in real time. Through this combined strategy, nanocomposites with both high lubrication performance and adaptability to diverse operating environments can be developed more rationally and efficiently.

In addition, the growing use of artificial intelligence (AI) and machine learning (ML) tools provides new opportunities to accelerate the discovery of high-performance nanocomposites. Unlike conventional trial-and-error or purely simulation-based approaches, AI can efficiently mine large experimental and computational datasets to identify hidden correlations between structure and tribological performance, rapidly screen vast compositional and structural spaces, and predict optimal design parameters with reduced cost and time. Recent progress has demonstrated the feasibility of ML algorithms in forecasting CoF, WSD, and dispersion stability from structural descriptors, as well as in guiding the rational selection of synthesis conditions [252, 253]. When integrated with high-throughput simulations and automated characterization pipelines, AI-driven approaches are expected to enable closed-loop optimization, thereby advancing the development of nanocomposites tailored for sustainable and application-specific lubrication [254].

Despite these promising prospects, current AI- and ML-assisted lubricant design still faces multiple technical challenges that must be addressed before large-scale implementation becomes feasible. Data-related limitations remain fundamental: experimental datasets are typically small, non-standardized, and lack detailed tribological descriptors, hindering cross-study model transferability. In addition, privacy and intellectual property concerns restrict access to industrial lubricant formulations, constraining collaborative database development. On the modeling side, black-box architectures often lack interpretability and physical consistency, leading to limited trust and generalization across materials and operating conditions. Integrating physical knowledge through physics-informed ML and coupling data-driven models with multi-scale simulations remain open research frontiers. Computational cost and model deployment further complicate real-time applications, particularly in adaptive lubrication systems operating under dynamic loads or temperature variations [255].

Future progress will depend on developing standardized tribological data protocols, establishing open-access databases, and building interpretable, physics-consistent ML frameworks capable of bridging molecular- to macro-scale behavior. Collaborative data-sharing platforms, hybrid modeling strategies combining first-principles and experimental data, and cross-disciplinary training between tribology and data science will be essential to translate the potential of AI into practical lubricant innovation.

5.2. Further research on the lubricating mechanism

The lubrication mechanisms of nanocomposites in lubricants remain incompletely understood, particularly under complex and variable operating conditions. Although improvements in friction and wear behavior have been demonstrated, the fundamental pathways-such as NPs adsorption, tribo-chemical reactions, and phase transformations often hypothesized rather than conclusively verified. Clarifying these processes requires the combined use of macroscopic tribological tests and microscopic or spectroscopic observations that capture the evolution of interfaces during sliding.

Recent research highlights that advanced characterization techniques are indispensable for revealing these mechanisms. For instance, Chen et al. [256] systematically investigated the superlubricity behavior of graphene oxide nanosheets in phosphoric acid through multi-technique analyses, including XPS, HRTEM, EDS, and Raman spectroscopy. Their findings demonstrated that the formation of hybrid tribofilms, hydrogen-bond-assisted hydration layers, and nanosheet-mediated interfacial shearing act synergistically to sustain ultralow friction. Although such studies mainly rely on ex-situ characterization rather than real-time in-situ observation, they nonetheless provide crucial mechanistic evidence that bridges tribochemical processes and structural lubrication effects. This work also underscores the potential of combining nanoscale structural analysis with macroscopic tribological data to develop a unified understanding of lubrication mechanisms.

Progress in this area depends on coupling advanced in situ techniques with theoretical modeling. Methods such as Raman mapping under load, X-ray photoelectron spectroscopy, and transmission electron microscopy can track the formation and degradation of tribofilms in real time, while atomistic and continuum simulations can predict interfacial energetics and particle dynamics. Such an integrated approach would enable the development of more accurate lubrication models, linking nanomaterial properties to performance under specific contact conditions and ultimately guiding the rational design of next-generation lubricant additives, formulation development, and enabling tailored solutions for specific industrial scenarios.

5.3. Adaptation to extreme and special operating conditions

With the advancement of modern industry, mechanical systems are increasingly required to operate under extreme and specialized conditions, such as ultra-high or ultra-low temperatures, strong radiation, high vacuum, and chemically aggressive environments. Under these demanding scenarios, conventional lubricant additives often fail due to thermal degradation, oxidative instability, or phase changes. Nanocomposites offer a promising pathway to address these challenges, as their multifunctional architectures can be engineered to combine thermal resilience, chemical inertness, and mechanical robustness. Designing lubricants specifically for these environments requires not only tailoring the intrinsic properties of nanomaterials, but also ensuring their stability within the base oil and compatibility with surrounding materials.

However, several technical challenges remain before such systems can be widely applied. At high temperatures, nanoparticles tend to aggregate or undergo structural oxidation that weakens tribofilm integrity [257]; at low temperatures, viscosity increases sharply, leading to poor lubricant flow and limited self-healing capability [258]. In vacuum or radiation environments, the absence of reactive species hinders tribochemical film formation, while radiation-induced defects may alter surface chemistry. Addressing these issues requires advanced approaches that couple in situ characterization under extreme conditions with multi-scale modeling to capture temperature and pressure-dependent phenomena.

Future research should therefore focus on systematically studying the performance evolution and failure mechanisms of nanocomposite lubricants under such extreme conditions. This includes investigating structural transformations at high temperatures, phase stability at cryogenic levels, and radiation-induced modifications to both NPs and lubricant matrices. By integrating innovative material design with performance optimization strategies, lubricants capable of meeting the rigorous demands of aerospace, nuclear, deep-sea, and other specialized applications can be developed. Such advancements would not only ensure reliable operation in critical systems but also foster technological progress in fields where conventional lubrication approaches are insufficient.

5.4. Dispersion stability and compatibility in lubricant matrices

The dispersion stability and compatibility of nanocomposites within lubricant matrices remain critical determinants of their tribological performance. Even when NPs possess excellent intrinsic properties, agglomeration or sedimentation can severely limit their effectiveness by reducing active contact with friction surfaces and promoting abrasive wear. Achieving long-term stability requires a detailed understanding of the physicochemical interactions between nanomaterials and base oils, including van der Waals forces, electrostatic interactions, and steric hindrance effects. These interactions are influenced by factors such as NPs size, surface charge, and the polarity and viscosity of the base oil.

However, maintaining stable and compatible nanocomposite dispersions remains a major technical challenge. The presence of detergents, dispersants, and anti-oxidants in industrial lubricant packages can compete with nanocomposite surfaces for adsorption sites, disrupting interfacial equilibrium and reducing additive effectiveness. Moreover, the absence of standardized evaluation methods makes it difficult to compare data across studies. Predicting long-term stability under thermal cycling and shear is equally complex, as subtle variations in surface energy or polarity can lead to delayed aggregation during service.

To address these challenges, future research should focus on developing advanced surface modification strategies and dispersion techniques that enhance the affinity of NPs for lubricant matrices without compromising other properties such as viscosity, oxidation stability, or additive compatibility. Techniques like grafting functional molecules, creating core-shell architectures, or employing dispersant-assisted stabilization have shown promise in preventing NPs aggregation. Systematic evaluation under both static storage and dynamic operating conditions will be necessary to ensure that nanocomposites maintain their dispersion, fully exert their intended functions, and avoid unintended negative effects on lubricant performance during long-term service.

Recent investigations have further highlighted the importance of evaluating nanocomposite-additive compatibility under realistic lubricant conditions. For instance, Yang et al. [259] reported that diatomite-encapsulated Mo_2CT_x MXene microcapsules (DE@Mo_2CT_x) exhibit excellent compatibility with traditional cutting fluids containing dispersants and detergents. The porous diatomite carrier not only prevents nanoparticle aggregation but also enables controlled release and sustained lubrication, avoiding unwanted chemical interactions with conventional additives. Similarly, Yang et al. [260] demonstrated that GO nanosheets could be uniformly dispersed in titanium alloy machining fluids, where their oxygen-containing functional groups enhanced thermal conductivity and reduced interfacial friction without destabilizing the base formulation. These findings suggest that rational surface engineering can effectively mitigate additive interference while maintaining the desired tribological synergy, such as microencapsulation or controlled functionalization. In future work, systematic compatibility testing with full additive packages will be essential to ensure that nanocomposite-enhanced lubricants achieve both superior performance and industrial robustness.

5.5. Industrialization, cost, and sustainability considerations

The outstanding tribological performance of nanocomposites demonstrated at the laboratory scale does not directly guarantee their applicability in industrial settings, where cost, process scalability, and long-term operational reliability are critical. Although raw materials such as CNTs are now available at approximately \$100 kg^{-1} [261], the fabrication of nanocomposites commonly involves additional steps, including surface functionalization, heterostructure assembly, and thermal or chemical post-treatment, which can substantially increase production cost. Therefore, industrial deployment will rely on synthesis routes that minimize processing complexity and enable the use of lower-cost precursor materials. Encouragingly, the market cost of graphene has shown a clear decreasing trend, ranging from \$26-680 kg^{-1} in 2022, with projections suggesting a potential decrease to ~\$12 kg^{-1} by 2028 [262], indicating a positive outlook for cost-accessible nanocomposite formulations.

Beyond cost, the environmental footprint associated with nanomaterial manufacturing remains a key consideration. For instance, energy consumption for graphene production typically ranges from 500-1000 MJ kg^{-1}, which is more than twice that of aluminum (200-300 MJ kg^{-1}) and nearly an order of magnitude higher than polypropylene [263]. A recent life-cycle assessment covering 71 categories of nanomaterials highlighted that environmental impacts vary widely depending on synthesis routes, reactor configuration, thermal treatment steps, and solvent usage [264]. Even processes designed to minimize chemical waste may still generate substantial greenhouse gas emissions if high-temperature or vacuum conditions are required [265]. As such, sustainable scale-up will require strategies including low-energy exfoliation approaches, heat recovery during batch processing, and solvent recycling systems to avoid negating the environmental benefits associated with improved lubrication efficiency.

Regulatory and ecological considerations introduce further complexity. Under the EU REACH framework (Commission Regulation (EU) 2018/1881), any nanoform intended for commercial deployment must undergo comprehensive characterization, including particle size distribution, surface chemistry, reactive byproduct formation, and toxicological impact. Similar obligations exist under the U.S. Toxic Substances Control Act (TSCA), which requires reporting of nanomaterial manufacturing and downstream release. In addition, the potential environmental fate of nanocomposites, including their persistence in wastewater and possible bioaccumulation, necessitates the development of "benign-by-design" additives and closed-loop end-of-life management strategies.

In summary, while nanocomposite-based additives hold considerable promise for enhancing lubricant performance, their industrial adoption requires parallel progress in scalable synthesis, cost reduction, environmental sustainability, and regulatory compliance. Advancing these dimensions in concert with deeper mechanistic understanding and application-specific formulation design will be essential to bridge the gap between laboratory innovation and reliable, sustainable industrial implementation.

6. Conclusion

Nanocomposites have emerged as promising additives in lubricant technology, offering practical routes to overcome the limitations of conventional formulations. Over the past few years, numerous studies have shown that adding nanocomposites can reduce the CoF by 15% -60% and the wear rate by 50% -90%, with specific effects varying depending on the operating conditions. This review has systematically summarized recent advances, focusing on their performance advantages, diverse synthesis routes, and multifaceted lubrication mechanisms.

The enhanced surface activity, tailored electrical conductivity, and synergistic phase interactions of nanocomposites enable them to outperform single-component analogues. Their mechanical robustness, thermal stability, and corrosion resistance make them particularly suited for extreme environments such as high-load (>1 GPa), elevated-temperature (>100 °C), and corrosive conditions. Dispersion strategies such as core-shell architectures and surface functionalization have proven effective in mitigating aggregation, maintaining stable tribological performance over extended test durations.

Synthesis methods, including hydrothermal, sol-gel, chemical deposition, and microwave-assisted processes, offer tunable control over particle size, morphology, and surface chemistry, which directly influence lubrication behavior. However, scaling these approaches while retaining product consistency and cost-effectiveness remains a bottleneck for industrial adoption.

The lubrication mechanisms of nanocomposites are diverse, encompassing the formation of physical adsorption layers, tribo-chemical reaction films, micro-bearing effects, and the restoration of worn surfaces. Synergistic interactions allow adaptation to varying tribological regimes. For example, core-shell systems have demonstrated simultaneous friction reduction and wear protection under both boundary and mixed lubrication conditions.

Despite substantial progress, challenges remain in optimizing NPs concentration, elucidating long-term environmental impacts, and developing energy-efficient, scalable synthesis processes. Addressing these issues will require the integration of eco-friendly fabrication techniques, high-resolution in situ characterization tools, and predictive computational models to clarify complex tribo-chemical pathways.

In conclusion, nanocomposites offer a viable path toward high-performance, sustainable lubrication solutions. With targeted research into their structure-property relationships, mechanistic behavior, and lifecycle impacts, they can deliver measurable gains in energy efficiency, wear reduction, and equipment durability, paving the way for their safe and cost-effective industrial deployment.

Acknowledgements

We acknowledge the financial support provided by the Key Specialized Research & Development and Promotion Project (Scientific and Technological Project) of Henan Province, China (252102230064 & 232102230049), the Basic and Frontier Technology Research Special Project of Nanyang City (24JCQY030), the Science and Technology Tackling Programme Projects of Nan-yang City (24KJGG057), the Interdisciplinary Sciences Project, Nanyang Institute of Technology

(24NGJY005), and the Doctoral Research Foundation Project, Nanyang Institute of Technology (NGBJ-2025-09).

Declaration of competing interest

The authors have no competing interests to declare that are relevant to the content of this article.

Reference

[1] Rosenkranz A, Costa HL, Baykara MZ, Martini A. Synergetic effects of surface texturing and solid lubricants to tailor friction and wear-a review. *Tribol. Int.* **155**: 106792 (2021)

[2] Wang R, Zhang F, Yang K, Xiong Y, Tang J, Chen H, et al. Review of two-dimensional nanomaterials in tribology: Recent developments, challenges and prospects. *Adv. Colloid Interface Sci.* **321**: 103004 (2023)

[3] Zhao J, Yang G, Zhang Y, Zhang S, Zhang C, Gao C, et al. Controllable synthesis of different morphologies of CuO nanostructures for tribological evaluation as water-based lubricant additives. *Friction*. **9**: 963-977 (2021)

[4] Gu Y, Ma L, Yan M, He C, Zhang J, Mou J, et al. Strategies for improving friction behavior based on carbon nanotube additive materials. *Tribol. Int.* **176**: 107875 (2022)

[5] Nyholm N, Espallargas N. Functionalized carbon nanostructures as lubricant additives-A review. *Carbon*. **201**: 1200-1228 (2023)

[6] Duan J, Li L, Tong Y, Chen Z, Deng D, Liu J, et al. Core-shell structured h-BN@ Ni reinforced CoCrNi-based self-lubricating composites. *Surf. Coat. Technol.* **448**: 128939 (2022)

[7] Zhang Y, Chromik RR. Tribology of Self-Lubricating Metal Matrix Composites. In: *Self-Lubricating Composites*. Menezes PL, Rohatgi PK, Omrani E, Ed. Berlin, Heidelberg: Springer Berlin Heidelberg; 2022: 31-71.

[8] Nahr MA, Mirsalehi SE. Additive Friction Stir Deposition of AA5083/MoS_2-Diamond Hybrid Nanocomposites: Investigating Their Metallurgical, Mechanical, Tribological, and Electrochemical Characteristics, and Process-Structure-Property Relationships. *J. Alloys Compd.* **1013**: 178553 (2025)

[9] Wang J, Zhuang W, Liang W, Yan T, Li T, Zhang L, et al. Inorganic nanomaterial lubricant additives for base fluids, to improve tribological performance: Recent developments. *Friction*. **10**(5): 645-676 (2021)

[10] Wang J, Zhang H, Hu W, Li J. Modified Ni Nanoparticles as Additives in Various Greases: Assessment of Comparative Performance Potential. *Lubricants*. **10**(12): 367 (2022)

[11] Pathak R, Punetha VD, Bhatt S, Punetha M. A review on copper-based nanoparticles as a catalyst: synthesis and applications in coupling reactions. *J. Mater. Sci.* **59**(15): 6169-6205 (2024)

[12] Jiang Z, Sun Y, Liu B, Yu L, Tong Y, Yan M, et al. Research progresses of nanomaterials as lubricant additives. *Friction*. **12**(7): 1347-1391 (2024)

[13] Tang W, Zhang Z, Li Y. Applications of carbon quantum dots in lubricant additives: a review. *J. Mater. Sci.* **56**(21): 12061-12092 (2021)

[14] Yu Z, Zhou M, Liu R, Wang Y, Zhang X. Carbon nanomaterials as additives in lubricating oils for tribological applications: A review. *Diamond Relat. Mater.* **156**: 112384 (2025)

[15] Opia AC, Bin Abdollah MF, Syahrullail S, Amiruddin H, Mamah CS, Veza I. Effectiveness of carbon nanomaterials as lubricant additives: Recent review. *Mater. Today Nano*. **30**: 100643 (2025)

[16] Zhang H, Han S, Hu W, Li J. Tribological study of TiO_2 nanoparticles modified with stearic acid as additives in lithium grease. *Ind. Lubr. Tribol.* **73**(6): 904-910 (2021)

[17] Liñeira del Río JM, Mariño F, López ER, Gonçalves DEP, Seabra JHO, Fernández J. Tribological enhancement of potential electric vehicle lubricants using coated TiO_2 nanoparticles as additives. *J. Mol. Liq.* **371**: 121097 (2023)

[18] Szabó ÁI, Tóth ÁD, Leskó MZ, Hargitai H. Investigation of the Applicability of Y_2O_3-ZrO-$_2$ Spherical Nanoparticles as Tribological Lubricant Additives. *Lubricants*. **10**(7): 152 (2022)

[19] Mariño F, Liñeira del Río JM, Gonçalves DEP, Seabra JHO, López ER, Fernández J. Effect of the addition of coated SiO_2 nanoparticles on the tribological behavior of a low-viscosity polyalphaolefin base oil. *Wear*. **530-531**: 205025 (2023)

[20] Li J, Chen B, Dong Z, Yang B, Qiu S, Zhang H, et al. Improved tribological performance of epoxy self-lubricating composite coating by BNNSs/Ag. *Prog. Org. Coat.* **171**: 107020 (2022)

[21] Yin Y, Shi P, Jiang Y, Zhang S, Qing T, Zhou N, et al. Carboxylated cellulose nanofibers and polytetrafluoroethylene nanoparticles as composite additives in poly-α-olefin oil to improve oil retention and tribological performance of oil-impregnated porous polyimide. *Tribol. Int.* **204**: 110507 (2025)

[22] Pham ST, Tieu AK, Sencadas V, Lei W, Liu D, Wan S, et al. Smart-Responsive Colloidal Capsules as an Emerging Tool to Design a Multifunctional Lubricant Additive. *ACS Appl. Mater. Interfaces*. **13**(6): 7714-7724 (2021)

[23] Song W, Yan J, Ji H. Tribological Performance of an Imidazolium Ionic Liquid-Functionalized SiO_2@Graphene Oxide as an Additive. *ACS Appl. Mater. Interfaces*. **13**(42): 50573-50583 (2021)

[24] Jiang H, Hou X, Ma Y, Su D, Qian Y, Ahmed Ali MK, et al. The tribological performance evaluation of steel-steel contact surface lubricated by polyalphaolefins containing surfactant-modified hybrid MoS_2/h-BN nano-additives. *Wear*. **504-505**: 204426 (2022)

[25] Liu R, He L, Li S, Ge C, Li W, Zhang X. Preparation and Tribological Behavior of γ-AlOOH/Hexagonal Boron Nitride Composites as Additives in Water-Based Lubricant. *J. Mater. Eng. Perform.* **34**(12): 11324-11333 (2024)

[26] Chen Y, Li C, Wang X, Zhang L, Tan X, Peng Y, et al. Preparation and Tribological Performance of the Ag/BN Nanocomposite as Additives for Lithium-Based Grease. *Lubricants*. **13**(1): 30 (2025)

[27] Li X, Shi W, Li X, Dong Z, Zhao S, He T, et al. Graphitic carbon nitrogen supporting h-BN nanosheets as lubricating additive: Enhancing mechanism on epoxy composite coating. *Colloids Surf., A*. **719**: 137032 (2025)

[28] Tu C, Yuan R, Qi H, Chen L, Qin X, Yuan J. Does the dispersion method affect the tribological properties of graphene oxide? *Surf. Coat. Technol.* **497**: 131737 (2025)

[29] Hayat A, Sohail M, Hamdy MS, Taha T, AlSalem HS, Alenad AM, et al. Fabrication, characteristics, and applications of boron nitride and their composite nanomaterials. *Surf. Interfaces*. **29**: 101725 (2022)

[30] GadelHak Y, Muhammad A, El-Azazy M, El-Shafie AS, Shibl MF, Mahmoud R. Computer-Aided Design of Large-Scale Nanomaterials Synthesis Processes: A Detailed Review. *ChemBioEng Rev.* **11**(4): e202300075 (2024)

[31] Kumar S, Kumar R. Tribological characteristics of synthesized hybrid nanofluid composed of CuO and TiO_2 nanoparticle additives. *Wear*. **518-519**: 204623 (2023)

[32] Kong W, Sun C, Kong D. Laser cladded TiO_2-Cu composite coatings with high TiO_2 content: Tribological properties by first-principle calculation. *Wear*. **530-531**: 204999 (2023)

[33] Momohjimoh I, Saheb N, Hussein M, Laoui T, Al-Aqeeli N. Electrical conductivity of spark plasma sintered Al-$_2O_3$-SiC and Al_2O_3-carbon nanotube nanocomposites. *Ceram. Int.* **46**(10): 16008-16019 (2020)

[34] Liu C, Zhang G, Yin Y, Li Y. Fabrication of graphene sheets coated with silver nanorods nanocomposite lubricant and their tribological behavior under current carrying. *J. Mater. Sci.* **60**(8): 3735-3750 (2025)

[35] Zhang G, Dong J, Liu C, Yang D, Li Y. Advanced tribological solutions for electrical contacts: graphene nanosheet-silver nanosphere hybrid lubricants. *J. Mater. Sci.*: 1-19 (2025)

[36] Ali A, Andriyana A. Properties of multifunctional composite materials based on nanomaterials: a review. *RSC Adv.* **10**(28): 16390-16403 (2020)

[37] Wu Q, Miao W, Zhang Y, Gao H, Hui D. Mechanical properties of nanomaterials: A review. *Chem. Eng. J.* **9**(1): 259-273 (2020)

[38] Lanfant B, Leconte Y, Debski N, Bonnefont G, Pinault M, Mayne L M, et al. Mechanical, thermal and electrical properties of nanostructured CNTs/SiC composites. *Ceram. Int.* **45**(2): 2566-2575 (2019)

[39] Song S, Gao Z, Lu B, Bao C, Zheng B, Wang L. Performance optimization of complicated structural SiC/Si composite ceramics prepared by selective laser sintering. *Ceram. Int.* **46**(1): 568-575 (2020)

[40] Sharma SK, Saxena KK, Salem KH, Mohammed KA, Singh R, Prakash C. Effects of various fabrication techniques on the mechanical characteristics of metal matrix composites: a review. *Adv. Mater. Process. Te*. **10**(2): 277-294 (2024)

[41] Zeng X, Zhou G, Xu Q, Xiong Y, Luo C, Wu J. A new technique for dispersion of carbon nanotube in a metal melt. *Mater. Sci. Eng., A*. **527**(20): 5335-5340 (2010)

[42] Liu S, Gao F, Zhang Q, Xue Z, Li W. Fabrication of carbon nanotubes reinforced AZ91D composites by ultrasonic processing. *Trans. Nonferrous Met. Soc. China*. **20**(7): 1222-1227 (2010)

[43] Sharifianjazi F, Moradi M, Abouchenari A, Pakseresht AH, Esmaeilkhanian A, Shokouhimehr M, et al. Effects of Sr and Mg dopants on biological and mechanical properties of SiO_{-2}-CaO-P_2O_5 bioactive glass. *Ceram. Int.* **46**(14): 22674-22682 (2020)

[44] Szabó ÁI, Hasan R. Synergistic Effects of CuO and ZnO Nanoadditives on Friction and Wear in Automotive Base Oil. *Appl. Sci.* **15**(15): 8258 (2025)

[45] Sun Q, Song J, Chen S, Shi J, Zhang X, Su Y, et al. Tribological behavior and lubrication mechanism of h-BN/ceramic composites: Effects of h-BN platelet size and ceramic phase. *Tribol. Int.* **187**: 108722 (2023)

[46] Adibnazari S, Imam A, Najafi M. Effects of two-and three-dimensional graphene-based nanomaterials on the fatigue behavior of epoxy nanocomposites. *Mater. Today Commun.* **24**: 101194 (2020)

[47] Wang R, Yue M, Xiong Y, Yue J. Experimental study on mechanism, aging, rheology and fatigue performance of carbon nanomaterial/SBS-modified asphalt binders. *Constr. Build. Mater.* **268**: 121189 (2021)

[48] Li L, Wang X, Du H, Han B. Comparison of compressive fatigue performance of cementitious composites with different types of carbon nanotube. *Int. J. Fatigue*. **165**: 107178 (2022)

[49] Zuo P, Srinivasan DV, Vassilopoulos AP. Review of hybrid composites fatigue. *Compos. Struct.* **274**: 114358 (2021)

[50] Prasadh S, Manakari V, Parande G, Wong RCW, Gupta M. Hollow silica reinforced magnesium nanocomposites with enhanced mechanical and biological properties with computational modeling analysis for mandibular reconstruction. *Int. J. Oral Sci.* **12**(1): 31 (2020)

[51] Shen Y, Lei W, Tang W, Ouyang T, Liang L, Tian ZQ, et al. Synergistic friction-reduction and wear-resistance mechanism of 3D graphene and SiO_2 nanoblend at harsh friction interface. *Wear*. **488-489**: 204175 (2022)

[52] Li P, Ji L, Li H, Chen L, Liu X, Zhou H, et al. Role of nanoparticles in achieving macroscale superlubricity of graphene/nano-SiO_2 particle composites. *Friction*. **10**(9): 1305-1316 (2022)

[53] Zhang R, Li J, Jerrams S, Hu S, Liu L, Wen S, et al. Constructing a fine dispersion and chemical interface based on an electrostatic self-assembly and aqueous phase compound in GO/SiO_2/SBR composites to achieve high-wear resistance in eco-friendly green tires. *Chem. Eng. J.* **452**: 139113 (2023)

[54] Sun Z, Li J, Yu M, Kathaperumal M, Wong C-P. A review of the thermal conductivity of silver-epoxy nanocomposites as encapsulation material for packaging applications. *Chem. Eng. J.* **446**: 137319 (2022)

[55] Jebasingh BE, Arasu AV. A detailed review on heat transfer rate, supercooling, thermal stability and reliability of nanoparticle dispersed organic phase change material for low-temperature applications. *Mater. Today Energy*. **16**: 100408 (2020)

[56] Rahman M, Islam KS, Dip TM, Chowdhury MFM, Debnath SR, Hasan SMM, et al. A review on nanomaterial-based additive manufacturing: Dynamics in properties, prospects, and challenges. *Prog. Addit. Manuf.* **9**(4): 1197-1224 (2024)

[57] Wang S, Ren G, Li W, Wang B, Wei F, Liang Z, et al. A green modification technology of carbon nanotubes toward enhancing the tribological properties of aqueous-based lubricants. *Tribol. Int.* **180**: 108268 (2023)

[58] Ali MKA, Xianjun H. Improving the heat transfer capability and thermal stability of vehicle engine oils using Al_2O_3/TiO_2 nanomaterials. *Powder Technol.* **363**: 48-58 (2020)

[59] Barani Z, Mohammadzadeh A, Geremew A, Huang CY, Coleman D, Mangolini L, et al. Thermal properties of the binary-filler hybrid composites with graphene and copper nanoparticles. *Adv. Funct. Mater.* **30**(8): 1904008 (2020)

[60] Pavía M, Alajami K, Estellé P, Desforges A, Vigolo B. A critical review on thermal conductivity enhancement of graphene-based nanofluids. *Adv. Colloid Interface Sci.* **294**: 102452 (2021)

[61] Huang X, Zhi C, Lin Y, Bao H, Wu G, Jiang P, et al. Thermal conductivity of graphene-based polymer nanocomposites. *Mater. Sci. Eng., R*. **142**: 100577 (2020)

[62] Moradi A, Zareh M, Afrand M, Khayat M. Effects of temperature and volume concentration on thermal conductivity of TiO_2-MWCNTs (70-30)/EG-water hybrid nano-fluid. *Powder Technol.* **362**: 578-585 (2020)

[63] Tian X, Kalbasi R, Qi C, Karimipour A, Huang H. Efficacy of hybrid nano-powder presence on the thermal conductivity of the engine oil: an experimental study. *Powder Technol.* **369**: 261-269 (2020)

[64] Asadi A, Asadi M, Rezaniakolaei A, Rosendahl LA, Afrand M, Wongwises S. Heat transfer efficiency of Al_2O_3-MWCNT/thermal oil hybrid nanofluid as a cooling fluid in thermal and energy management applications: An experimental and theoretical investigation. *Int. J. Heat Mass Transfer*. **117**: 474-486 (2018)

[65] Cao F, Zhang Y, Wang H, Khan K, Tareen AK, Qian W, et al. Recent Advances in Oxidation Stable Chemistry of 2D MXenes. *Adv. Mater.* **34**(13): 2107554 (2022)

[66] Iqbal A, Hong J, Ko TY, Koo CM. Improving oxidation stability of 2D MXenes: synthesis, storage media, and conditions. *Nano Convergence*. **8**(1): 9 (2021)

[67] Sun B, Hu P, Ji X, Fan M, Zhou L, Guo M, et al. Excellent stability in polyetherimide/SiO_2 nanocomposites with ultrahigh energy density and discharge efficiency at high temperature. *Small*. **18**(28): 2202421 (2022)

[68] Hu R, Wen S, Chen Q, Sun X, Liu H, Gao W, et al. Universal Construction of Electrical Insulation and High-Thermal-Conductivity Composites Based on the In Situ Exfoliation of Boron Nitride-Graphene Hybrid Filler. *ACS Appl. Mater. Interfaces*. **17**(4): 6783-6792 (2025)

[69] Jiang H, Li J, Xie Y, Guo H, He M, Shi X, et al. Design of efficient microstructured path by magnetic orientation boron nitride nanosheets/$MnFe_2O_4$ enabling waterborne polyurethane with high thermal conductivity and flame retardancy. *J. Mater. Sci. Technol.* **209**: 207-218 (2025)

[70] Marian M, Berman D, Rota A, Jackson RL, Rosenkranz A. Layered 2D nanomaterials to tailor friction and wear in machine elements-A review. *Adv. Mater. Interfaces*. **9**(3): 2101622 (2022)

[71] Fu Q, Zhang P, Zhuang L, Zhou L, Zhang J, Wang J, et al. Micro/nano multiscale reinforcing strategies toward extreme high-temperature applications: Take carbon/carbon composites and their coatings as the examples. *J. Mater. Sci. Technol.* **96**: 31-68 (2022)

[72] Randis R, Darmadi DB, Gapsari F, Sonief AAa, Akpan ED, Ebenso EE. The potential of nanocomposite-based coatings for corrosion protection of metals: a review. *J. Mol. Liq.* **390**: 123067 (2023)

[73] Mathew ZP, Shamnamol G, Greeshma K, John S. Insight on the corrosion inhibition of nanocomposite chitosan/boron nitride integrated epoxy coating system against mild steel. *Corrosion Communications*. **9**: 36-43 (2023)

[74] Yang P, Huang Y, Li R, Huang X, Ruan H, Shou M, et al. Optimization of Fe@Ag core-shell nanowires with improved impedance matching and microwave absorption properties. *Chem. Eng. J.* **430**: 132878 (2022)

[75] Han F, Song Z, Xu J, Dai M, Luo S, Han D, et al. Oxidized titanium carbide MXene-enabled photoelectrochemical sensor for quantifying synergistic interaction of ascorbic acid based antioxidants system. *Biosens. Bioelectron.* **177**: 112978 (2021)

[76] Wang L, Fu Q, Zhao F. Improving oxidation resistance of $MoSi_2$ coating by reinforced with Al_2O_3 whiskers. *Intermetallics*. **94**: 106-113 (2018)

[77] AhadiParsa M, Dehghani A, Ramezanzadeh M, Ramezanzadeh B. Rising of MXenes: Novel 2D-functionalized nanomaterials as a new milestone in corrosion science-a critical review. *Adv. Colloid Interface Sci.* **307**: 102730 (2022)

[78] Farag AA. Applications of nanomaterials in corrosion protection coatings and inhibitors. *Corros. Rev.* **38**(1): 67-86 (2020)

[79] Pourhashem S, Ghasemy E, Rashidi A, Vaezi MR. A review on application of carbon nanostructures as nanofiller in corrosion-resistant organic coatings. *J. Coat. Technol. Res.* **17**(1): 19-55 (2020)

[80] Liu L, Zhao M, Pei X, Liu S, Luo S, Yan M, et al. Improving corrosion resistance of epoxy coating by optimizing the stress distribution and dispersion of SiO_2 filler. *Prog. Org. Coat.* **179**: 107522 (2023)

[81] Chen C, Yu M, Xiao J, Jiang M, Liu Y, Wang R, et al. One-step in-situ growth by one-pot method for uniform BTA@ZIF-8 layer to improve the corrosion protection of sol-gel coatings. *Corros. Sci.* **250**: 112887 (2025)

[82] Zafar S, Kahraman R, Shakoor R. Silane functionalization of titania-graphene oxide nanocomposite for superior anticorrosion polyurethane coatings on steel. *Colloids Surf., A*. **703**: 135434 (2024)

[83] Huo S, Guo Y, Yang Q, Wang H, Song P. Two-Dimensional Nanomaterials for Flame Retardant Polymer Composites: A Mini Review. *Adv. Nanocompos.* **1**(1): 240-247 (2024)

[84] Lavagna L, Nisticò R, Musso S, Pavese M. Functionalization as a way to enhance dispersion of carbon nanotubes in matrices: A review. *Mater. Today Chem.* **20**: 100477 (2021)

[85] Kamae T, Drzal LT. Carbon fiber/epoxy composite property enhancement through incorporation of carbon nanotubes at the fiber-matrix interphase-Part I: The development of carbon nanotube coated carbon fibers and the evaluation of their adhesion. *Composites, Part A*. **43**(9): 1569-1577 (2012)

[86] Wei Y, Dai L, Sheng C, Liao H, Hou X. Tribological Properties of $TiO\text{-}_2$@CTAB Core-Shell Nanopowders as Lubricating Additives. *ACS Appl. Nano Mater.* **6**(15): 14177-14190 (2023)

[87] Samanta S, Sahoo RR. Covalently Linked Hexagonal Boron Nitride-Graphene Oxide Nanocomposites as High-Performance Oil-Dispersible Lubricant Additives. *ACS Appl. Nano Mater.* **3**(11): 10941-10953 (2020)

[88] Gong K, Lou W, Zhao G, Wu X, Wang X. MoS_2 nanoparticles grown on carbon nanomaterials for lubricating oil additives. *Friction*. **9**(4): 747-757 (2020)

[89] Sun J, Ge C, Wang C, Li S. Tribological behavior of graphene oxide-Fe_3O_4 nanocomposites for additives in water-based lubricants. *Fullerenes, Nanotubes Carbon Nanostruct.* **30**(8): 863-872 (2022)

[90] Yang Z, Guo J, Dang P, Gong B. Tribological properties of GO/modified SiO_2 combination as lubricant additive for bearings. *Tribol. Int.* **199**: 109946 (2024)

[91] Morshed A, Wu H, Ren M, Xing Z, Jiao S, Jiang Z. A Study of Water-Based Nanolubricants Using Hexagonal Boron Nitride (hBN)-Based Nanocomposites as Lubricant Additives. *Lubricants*. **12**(4): 123 (2024)

[92] Jin B, Zhao J, Chen G, He Y, Huang Y, Luo J. In situ synthesis of Mn_3O_4/graphene nanocomposite and its application as a lubrication additive at high temperatures. *Appl. Surf. Sci.* **546**: 149019 (2021)

[93] Jia S, Zhao J, Hao G, Feng J, Zhang C, Wang Z, et al. Preparation and Tribological Behavior of Nitrogen-Doped Carbon Nanotube/Ag Nanocomposites as Lubricant Additives. *Lubricants*. **11**(10): 443 (2023)

[94] Liñeira del Río JM, Rial R, López ER, Fernández J. Tribological enhancement using Mn_3O_4-Graphene nanocomposites as additives for potential transmission fluids of electric vehicles. *J. Mol. Liq.* **366**: 121097 (2022)

[95] Yang H, Cui Y, Yang K, Wang Y, Wang Y, Ye Q, et al. Boosting the tribological properties by developing a g-C3N4/RGO nanocomposite as lubricant additive. *Tribol. Int.* **199**: 109996 (2024)

[96] Wang L, Gong P, Li W, Luo T, Cao B. Mono-dispersed Ag/Graphene nanocomposite as lubricant additive to reduce friction and wear. *Tribol. Int.* **146**: 106228 (2020)

[97] Yi S, Li J, Zuo Z, Fu J, Chen H, Yang L, et al. Mechanochemical exfoliation of sugar-assisted boron nitride nanosheets for achieving superlubricity and wear distinction. *Wear*. **554-555**: (2024)

[98] Kumara C, Luo H, Leonard DN, Meyer HM, Qu J. Organic-Modified Silver Nanoparticles as Lubricant Additives. *ACS Appl. Mater. Interfaces*. **9**(42): 37227-37237 (2017)

[99] Wang X, Liu H, Zhao Q, Wang X, Lou W. Viscosity Variations and Tribological Performances of Oleylamine-Modified Fe_3O_4 Nanoparticles as Mineral Oil Additives. *Lubricants*. **11**(3): 149 (2023)

[100] Wang X, Ye X. Effect of morphology on tribological properties of Fe_3O_4 as lubricant additive: Nanospheres, nanowires and nanosheets. *Tribol. Int.* **191**: 109201 (2024)

[101] Gong P, Wang W, Xue M, Liu P, Ding S, Yu C. Tribological Behaviors and the Lubrication Mechanism of Functionalized Boron Nitride Nanosheet-Containing Fluid for Titanium Alloy Cold Rolling. *ACS Appl. Nano Mater.* **7**(8): 9745-9756 (2024)

[102] Zhang Y, Cheng J, Lu C, Chen H, Xie G, Zhang L, et al. Tribological Properties of Polydopamine-Modified Ag as Lubricant Oil Additives. *Lubricants*. **10**(12): 343 (2022)

[103] Ghasemy Piranloo F, Bavarsiha F, Dadashian S. Tribological properties of core/shell Fe_3O_4/TiO_2 composites as additives in base oil. *J. Sol-Gel Sci. Technol.* **103**(3): 908-920 (2022)

[104] Dong S, Wang W, Gao Y, Wang K. Black Phosphorus Quantum Dots with a Core-Shell Nanostructure as a Water-Based Lubrication Additive. *ACS Appl. Nano Mater.* **6**(10): 8506-8514 (2023)

[105] Ao D, Fan X, Zhu M. C@Ag core-shell structure as lubricating additives towards high efficient lubrication. *Friction*. **12**(9): 1991-2003 (2024)

[106] Du G, Zhang Y, Fan S, Song N, Zhang S, Zhang P. Self-dispersed molybdenum disulfide quantum dot/graphene crumpled ball as efficient high temperature lubricant additive. *Friction*. **12**(8): 1771-1784 (2024)

[107] Jia Q, Yin J, Dai B, Wang X, Han Y, Liu W. Silver-modified polydopamine-coated silica core-shell nanospheres as functional additives for lubricants and shear thickening fluids. *Tribol. Int.* **201**: 110192 (2025)

[108] Li S, Wu Y, Zhao W. P(MMA-GMA-AM-St) as transition layer for constructing GO@pPTFE core-shell nanoparticles as hydro-based lubricant additives towards excellent friction reduction and wear resistance. *Carbon*. **232**: 119828 (2025)

[109] Xu X, Su F, Yu H, Liu R, Xu Z. Black phosphorus nanosheet dotted with Fe_3O_4-PDA nanoparticles: A novel lubricant additive for tribological applications. *Tribol. Int.* **207**: 110607 (2025)

[110] Fei J, Zhao L, Zheng Q, Wei W, Liang L, Tian ZQ. Tribological properties and molecular dynamics analysis of citric acid modified 3D porous graphene/carbon black as lubricant additives. *Tribol. Int.* **208**: 110648 (2025)

[111] Liu R, Guo D, Du X, Du G, Zhang X. Fabrication of surface-carbonated boron nitride nanosheets and their application as water-based lubrication additives. *Wear*. **560-561**: 205633 (2025)

[112] Li Z, Guan Q, Liu S, Bao J, Ding H, Wang W. Friction-reducing and anti-wear performance of SiO_2-Coated TiN nanoparticles in gear oil. *Wear*. **538-539**: 205219 (2024)

[113] Spikes H. Mechanisms of ZDDP-An Update. *Tribol. Lett.* **73**(1): 38 (2025)

[114] Hong Y, Mo Y, Lv J, Wang J. Tribological Properties of Polymer Friction Improvers Combined with MoDTC/ZDDP at Different Temperatures. *Lubricants*. **11**(5): 196 (2023)

[115] Lei X, Zhang Y, Zhang S, Yang G, Zhang C, Zhang P. Study on the mechanism of rapid formation of ultra-thick tribofilm by CeO_2 nano additive and ZDDP. *Friction*. **11**(1): 48-63 (2022)

[116] Mittal P, Rai H, Kumari S, Khatri OP, Gosvami NN. Efficient friction and wear reduction of Al-Si alloy via tribofilms generated from synergistic interaction of ZDDP and chemically functionalized h-BN additives. *Appl. Surf. Sci.* **595**: 153520 (2022)

[117] Segu DZ, Kim CL. Performance of composite ZrO_2/MoDTC nanolubricant as an effective anti-friction and - Wear oil-based additive. *Wear*. **536-537**: 205178 (2024)

[118] Zhang L, Li N. Tribological investigation of graphene or/and MoDTC as additives in PAO base oil. *Diamond Relat. Mater.* **136**: 110043 (2023)

[119] Zhang Y, Zhang Y, Zhang S, Yang G, Gao C, Zhou C, et al. One step synthesis of ZnO nanoparticles from ZDDP and its tribological properties in steel-aluminum contacts. *Tribol. Int.* **141**: 105890 (2020)

[120] Wang J, Li Z, Zhao H, Ren S, Wang C, Huang X, et al. Synergistic effects between sulfur- and phosphorus-free organic molybdenums and ZDDP as lubricating additives in PAO 6. *Tribol. Int.* **165**: 107324 (2022)

[121] Maurya U, Vasu V, Kashinath D. Ionic Liquid-Nanoparticle-Based Hybrid-Nanolubricant Additives for Potential Enhancement of Tribological Properties of Lubricants and Their Comparative Study with ZDDP. *Tribol. Lett.* **70**(1): 11 (2022)

[122] Farfan Cabrera LI, Hernández Peña A, Resendiz Calderon CD, Lee P, Sanchez C, Lee S, et al. Electrified four-ball testing of ZDDP and MoDTC as additives in low-viscosity synthetic oil. *Wear*. **571**: 205835 (2025)

[123] Yadav S, Sharma A. Importance and challenges of hydrothermal technique for synthesis of transition metal oxides and composites as supercapacitor electrode materials. *J. Storage Mater.* **44**: 103295 (2021)

[124] Lomakin M, Proskurina O, Sergeev A, Buryanenko I, Semenov V, Voznesenskiy S, et al. Crystal structure and optical properties of the Bi-Fe-W-O pyrochlore phase synthesized via a hydrothermal method. *J. Alloys Compd.* **889**: 161598 (2021)

[125] Amaya-García F, Caldera M, Koren A, Kubicek S, Menche J, Unterlass MM. Green Hydrothermal Synthesis of Fluorescent 2, 3-Diarylquinoxalines and Large-Scale Computational Comparison to Existing Alternatives. *ChemSusChem*. **14**(8): 1853-1863 (2021)

[126] Lai H, Zhao Z, Yu W, Lin Y, Feng Z. Physicochemical and Antibacterial Evaluation of TiO_2/CNT Mesoporous Nanomaterials Prepared by High-Pressure Hydrothermal Sol-Gel Method under an Ultrasonic Composite Environment. *Molecules*. **28**(7): 3190 (2023)

[127] Liu MM, Ma SY, Cai YH, Ma NN, Wang L, Sheng H. ZnO/$ZnCo_2O_4$ composite prepared by one-step hydrothermal method for high-performance ethylene glycol sensor. *Ceram. Int.* **48**(15): 22305-22312 (2022)

[128] Zhang H, Chang Q. Friction-induced rehybridization of hydrothermal amorphous carbon in magnesium silicate hydroxide-based nanocomposite. *Carbon*. **155**: 650-659 (2019)

[129] Wang B, Chang Q, Gao K, Wang K. Hydrothermal synthesized magnesium silicate hydroxide/graphene nanocomposites in a MgO-SiO_2-graphite-H_2O alkaline system and its application in anti-wear additive toward infinitesimal wear. *Tribol. Int.* **148**: 106313 (2020)

[130] Mou Z, Yang Q, Peng J, Yan R, Zhao B, Ge Y, et al. One-step green synthesis of oil-dispersible carbonized polymer dots as eco-friendly lubricant additives with superior dispersibility, lubricity, and durability. *J. Colloid Interface Sci.* **623**: 762-774 (2022)

[131] Liu X, Le K, Wang J, Lin H, Liu Y, Jiang F, et al. Synergistic lubrication of multilayer $Ti_3C_2T_x$@ MoS_2 composite coatings via hydrothermal synthesis. *Appl. Surf. Sci.* **668**: 160400 (2024)

[132] Guan Z, Zhang P, Florian V, Wu Z, Zeng D, Liu J, et al. Preparation and tribological behaviors of magnesium silicate hydroxide-MoS_2 nanoparticles as lubricant additive. *Wear*. **492-493**: 204237 (2022)

[133] Xiong S, Zhang J, Wu C. Effect of Nano-BN/Si and BN/Al_2O_3 on Friction and Wear Properties of AlN Plate Immersed in the Lubricants. *Tribol. Lett.* **71**(3): 103 (2023)

[134] Zhao Z, Fan X, Li W, He Y, Sun Q, Zhu M. Multi-layer interface lubrication of in-situ synthesized titanium dioxide/reduced graphene oxide nanocomposites. *Appl. Surf. Sci.* **604**: 154571 (2022)

[135] Meng FS, Li Z, Ding HH, Hu JS, Wang WJ, Guo J, et al. Study on the preparation and tribological properties of BN@C-OA nano-additive lubricants. *Wear*. **474-475**: 203876 (2021)

[136] Mezentseva L, Osipov A, Ugolkov V, Kruchinina I, Maslennikova T, Koptelova L. Sol-gel synthesis of precursors and preparation of ceramic composites based on $LaPO_4$ with Y_2O_3 and ZrO_2 additions. *J. Sol-Gel Sci. Technol.* **92**: 427-441 (2019)

[137] Gevaudan JP, Wallat JD, Lama B, Srubar III WV. PVA-and PEG-assisted sol-gel synthesis of aluminosilicate precursors for N-A-S-H geopolymer cements. *J. Am. Ceram. Soc.* **103**(2): 859-877 (2020)

[138] De A, Kim MS, Adhikari A, Patel R, Kundu S. Sol-gel derived nanostructure electrocatalysts for oxygen evolution reaction: A review. *J. Mater. Chem. A*. **12**(31): 19720-19756 (2024)

[139] Tinoco Navarro LK, Jaroslav C. Enhancing photocatalytic properties of TiO_2 photocatalyst and heterojunctions: a comprehensive review of the impact of biphasic systems in aerogels and xerogels synthesis, methods, and mechanisms for environmental applications. *Gels*. **9**(12): 976 (2023)

[140] Bokov D, Turki Jalil A, Chupradit S, Suksatan W, Javed Ansari M, Shewael IH, et al. Nanomaterial by sol-gel method: synthesis and application. *Adv. Mater. Sci. Eng.* **2021**(1): 5102014 (2021)

[141] Lei Q, Guo J, Noureddine A, Wang A, Wuttke S, Brinker CJ, et al. So-gel-based advanced porous silica materials for biomedical applications. *Adv. Funct. Mater.* **30**(41): 1909539 (2020)

[142] Sivasamy R, Venugopal P, Mosquera E. Synthesis of Gd_2O_3/CdO composite by sol-gel method: Structural, morphological, optical, electrochemical and magnetic studies. *Vacuum*. **175**: 109255 (2020)

[143] Sobhani A. $CuMn_2O_4/Mn_2O_3$ micro composites: Sol-gel synthesis in the presence of sucrose and investigation of their photocatalytic properties. *Arabian J. Chem.* **16**(10): 105201 (2023)

[144] Yetim T, Turalioğlu K, Taftali M, Tekdir H, Kovaci H, Yetim AF. Synthesis and characterization of wear and corrosion resistant Ni-doped Al_2O_3 nanocomposite ceramic coatings by sol-gel method. *Surf. Coat. Technol.* **444**: 128659 (2022)

[145] Ge H, Yao X, Wang J, Li G, Li D, You N, et al. Sol-gel derived red fluorescent nanocomposites of copper nanoclusters conjugated silica for visualizing latent fingerprints. *Compos. Commun.* **49**: 101979 (2024)

[146] Sang W, Yang X, Tian H, Wang J, Wang Y, Li Z. Properties of SiO_2-B_2O_3-Li_2O-ZnO-Al_2O_3 glass-ceramic-coated diamond particles prepared by sol-gel method. *Diamond Relat. Mater.* **139**: 110392 (2023)

[147] Haldorai Y, Kumar RS, Ramesh S, Kumar RTR, Yang W. Sol-gel synthesized CuO nanoparticles supported on reduced graphene oxide nanocomposite for sunlight-catalytic methylene blue degradation and nanofluid applications. *J. Sol-Gel Sci. Technol.* **111**(3): 689-702 (2024)

[148] Wang W, Chang W, Ding S, Qu Y, Gao Y, Wang K. Preparation and tribological properties of multi-layer graphene/silicon dioxide composites-based solid lubricant coatings at elevated temperatures. *R. Soc. Open Sci.* **10**(2): 220740 (2023)

[149] Zhang C, Zhang S, Yu L, Zhang Z, Wu Z, Zhang P. Preparation and tribological properties of water-soluble copper/silica nanocomposite as a water-based lubricant additive. *Appl. Surf. Sci.* **259**: 824-830 (2012)

[150] López TD-F, González AF, Del Reguero Á, Matos M, Díaz-García ME, Badía-Laíño R. Engineered silica nanoparticles as additives in lubricant oils. *Sci. Technol. Adv. Mater.* **16**(5): 055005 (2015)

[151] Kumar A, Yadav N, Bhatt M, Mishra N, Chaudhary P, Singh R. Sol-Gel Derived Nanomaterials and It's Applications: A Review. *Res. J. Chem. Sci.* **5**: 1-6 (2015)

[152] Barrino F. Hybrid Organic-Inorganic Materials Prepared by Sol-Gel and Sol-Gel-Coating Method for Biomedical Use: Study and Synthetic Review of Synthesis and Properties. *Coatings*. **14**(4): 425 (2024)

[153] Yang T, Zhao Q, Hu M, Wang X, Zhao G, Gong K, et al. Tribological behavior of novel core-shell Fe_3O_4@PEG nano-additives. *Tribol. Lett.* **70**(4): 116 (2022)

[154] Zhang Y, Guo X, Li Z, Wang C, Liu T, Zhang K. Study on the tribological properties of Fe_3O_4@ CNTs nanofluids acting on the textured ceramics. *Appl. Phys. A*. **128**(2): 161 (2022)

[155] Xiang S, Zhi X, Bao H, He Y, Zhang Q, Lin S, et al. Tribological Behavior of GTL Base Oil Improved by Ni-Fe Layered Double Hydroxide Nanosheets. *Lubricants*. **12**(5): 146 (2024)

[156] Lawal Su, Dambatta YS, Kuburi LS, Kaisan MU. Analysis of physicochemical and tribological properties of nano alumina-based gear oil developed from effluent of lube oil blending plant. *Ind. Crops Prod.* **209**: 117936 (2024)

[157] Dippong T, Levei EA, Cadar O. Recent advances in synthesis and applications of MFe_2O_4 (M= Co, Cu, Mn, Ni, Zn) nanoparticles. *Nanomaterials*. **11**(6): 1560 (2021)

[158] Sobhani A, Alinavaz S. Co-precipitation synthesis of $CuMn_2O_4$/CuMnO nanocomposites without capping agent and investigation of their applications for removing pollutants from wastewater. *Biomass Convers. Biorefin.* **14**(22): 28901-28911 (2024)

[159] Patil S, Jagadale S. Chapter 3 - Co-precipitation methods for the synthesis of metal oxide nanostructures. In: *Solution Methods for Metal Oxide Nanostructures*. Mane R, Jadhav V, Al-Enizi A, Ed. Amsterdam: Elsevier; 2023: 39-60.

[160] Saremi A, Mirkazemi SM, Sazvar A, Rezaie H. Controlling magnetic and surface properties of cobalt ferrite nanoparticles: A comparison of co-precipitation and solvothermal synthesis methods. *Solid State Sci.* **148**: 107432 (2024)

[161] Wu C, Li S, Chen Y, Yao L, Li X, Ni J. Tribological properties of chemical composite and physical mixture of ZnO and SiO_2 nanoparticles as grease additives. *Appl. Surf. Sci.* **612**: 155932 (2023)

[162] Wu C, Li S, Ni J, Yao L, Xia Q. Effect of structure of ZnO and SiO_2 core-shell composite nanoparticles as lubricant additive on tribological properties of greases. *Appl. Surf. Sci.* **657**: 159745 (2024)

[163] Yang K, Xia Y, Chen W, Zhang Y. Improving frictional and insulation performance with silica-coated titanium dioxide additives in grease. *Ind. Lubr. Tribol.* **76**(6): 737-746 (2024)

[164] Fang JH, Chen BS, Wang XC, Wang J, Wu J. Synthesis and tribological behaviors of SiO_2/SnO_2 composite nanoparticles in rapeseed oil. *Appl. Mech. Mater.* **713**: 2928-2932 (2015)

[165] Zhao J, Huang Y, He Y, Shi Y. Nanolubricant additives: A review. *Friction*. **9**(5): 891-917 (2021)

[166] Schwenke AM, Hoeppener S, Schubert US. Synthesis and modification of carbon nanomaterials utilizing microwave heating. *Adv. Mater.* **27**(28): 4113-4141 (2015)

[167] Głowniak S, Szczęśniak B, Choma J, Jaroniec M. Advances in microwave synthesis of nanoporous materials. *Adv. Mater.* **33**(48): 2103477 (2021)

[168] Kumar A, Kuang Y, Liang Z, Sun X. Microwave chemistry, recent advancements, and eco-friendly microwave-assisted synthesis of nanoarchitectures and their applications: a review. *Mater. Today Nano*. **11**: 100076 (2020)

[169] Wang S, Liang Z, Wang B, Gui Y, Ren G, Cao Y, et al. Synthesis of lubricant additive for castor oil: A green and fast approach. *J. Mol. Liq.* **411**: 125800 (2024)

[170] Fu M, Zhu Z, Chen W, Yu H, Liu Q. Microwave-assisted synthesis of MoS_2/graphene composites for supercapacitors. *J. Mater. Sci.* **55**(34): 16385-16393 (2020)

[171] Sun Y, Du X, Zhang J, Huang N, Yang L, Sun X. Microwave-assisted preparation and improvement mechanism of carbon nanotube@$NiMn_2O_4$ core-shell nanocomposite for high performance asymmetric supercapacitors. *J. Power Sources*. **473**: 228609 (2020)

[172] Sahoo S, Al Mahmud A, Sood A, Dhakal G, Tiwari SK, Zo S, et al. Microwave-assisted facile synthesis of graphitic-C_3N_4/reduced graphene oxide/MoS_2 composite as the bifunctional electrocatalyst for electrochemical water splitting. *J. Sci.: Adv. Mater. Devices*. **10**(1): 100843 (2025)

[173] Liu H, Xie M, Pan B, Wang B, Zhang L, Zhou Y, et al. Boosting the tribological properties of PEG200 by a novel face-to-face FeOCl/Zn-MOF lubricant additive. *J. Mol. Liq.* **391**: 123409 (2023)

[174] Jaiswal V, Kalyani, Umrao S, Rastogi RB, Kumar R, Srivastava A. Synthesis, characterization, and tribological evaluation of TiO_2-reinforced boron and nitrogen co-doped reduced graphene oxide based hybrid nanomaterials as efficient antiwear lubricant additives. *ACS Appl. Mater. Interfaces*. **8**(18): 11698-11710 (2016)

[175] Salah N, Alshahrie A, Abdel-wahab MS, Alharbi ND, Khan ZH. Carbon nanotubes of oil fly ash integrated with ultrathin CuO nanosheets as effective lubricant additives. *Diamond Relat. Mater.* **78**: 97-104 (2017)

[176] Kumar A, Behera B, Ray SS. Microwave-assisted surface-initiated redox polymerization of acrylamide with functionalized graphene oxide for aqueous lubricant additive. *RSC Adv.* **5**(49): 39474-39481 (2015)

[177] Saxena M, Sharma AK, Srivastava AK, Singh RK, Dixit AR, Nag A, et al. Microwave-Assisted Synthesis, Characterization and Tribological Properties of a *g*-C_3N_4/MoS_2 Nanocomposite for Low Friction Coatings. *Coatings*. **12**(12): 1840 (2022)

[178] Meng LY, Wang B, Ma MG, Lin KL. The progress of microwave-assisted hydrothermal method in the synthesis of functional nanomaterials. *Mater. Today Chem.* **1**: 63-83 (2016)

[179] Kim SC, Ri YS, Ju DG. A new method to improve homogeneity and oxidation stability of Cu nanoparticles for lubricant additive in liquid phase reduction process. *Mater. Res. Express*. **10**(3): 035007 (2023)

[180] Cui Y, Xue S, Wang T, Liu S, Ye Q, Zhou F, et al. Core-rim structured MXene@SiO_2 composites as oil-based additives for enhanced tribological properties. *Friction*. **12**(8): 1728-1740 (2024)

[181] Wu L, Wang F, Zhang C, Zhang X, Gu L, Shi W. Silver/Graphene Nanocomposite as an Additive for Aqueous Lubrication. *ACS Appl. Nano Mater.* **6**(3): 1603-1609 (2023)

[182] Liang F, Chen C, Xue H, He Q, Cai M, Zhou Y, et al. Toward high-performance lubricants: Rational design and construction of supramolecular oil gels by amphiphilic telechelic polymers to stabilize two-dimensional nanomaterials in base oils. *Tribol. Int.* **184**: 108468 (2023)

[183] Zhang J, Jiang D, Wang D, Yu Q, Bai Y, Cai M, et al. MoS_2 lubricating film meets supramolecular gel: a novel composite lubricating system for space applications. *ACS Appl. Mater. Interfaces*. **13**(48): 58036-58047 (2021)

[184] Wang T, Xue S, He B, Liu S, Ye Q, Zhou F, et al. Liquid Metal-Based Supramolecular Oleogel Lubricants Constructed by Dynamic Disulfide and Hydrogen Bonds for Antiwear and Friction Reduction. *Chem. Mater.* **36**(10): 5110-5119 (2024)

[185] Wang Q, Wang H, Zhao G, Ren J, Gao G, Yang S, et al. Tribological property of dendritic fibrous nano silica composite particle as lubricant additive. *Tribol. Int.* **195**: 109589 (2024)

[186] Wang T, Wang Y, Wang X, He B, Liu S, Ye Q, et al. Fabrication of Ionic Supramolecular Oleogel Lubricants Enhanced with Liquid Metal Nanodroplets for Superior Tribological Performance. *ACS Nano*. **18**(49): 33468-33478 (2024)

[187] Jin G, Cui Y, Wang T, Liu S, Xue S, Liu S, et al. Dynamic Directional Ultrasonically In Situ-Generated N,S-Codoped Carbon Dots in Poly(ethylene glycol) for Improved Tribological Performance. *ACS Appl. Mater. Interfaces*. **16**(30): 39896-39905 (2024)

[188] Wei Y, Dai L, Zhong H, Liao H, Hou X. Preparation and Tribological Properties of a Multilayer Graphene-Reinforced TiO_2 Composite Nanolubricant Additive. *ACS Omega*. **7**(46): 42242-42255 (2022)

[189] Krim J, Smirnov AI. Fundamental Mechanisms Underlying the Effectiveness of Nanoparticle Additives to Lubricants: 25 Examples Linking Nano-to Macroscale Friction. *Lubricants*. **12**(6): 225 (2024)

[190] Meng Y, Su F, Chen Y. A novel nanomaterial of graphene oxide dotted with Ni nanoparticles produced by supercritical CO_2-assisted deposition for reducing friction and wear. *ACS Appl. Mater. Interfaces*. **7**(21): 11604-11612 (2015)

[191] Jiang Z, Sun Y, Liu B, Yu L, Tong Y, Yan M, et al. Research progresses of nanomaterials as lubricant additives. *Friction*. **12**(7): 1347-1391 (2024)

[192] Borda FLG, de Oliveira SJR, Lazaro LMSM, Leiróz AJK. Experimental investigation of the tribological behavior of lubricants with additive containing copper nanoparticles. *Tribol. Int.* **117**: 52-58 (2018)

[193] Zhang Y, Zhang S, Sun D, Yang G, Gao C, Zhou C, et al. Wide adaptability of Cu nano-additives to the hardness and composition of DLC coatings in DLC/PAO solid-liquid composite lubricating system. *Tribol. Int.* **138**: 184-195 (2019)

[194] Guo J, Zhao Y, Sun B, Wang P, Wang Z, Dong H. Research progress of nano copper lubricant additives on engineering tribology. *Metals*. **11**(12): 2006 (2021)

[195] Guo P, Chen L, Wang J, Geng Z, Lu Z, Zhang G. Enhanced Tribological Performance of Aminated Nano-Silica Modified Graphene Oxide as Water-Based Lubricant Additive. *ACS Appl. Nano Mater.* **1**(11): 6444-6453 (2018)

[196] Wang D, Jia X, Shan Z, Gao L, Yang J, Wang Z, et al. Zr-MOFs (UIO-66-NH_2)@Fluorinated Graphene for Developing Highly Antiwear, Friction-Reduction Lubricating Additives. *Langmuir*. **40**(51): 27061-27072 (2024)

[197] Gao L, Jia X, Wang D, Song H. MoS_2 Compounded with FG through Layered Loading for Synergistic Lubrication: A High-Performance Lubricant for Extreme Environmental Condition. *ACS Appl. Mater. Interfaces*. **17**(32): 46238-46250 (2025)

[198] Hou X, Liu X, Dai L, Yang Y, Du J, Wang Y, et al. Preparation and Tribological Properties of Potassium Borate/Graphene Nano-composite as Lubricant Additive. *J. Mater. Eng. Perform.* **33**(4): 1827-1841 (2023)

[199] Yu H, Liu X, Zheng Z, Qiao D, Feng D, Gong Z, et al. In Situ Graphene Formation Induced by Tribochemical Reaction for Sustainable Lubrication. *ACS Sustainable Chem. Eng.* **11**(6): 2238-2248 (2023)

[200] Zhang L, Yin Z, Zhang K, Li S, Wang J, Wei X. Study on friction properties of silver/polydopamine modified graphene oxide nanocomposites as lubricant additive. *Fullerenes, Nanotubes Carbon Nanostruct.* **31**(3): 209-223 (2022)

[201] Sun B, Chen W, Zhang H, Feng T, Xing W, Elmarakbi A, et al. CeO_2-decorated reduced graphene oxide for lubricative, anticorrosive and photocatalytic purposes. *Mater. Chem. Phys.* **308**: 128255 (2023)

[202] Wang S, Chen D, Chen Y, Zhu K. Dispersion stability and tribological properties of additives introduced by ultrasonic and microwave assisted ball milling in oil. *RSC Adv.* **10**(42): 25177-25185 (2020)

[203] Gou R, Chen J. Tribological properties of Graphene/MoS_2 combinations as lubricant additives for polycrystalline diamond compact. *Ceram. Int.* **50**(8): 12713-12723 (2024)

[204] Lu Z, Qiu F, Song H, Hu X. Tribological performances of MoS_2/C_{60} nanocomposite as lubricating additive in dioctyl sebacate. *Ind. Lubr. Tribol.* **76**(4): 486-499 (2024)

[205] He J, Sun J, Choi J, Wang C, Su D. Synthesis of N-doped carbon quantum dots as lubricant additive to enhance the tribological behavior of MoS_2 nanofluid. *Friction*. **11**(3): 441-459 (2022)

[206] Lv W, Wang T, Wang Q, Yap KK, Song F, Wang C. Tribological and Mechanochemical Properties of Nanoparticle-Filled Polytetrafluoroethylene Composites under Different Loads. *Polymers (Basel)*. **16**(7): 894 (2024)

[207] Nassef MGA, Nassef BG, Hassan HS, Nassef GA, Elkady M, Pape F. Tribological and Chemical-Physical Behavior of a Novel Palm Grease Blended with Zinc Oxide and Reduced Graphene Oxide Nano-Additives. *Lubricants*. **12**(6): 191 (2024)

[208] Wen G, Wen X, Cao H, Bai P, Meng Y, Ma L, et al. Fabrication of Ti_3C_2 MXene and tetradecylphosphonic acid@MXene and their excellent friction-reduction and anti-wear performance as lubricant additives. *Tribol. Int.* **186**: 108590 (2023)

[209] Feng P, Ren Y, Li Y, He J, Zhao Z, Ma X, et al. Synergistic lubrication of few-layer $Ti_3C_2T_x/MoS_2$ heterojunction as a lubricant additive. *Friction*. **10**(12): 2018-2032 (2022)

[210] Alazemi AA, Etacheri V, Dysart AD, Stacke L, Pol VG, Sadeghi F. Ultrasmooth Submicrometer Carbon Spheres as Lubricant Additives for Friction and Wear Reduction. *ACS Appl. Mater. Interfaces*. **7**(9): 5514-5521 (2015)

[211] He T, Chen N, Fang J, Cai G, Wang J, Chen B, et al. Micro/nano carbon spheres as liquid lubricant additive: Achievements and prospects. *J. Mol. Liq.* **357**: 119090 (2022)

[212] Song H, Wang Z, Yang J. Tribological properties of graphene oxide and carbon spheres as lubricating additives. *Appl. Phys. A*. **122**: 1-9 (2016)

[213] Gu Y, Fei J, Huang J, Zhang L, Qu M. Synthesis and tribological performance of carbon microspheres/poly (methyl methacrylate) core-shell particles as highly efficient lubricant. *J. Phys. Chem. C*. **123**(47): 29037-29046 (2019)

[214] Shan Z, Jia X, Tian R, Yang J, Fan H, Song H. Cellulose-armored “CNTs-soft metal” hybrid nanomaterials to improving the friction-reduction and anti-wear performance of bio-lubricants. *Tribol. Int.* **191**: 109085 (2024)

[215] Wang F, Wang X, Ye X. The tribological properties of the heterogeneous core-shell nano/microspheres as lubricating additives: Based on Fe_3O_4 and C. *J. Ind. Eng. Chem.* **in press**: (2025)

[216] Xue H, Zhao F, Song Y, Ma S, Wang H. Synthesis of nanoSiO_2/graphene oxide nanocomposite as a novel engine oil additive for reducing friction and wear. *J. Mater. Sci.* **59**(3): 896-914 (2024)

[217] Chen G, Zhao J, Chen K, Liu S, Zhang M, He Y, et al. Ultrastable lubricating properties of robust self-repairing tribofilms enabled by in situ-assembled polydopamine nanoparticles. *Langmuir*. **36**(4): 852-861 (2020)

[218] Maurya U, Vasu V. Boehmite nanoparticles for potential enhancement of tribological performance of lubricants. *Wear*. **498**: 204311 (2022)

[219] Ma W, Li T, Fang Z, Li W, Tang H, Zhang L, et al. $Ti_3C_2T_x$ MXenes modified with dodecylphosphonic acid as an effective lubricant additive. *Tribol. Int.* **186**: 108565 (2023)

[220] Wang Y, Zhao F, Yang H, Yang K, Zhang T, Ye Q, et al. Constructing MXene quantum dots decorated covalent organic frameworks as oil-based lubricant additive. *Sci. China Mater.* **68**(4): 1220-1229 (2025)

[221] Wu Z, Fei J, Li C, Yan J, Ke X, Qi L. Effect of 2D Cu-MOFs modified carbon spheres nanoparticles as an environmentally friendly lubricating additive on tribological properties. *Tribol. Int.* **192**: 109321 (2024)

[222] Zhang Z, Fan X, Ma X, Zhu M. Synergistic lubrication mechanism of core/shell C@MoS_2 particles as lubricant additives. *Appl. Surf. Sci.* **639**: 158234 (2023)

[223] Jin Y, Cai X, Zhang P, Zeng D, Tu X, Chen D. Friction and self-repairing behaviour of magnesium silicate hydroxide-MoS_2 lubricant additives on gray cast iron with Cr-coated steel ball friction pairs. *Tribol. Int.* **195**: 109665 (2024)

[224] Zhao J, Li Y, He Y, Luo J. In situ green synthesis of the new sandwichlike nanostructure of Mn_3O_4/graphene as lubricant additives. *ACS Appl. Mater. Interfaces*. **11**(40): 36931-36938 (2019)

[225] Man W, Huang Y, Gou H, Li Y, Zhao J, Shi Y. Synthesis of novel CuO@ Graphene nanocomposites for lubrication application via a convenient and economical method. *Wear*. **498**: 204323 (2022)

[226] Chen B, Zhang M, Zhang K, Dong Z, Li J, Zhao G. Mono-dispersed Ag nanoparticles decorated graphitic carbon nitride: An excellent lubricating additive as PPESK composite film. *Friction*. **10**(5): 717-731 (2022)

[227] Liu S, Hu G, Wang Y, Liu S, Ye Q, Zhou F, et al. Hybrid Carbon Nanospheres with Encapsulated (Bi) Metallic Nanocrystals as Lubricant Additives for Antiwear and Friction Reduction. *ACS Appl. Mater. Interfaces*. **16**(3): 3911-3921 (2024)

[228] Ma X, Gan C, Li X, Li Y, Feng P, Fan X, et al. Tribological properties of SiO_2@Cu and SiO_2@ MoS_2 core-shell microspheres as lubricant additives. *Tribol. Lett.* **69**: 1-15 (2021)

[229] Wang Y, Zhang G, Yang D, Li Y, Yin W, Weng Y. Electronic-Control Friction Behavior of Porous Metal-Organic Framework@Ag Nanocrystals as Self-Repairing Lubricant Additive. *ACS Appl. Mater. Interfaces*. **15**(29): 35732-35740 (2023)

[230] Shang L, Zhang G, Liu F, Han L, Liang E, Qi H. Electric-tuned wear resistance of NaFe-PBA composite lubricant. *Tribol. Int.* **213**: 111062 (2026)

[231] Hou F, Zhang G, Lu S, Qi J, Li Y. Design of Intercalated Graphene/CNTs nanocomposite lubricants with load-bearing and their intelligent electric current-controlled friction performance. *Diamond Relat. Mater.* **151**: 111832 (2025)

[232] Yi S, Li J, Liu Y, Ge X, Zhang J, Luo J. In-situ formation of tribofilm with $Ti_3C_2T_x$ MXene nanoflakes triggers macroscale superlubricity. *Tribol. Int.* **154**: (2021)

[233] Yi S, Li J, Rao J, Ma X, Zhang Y. Alkyl-functionalized black phosphorus nanosheets triggers macroscale superlubricity on diamond-like carbon film. *Chem. Eng. J.* **449**: (2022)

[234] Yi S, Guo Y, Li J, Zhang Y, Zhou A, Luo J. Two-dimensional molybdenum carbide (MXene) as an efficient nanoadditive for achieving superlubricity under ultrahigh pressure. *Friction*. **11**(3): 369-382 (2022)

[235] Chen J, Yu J, Liu D, He K, Liu Z, Liang L, et al. Tribological properties and synergistic lubrication mechanism of 3D graphene/nano-TiO_2 (G@TiO_2) composite castor oil: A microscopic view and molecular dynamics perspective. *Tribol. Int.* **188**: 108821 (2023)

[236] Granja V, Jogesh K, Taha Tijerina J, Higgs CF. Tribological Properties of h-BN, Ag and MgO Nanostructures as Lubricant Additives in Vegetable Oils. *Lubricants*. **12**(3): 66 (2024)

[237] Guo W, Chen W, Wang Z, Mao Y. Study on Friction Reduction and Photocatalytic Properties of nano-ZnO/TiO_2 Composite Lubricants. *J. Mater. Eng. Perform.* **34**(14): 14822-14831 (2024)

[238] Huang J, Min C, Sun Z, Yu H, Liang H. Unique synergistic effects of ternary multi-dimensional CNT/g-C_3N_4/MoS_2 hybrid as a paraffin oil additive for improved tribological properties. *Colloids Surf., A*. **689**: 133635 (2024)

[239] Opia AC, Abdollah MF, Amiruddin H. Lubricity performance of Jatropha oil incorporated PTFE and h-BN as additives for electric vehicles transmission lubrication. *Ind. Lubr. Tribol.* **77**(1): 93-104 (2024)

[240] Que L, Zhang Z, Su J, Dai M, Han R, Xu X, et al. Synergistic effect of in-situ synthetic GE@Cu particles as additives for enhancement in lubrication performances. *Diamond Relat. Mater.* **144**: 110984 (2024)

[241] Xiong S, He J, Wang C. Preparation and Tribological Behavior of N-doped Graphene Oxide Quantum Dots with MoS_2 and Al_2O_3 Nanocomposites as Lubricant Additive in Aqueous Glycerol. *Tribol. Lett.* **72**(3): 86 (2024)

[242] Li W, Zeng Z, Le S, Zhu K, Huang X, Hegab H, et al. Investigation of a green nanofluid added with graphene and Al_2O_3 nano-additives for grinding hard-to-cut materials. *Tribol. Int.* **195**: 109580 (2024)

[243] Hettiarachchi SJ, Bowen J, Kershaw M, Baragau IA, Nicolaev A, Kellici S. Nanostructured Al_2O_3/graphene additive in bio-based lubricant: A novel approach to improve engine performance. *Tribol. Int.* **186**: 108619 (2023)

[244] Chen J, He K, Fei J, Yu J, Meng Z, Pang Y, et al. Extreme pressure and anti-wear properties of polycarboxylate superplasticizer modified 3D porous graphene/SiO_2 as water-based lubricant additives. *Wear*. **540-541**: 205239 (2024)

[245] Cai X, Li S, Zeng W, Huang K, Zhao L, Zeng D, et al. Improving dispersion and tribological performance of MoS_2 lubricant additive with the synergistic effects of MSH and amorphous carbon. *J. Mater. Res. Technol.* **29**: 2509-2519 (2024)

[246] Ouyang T, Sun X, Tang W, Li Y, Tian ZQ, Li Y. Anti-wear and vibration-noise control of nitrogen-doped graphene/C_{60} nano additives. *Wear*. **536-537**: 205173 (2024)

[247] Ouyang T, Sun X, Tuo X, Yang Y, Deng Q, Qin S. Anti-wear effects of modified graphene/nanodiamond hybrid additives in lubricating oils. *Wear*. **576-577**: 206116 (2025)

[248] Qiu S, Chen B, Yang B, Dong W, Tong Y, Li J, et al. Facile construction of graphene oxide/CeO_2 nanohybrid for enhancing tribological properties of green rapeseed oil. *Colloids Surf., A*. **676**: 132248 (2023)

[249] Xia D, Wang Y, Liu H, Lin H, Han S. The tribological properties and synergistic lubrication mechanism of MoS_2/AlOOH nanosheets as lubricant additives. *J. Alloys Compd.* **1007**: 176236 (2024)

[250] Liñeira del Río JM, Fernandes CMCG, Gonçalves DEP, Seabra JHO. Synergistic Effects of Functionalized WS_2 and SiO_2 Nanoparticles and a Phosphonium Ionic Liquid as Hybrid Additives of Low-Viscosity Lubricants. *Lubricants*. **12**(2): 58 (2024)

[251] Nagarajan T, Sridewi N, Wong WP, Walvekar R, Khalid M. Enhanced tribological properties of diesel-based engine oil through synergistic MoS_2-graphene nanohybrid additive. *Sci. Rep.* **13**(1): 17424 (2023)

[252] Pasha MB, Rao RN, Ismail S, Gupta M, Prasad PS. Tribo-informatics approach to predict wear and friction coefficient of Mg/Si3N4 composites using machine learning techniques. *Tribol. Int.* **196**: 109696 (2024)

[253] Wen G, Liu W, Wen X, Wei P, Cao H, Bai P, et al. Effective tribological performance-oriented concentration optimization of lubricant additives based on a machine learning approach. *Tribol. Int.* **197**: 109770 (2024)

[254] Yin N, Yang P, Liu S, Pan S, Zhang Z. AI for tribology: Present and future. *Friction*. **12**(6): 1060-1097 (2024)

[255] Shah R, Jaramillo R, Thomas G, Rayhan T, Hossain N, Kchaou M, et al. Artificial intelligence and machine learning in tribology: selected case studies and overall potential. *Adv. Eng. Mater.*: 2401944 (2025)

[256] Chen H, Yi S, Li J, Fu J, Yang L, Xu Y, et al. Facilitating macroscopic superlubricity through graphene oxide nanosheet additives in phosphoric acid. *Mater. Today Nano*. **27**: (2024)

[257] Li H, Zhang Y, Li C, Zhou Z, Nie X, Chen Y, et al. Extreme pressure and antiwear additives for lubricant: academic insights and perspectives. *Int. J. Adv. Manuf. Tech*. **120**(1): 1-27 (2022)

[258] Kumar S, Kumar A, Kumar A, Kumar A, Choudhari A, Gupta AK, et al. State of the art in lubricants for extreme cold weather. In: *Performance Characterization of Lubricants*2024: 227-261.

[259] Yang Z, Wang Z, Li J, Ding S, Yi S. Tribological and machining performance of novel DE@Mo_2CTx MXene bio-microcapsule nanofluids in machining of magnesium alloys. *Tribol. Int.* **211**: (2025)

[260] Yang Z, Yi S, Li J, Ding S. Thermal and force simulation modelling of graphene oxide nanosheets as cutting fluid additives during Ti-6Al-4V drilling process. *Int. J. Therm. Sci.* **210**: (2025)

[261] Zhang YS, Zhu HL, Yao D, Williams PT, Wu C, Xu D, et al. Thermo-chemical conversion of carbonaceous wastes for CNT and hydrogen production: a review. *Sustainable Energy Fuels*. **5**(17): 4173-4208 (2021)

[262] Schmaltz T, Wormer L, Schmoch U, Döscher H. Graphene Roadmap Briefs (No. 3): meta-market analysis 2023. *2D Mater.* **11**(2): 022002 (2024)

[263] Arvidsson R, Kushnir D, Sanden BA, Molander S. Prospective life cycle assessment of graphene production by ultrasonication and chemical reduction. *Environ. Sci. Technol.* **48**(8): 4529-4536 (2014)

[264] Nizam NUM, Hanafiah MM, Woon KS. A Content Review of Life Cycle Assessment of Nanomaterials: Current Practices, Challenges, and Future Prospects. *Nanomaterials (Basel)*. **11**(12): 3324 (2021)

[265] Munuera J, Britnell L, Santoro C, Cuéllar-Franca R, Casiraghi C. A review on sustainable production of graphene and related life cycle assessment. *2D Mater.* **9**(1): 012002 (2021)

Author biography

Siyuan WANG He received his Ph.D. degree from Hunan University, China, in 2024. He subsequently joined the School of Intelligent Manufacturing, Nanyang Institute of Technology, China. His main research interests are the preparation and application of lubricant nano-additive materials.

Guanlin REN He received his Ph.D. degree from Hunan University, China, in 2024. He subsequently joined the State Key Laboratory of Solid Lubrication, Lanzhou Institute of Chemical Physics, Chinese Academy of Sciences, China. His main research interests are the synthesis and lubrication mechanism of high-performance lubricants.